ESTIMATION OF GROUNDWATER RECHARGE USING NEUTRON PROBE MOISTURE READINGS NEAR GOLDEN, COLORADO

by

Nicholas J. Kiusalaas and Eileen P. Poeter

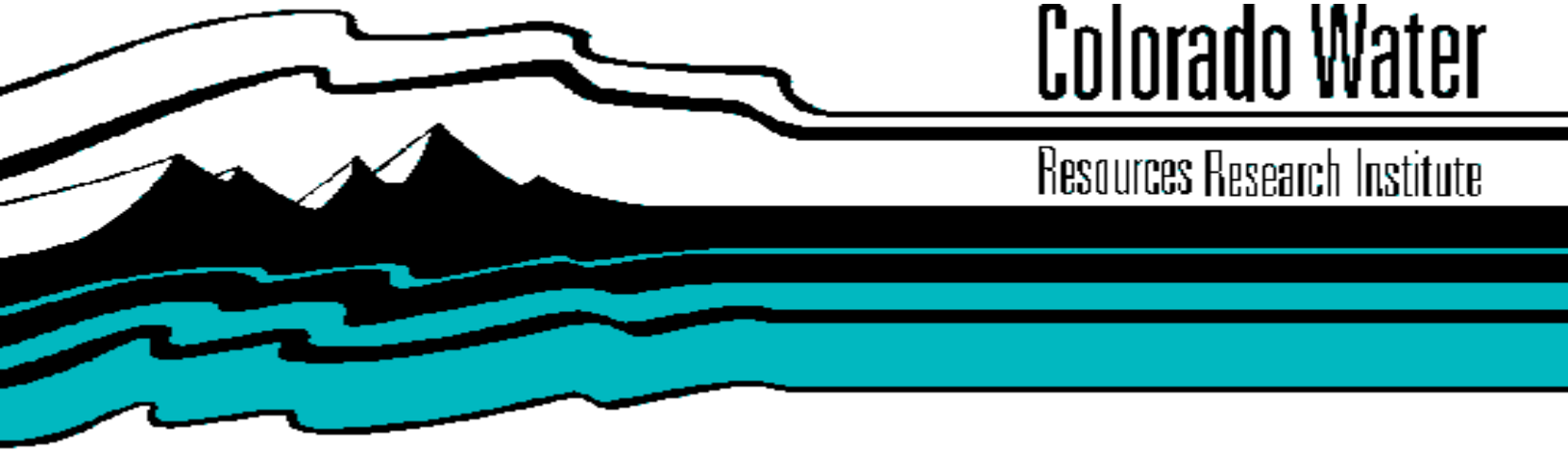

Completion Report No. 165

ESTIMATION OF GROUNDWATER RECHARGE USING NEUTRON PROBE MOISTURE READINGS NEAR GOLDEN, COLORADO

by

Nicholas J. Kiusalaas
Eileen P. Poeter

Department of Geology and Geological Engineering
Colorado School of Mines

November 16, 1992

Grant No. 14-08-0001-G1551-04
Project No. 11

The research on which this report is based was financed in part by the U.S. Department of the Interior, Geological Survey, through the Colorado Water Resources Institute; and the contents of this publication do not necessarily reflect the views and policies of the U.S. Department of the Interior, nor does the mention of trade names or commercial products constitute their endorsement by the United States Government.

COLORADO WATER RESOURCES RESEARCH INSTITUTE
Colorado State University
Fort Collins, Colorado 80523

Robert C. Ward, Director

ABSTRACT

To better understand recharge processes under natural conditions in the Denver Basin, a vadose zone monitoring study was conducted from September 1991 through September 1992 at a site near Golden, Colorado. Six access tubes were monitored with a neutron probe to a depth of 8.75 feet to determine moisture profiles several times a month. Moisture characteristic curves were developed for soil samples which were extracted during access tube installation. The van Genuchten function was fitted to experimental moisture characteristic curve data and combined with saturated hydraulic conductivity from laboratory analysis to estimate unsaturated hydraulic conductivity. Numerical analysis based on moisture profiles and hydraulic properties was used to estimate vertical flux.

Moisture profiles were static below 3 feet from September 1991 through February 1992. A wetting front began to move below 3 feet in March and progressed to a depth of 6.75 by April. Moisture content below 6.75 feet did not change throughout the monitoring period. At the conclusion of the study, moisture profiles had not returned to the condition that existed at the same time the previous year. The

additional water in storage is believed to be due to unusually heavy March precipitation when evapotranspiration demands were low, and is expected to be depleted to meet evapotranspiration demands before a significant amount of water percolates downwards to recharge the groundwater. Average spring precipitation is not believed to result in wetting fronts of the magnitude witnessed during this study.

Downward vertical flow of water at the study site is believed to occur under near steady-state conditions represented by the static moisture profiles recorded in the late summer and fall of 1991. Soil compaction during sampling resulted in imprecise moisture characteristic curves. As a consequence, it is uncertain if a downward gradient existed below 6.75 feet at any time during the monitoring period. If downward flow occurs, it is estimated to range from $4.9(10)^{-4}$ to $9.7(10)^{-6}$ inches per year [$1.2(10)^{-3}$ to $2.5(10)^{-5}$ cm/year] during the study period based on one dimensional numerical simulations.

TABLE OF CONTENTS

LIST OF FIGURES

LIST OF TABLES

1.0 INTRODUCTION

1.1 Purpose

The purpose of this study is to determine the amount of recharge to the groundwater table resulting from precipitation at one site in the Denver Basin. Neutron moisture logging and lysimetry methods are used to obtain quantitative field measurements for calculation of recharge rates.

Recharge rates in the Denver Basin are currently uncertain even though they are vital parameters when addressing water management concerns such as safe yield. Until present, recharge rates have primarily been obtained indirectly from sources such as calibrated models. The goal of this study is to use direct field measurements in the vadose (unsaturated) zone to provide a better understanding of the nature of recharge to a portion of the Denver Basin.

1.2 Site Location

The study area is a 30 by 20 foot plot located 3 miles north of Golden, Colorado in Section 15, T. 3 S., R. 70 W., (Figure 1.1). The elevation of the site is approximately 5900

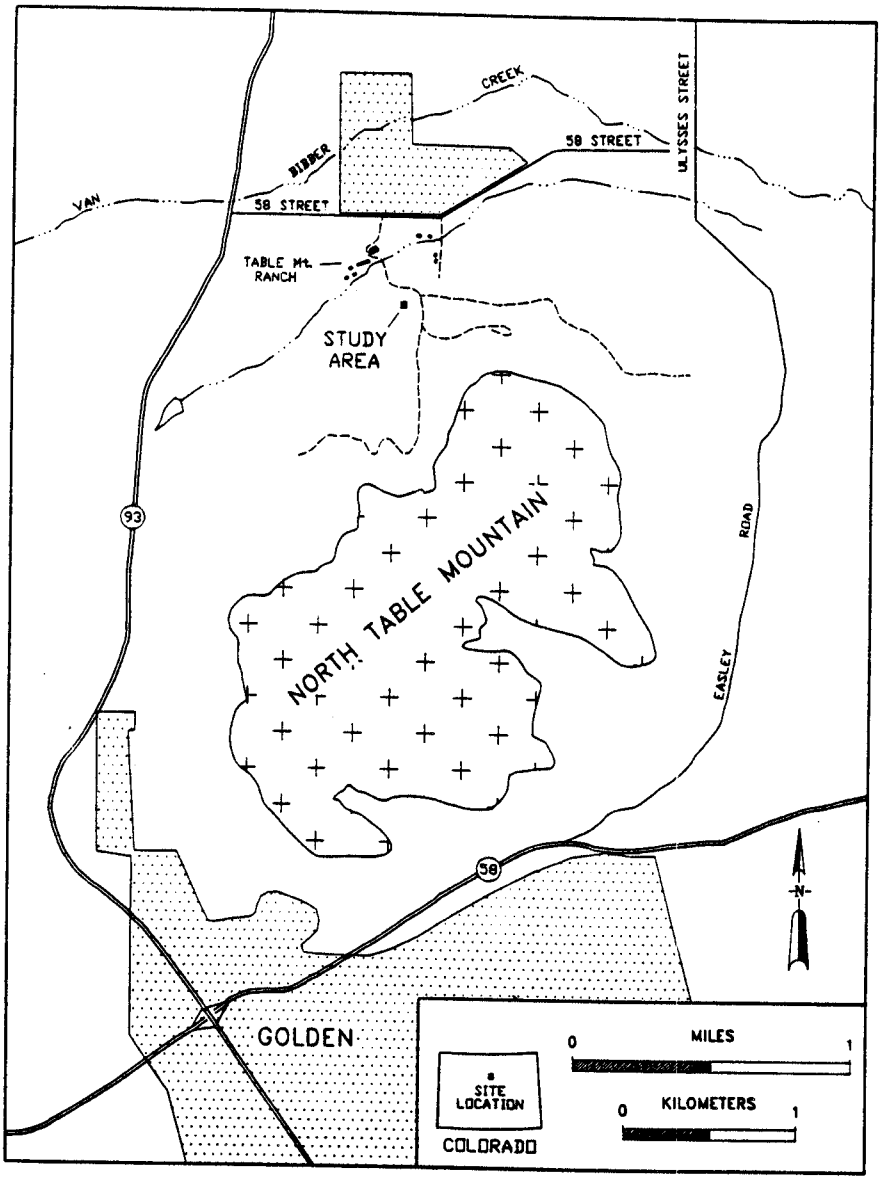

Figure 1.1 Study Site Location

feet above mean sea level and slopes to the north-west at 3 to 5 degrees. Access to the study site is through an unpaved road on the Table Mountain Ranch which lies 0.5 miles west of Colorado State Highway 93 on 58th street.

1.3 Site Geology, Surficial Materials and Vegetation

The study area lies above the approximate contact of the upper Arapahoe Formation and the lower Denver Formation (Van Horn, 1957). The Arapahoe Formation consists of conglomerates, brown quartoze sandstones, and silty claystones. The upper portion of the formation is not exposed near the study area. The Denver Formation consists of andesitic conglomerates, tuffaceous sandstones and silty claystones.

The soil at the study site is the Nunn Clay Loam (Price and Amen, 1983). It is a well drained soil that forms on high terraces and hill slopes from 5% to 9%, and has "slow permeability". Vegetation consists of western wheatgrass, green needlegrass and blue gramma.

1.4 Arid and Semiarid Zone Recharge Concepts

Groundwater recharge occurs when infiltration exceeds the demands of evapotranspiration and water drains from the root zone, and flows downwards to replenish the groundwater

reservoir (Gee, W. *et al.*, 1988). Typically, infiltration does not exceed evapotranspiration for most of the year in arid and semiarid regions. Recharge is often episodic or seasonal in nature (Balek, 1988). There may only be a few times of the year when precipitation is high enough to exceed evapotranspiration. For example, some regions have high precipitation in winter or early spring when the water needs of vegetation and evaporation rates are low. In some areas, recharge may not occur every year.

Gee *et al* (1988) make a distinction between two modes of recharge; continuous, diffuse recharge from widespread percolation through the vadose zone and transient recharge from short term penetration of water through preferred pathways. Diffuse recharge is often localized and only occurs in limited portions of a region. This localized recharge may be controlled by a number of factors including topography, vegetation, heterogeneity of soil hydraulic properties and depth to the water table (Rushton, 1988). The lack of change in moisture content at depth does not necessarily indicate a static water condition. Vertical gradients are often found to be near unity in homogeneous soils with flow occurring under the gravity gradient (Gee, 1988). Under these conditions, the vertical flux is equal to the hydraulic conductivity. Steady state conditions may also be present in heterogeneous soil.

Under these conditions the gradient is not unity, therefore the flux must be calculated using Darcy's law or other methods discussed later. Static moisture profiles have been reported in heterogeneous soil conditions by Davis (1990) and Hammermeister (1985).

1.5 Previous Work

Few field studies using quantitative field measurements to calculate natural recharge from natural precipitation in arid and semiarid environments have been documented in the literature. To the author's knowledge, studies of natural recharge have not been conducted in the western portion of the Denver Basin.

The most closely related study was conducted by Klute *et al.* (1972). The purpose of this study was to assess the impact of agricultural land management practices on groundwater recharge to the Ogallala Aquifer near Burlington, Colorado. The authors cite studies that report average recharge rates to the high plains as approximately 0.8 inches per year (Boettcher, 1966; Cardwell and Jenkins, 1963; McGovern, 1964,; Weist 1964) and 0.4 inches per year for Kit Carson County where this study was conducted (Riddell, 1967). To assess groundwater recharge rates and the impact agricultural surface treatments has on it, a site was

established that consisted of Peorian loess overlying the Ogallala formation. The site was divided into 12, 100 x 80 foot plots and each was assigned one of six surface treatments consisting of native rangeland, mechanical fallow, pitting, chemical fallow, gravel mulch, and gravel mulch with herbicide. Soil water moisture content was monitored using a neutron probe to 9.5 feet in all plots except the gravel mulch with herbicide which was monitored to 18 feet. Readings were taken at 1-foot intervals. Moisture characteristic curves were developed for selected samples using 1, 5, and 15 bar measurements. In addition to moisture characteristic curves, matric potential was determined using thermocouple psychrometers installed on the native rangeland plots.

Throughout the monitoring period, the native rangeland showed no significant change in moisture content below 4 feet. In situ matric potential determined from the moisture characteristic curves were below 15 bars from 2 feet to the bottom of the measured interval. Thermocouple psychrometer measurements indicated very high matric potentials throughout most of the year. These readings are presented in table 1.1.

The authors concluded that no significant recharge occurs from precipitation at this site under natural rangeland conditions. If previous recharge estimates of 0.8 inches

(2.03 cm) per year are correct, substantially larger rates must occur at isolated areas such as playa lakes, stream beds,

Table 1.1 Matric potentials from thermocouple psychrometer readings in native rangeland near Burlington, Colorado

Depth (ft)	Matric Potential (bars)			
	Date	7/20/71	12/15/71	5/20/72
20		23.0	23.5	20.5
20		23.5	22.0	20.5
20		18.0	17.5	16.0
10		16.0	11.5	13.0
10		14.0	8.5	7.0

Source: Klute, A., R.E. Danielson, D.R. Linden, and P. Hamaker, 1972. Ground Water Recharge as Affected by Surface Vegetation and Management: Colorado Water Resources Research Institute, Completion Report No. 41

terrace channels, or irrigated farmland.

Other relevant studies conducted in semiarid regions include Stephens *et al* (1986) who worked near Socorro, New Mexico. Fluxes were calculated in the vadose zone by applying Darcy's equation to in situ pressure head data from tensiometers assuming only vertical flow. Fluxes ranged from 0.70 cm/yr to 3.66 cm/yr using the harmonic mean and geometric mean respectively to calculate hydraulic conductivity. Summer

rains were found to take up to 4 months to penetrate to 2.4 meters in this "relatively uniform, unconsolidated, dry sand".

Stephens *et al* (1987) continued their work by examining the effect of topography on recharge. They concluded that recharge can be very localized in arid and semiarid climates with a higher potential for recharge existing in topographically concave locations as opposed to hilltops or slopes. Large lateral flow components were found using tracer tests on apparently uniform sandy hill slopes even in the absence of low permeability horizons. The lateral flow was believed to be due to the anisotropy of hydraulic conductivity.

Nixon *et al*. (1972) conducted a 10 year study in a semiarid watershed. They found that rain penetrates as a wetting front during the rainy season but does not reach the bottom of the root zone every year. Extrapolation of the data collected at 4 sites indicated that recharge resulting from precipitation occurred on an average of once every 7 years. The wetting front at a grass - weed site only penetrated below the root zone 3 times in the 10 years of monitoring to contribute to recharge. The strongest wetting front that contributed to recharge took 2 months to travel 8.5 feet from the bottom of the root zone to the full monitored depth in this sandy soil. The authors concluded that recharge occurred

at irregular intervals that depend on the sequence and amount of precipitation events, and the moisture holding capacity of the root zone.

Van Tonder *et al.* (1990) conducted a recharge study of the Karoo Aquifer in South Africa using neutron probe measurements. They found no increase in soil moisture content below a depth of 1 meter despite "exceptionally high rainfall" during part of study duration and a corresponding rise in the water table. They attributed this to recharge along preferential pathways (cracks) that were not detected with the neutron probe.

Enfield et. al (1973) applied thermocouple psychrometer data to a site at the Hanford Reservation in Washington. They used a modified version of the Millington and Quirk equation to allow for thermal gradients and hydraulic conductivity values calculated using the method outlined by Jackson *et al.* (1965). Steady-state conditions were believed to exist throughout the monitored interval (10 meters to 80 meters). Vertical flux was calculated at 80 meters where matric potential was 1 bar and a gradient of 0.04 bars/meter (0.41 cm/cm) was inferred from other psychrometers. The authors concluded that the rate and direction of flux was uncertain although if a downward flux did exist, it was less than 1

centimeter per year. They attributed the uncertainty to limitations of calculated hydraulic conductivity values and thermal diffusivities and neglecting osmotic potentials.

Recharge estimates for the Denver Basin reported by Robson (1987), range from 0 to 1.0 inches per year with an average of 0.1 inches per year. These estimates were obtained from a calibrated numerical model.

2.0

FIELD SITE OVERVIEW

2.1 Site Selection Criteria

Site selection was based on 3 criteria. These criteria and their rational are as follows:

1) The property is accessible and within close proximity to the Golden area. This allows access at regular intervals when frequent monitoring is needed such as after precipitation events.

2) The site contains native vegetation representative of the Front Range area and is not farmland. This study is concerned with recharge under natural conditions. The presence of non-native vegetation, such as crops, and disturbed soil would not permit recharge estimates representative of undisturbed conditions throughout most of the Front Range.

3) And finally, the underlying geologic formation should be an aquifer in the Denver Basin. The ultimate concern of this study is the amount of water that is replenishing the bedrock aquifers in the Denver Basin. Although this

study is of limited areal extent, the site should provide insight into recharge of groundwater in the Denver Basin.

2.2 Instrumentation

Field instrumentation and monitoring equipment consist of one draining lysimeter, one neutron probe and 6 neutron probe access tubes. Figure 2.1 illustrates site dimensions, the location of neutron probe access tubes and the weighing lysimeter. The site is surrounded by general purpose wire fence to prevent tampering and trampling by horses. Throughout this report, neutron probe access tubes and their corresponding holes will be referred to by the numbers designated in Figure 2.1. The weighing lysimeter was installed August 29, 1991. Table 2.1 provides a summary of relevant information on the neutron probe access tubes.

2.3 Soil Sampling

Holes for neutron probe access tubes were drilled with a 3¼-inch diameter hand auger and soil samples 6 inches long were taken every foot from ½ foot to 9 feet. Sampling equipment consisted of a hollow tube sampler, 2-inch by 6-inch brass liners with end caps, and an 8-pound slide hammer. Samples were immediately labeled and capped after extraction, and stored in a humidity room at the end of the day on which

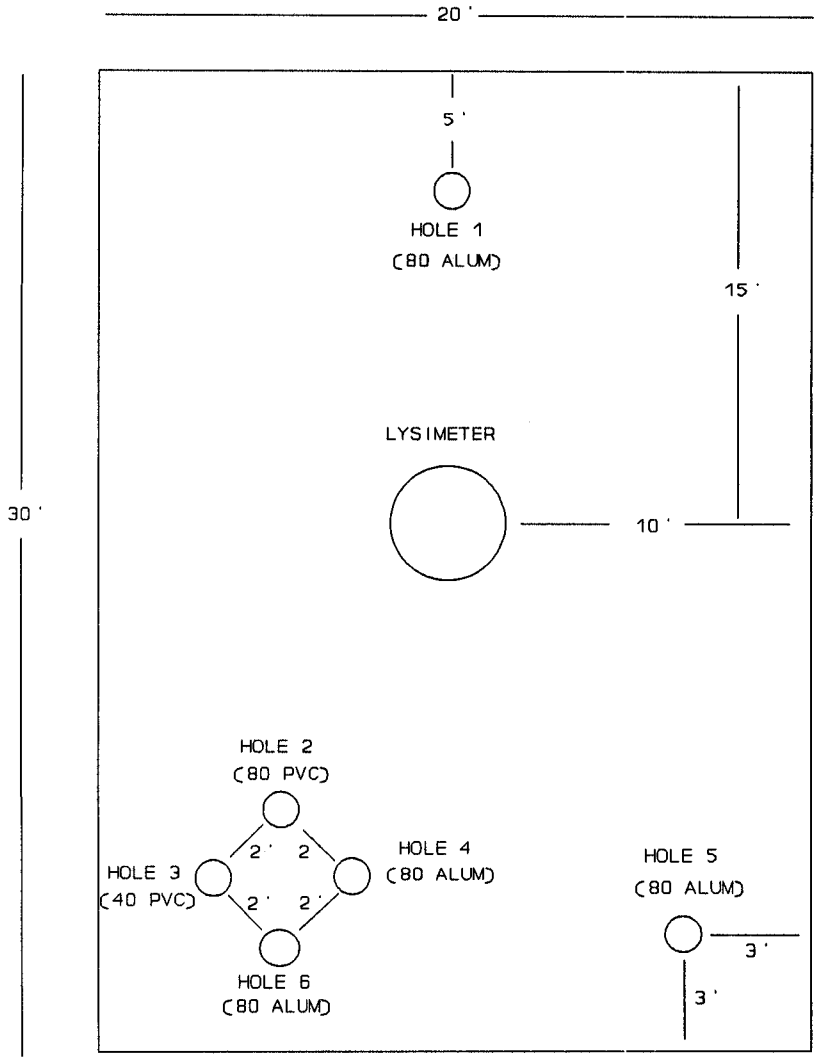

Figure 2.1 Study area geometry and monitoring equipment

Table 2.1 Summary of Neutron Probe Access Tube Information

Hole #	Casing Material	Casing Length	Installation Date
1	3" SCH 80 ALUMINUM	10.0 ft	7/30/91
2	3" SCH 80 PVC	9.8 ft	7/31/91
3	3" SCH 40 PVC	9.8 ft	8/6/91
4	3" SCH 80 ALUMINUM	10.0 ft	7/31/91
5	3" SCH 80 ALUMINUM	6.6 ft	8/6/91
6	3" SCH 80 ALUMINUM	10.0 ft	3/19/92

they were collected. These samples were later used for hydraulic parameter testing and neutron probe calibration as will be discussed in detail in later sections.

2.4 Field Measurements

The field site was monitored several times a month throughout most of the year and more frequently after precipitation or snow melt events. Measurements consisted of weighing the lysimeter and taking moisture readings with the neutron probe. The lysimeter was not weighed when snow cover was present as this would disturb the snow cover and disrupt natural conditions. A standard count was taken with the neutron probe to check for malfunctions (discussed later). Having determined the probe was functioning correctly, neutron

count ratios were taken at 1-foot intervals that corresponded to the center of the 6-inch sampling intervals.

2.5 Hydraulic Parameter Determination

Hydraulic parameters were determined for soil samples and later used for numerical modeling. Hydraulic testing consisted of pressure plate and saturated hydraulic conductivity tests. Data from the pressure plate tests were used as input to SOHYP to determine van Genuchten parameters. Grain size distribution was determined on samples used for pressure plate tests and to calibrate the neutron probe. A flow chart summarizing sample testing is presented in Figure 2.2.

2.6 Moisture Profiles

Moisture profiles were static below 3.75 feet from August 1991 through the end of March 1992 (Figures 2.3 through 2.5). Although these Figures suggest slight changes in moisture content below 3.75 feet, these variations are within the range of variation expected due to the random radioactive decay of the neutron source. Consequently, it is not possible to determine if slight changes in moisture content are occurring. Increased moisture contents from the surface to 3.75 feet indicate water did infiltrate and percolate short

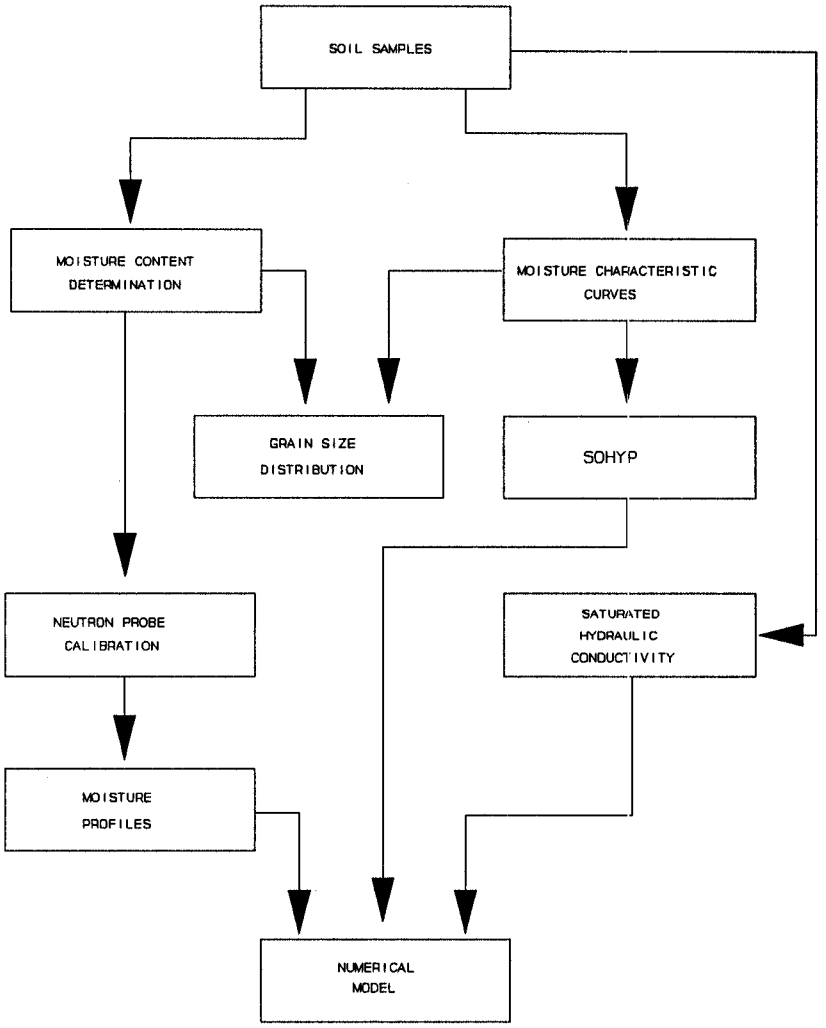

Figure 2.2 Flow chart summarizing sample testing

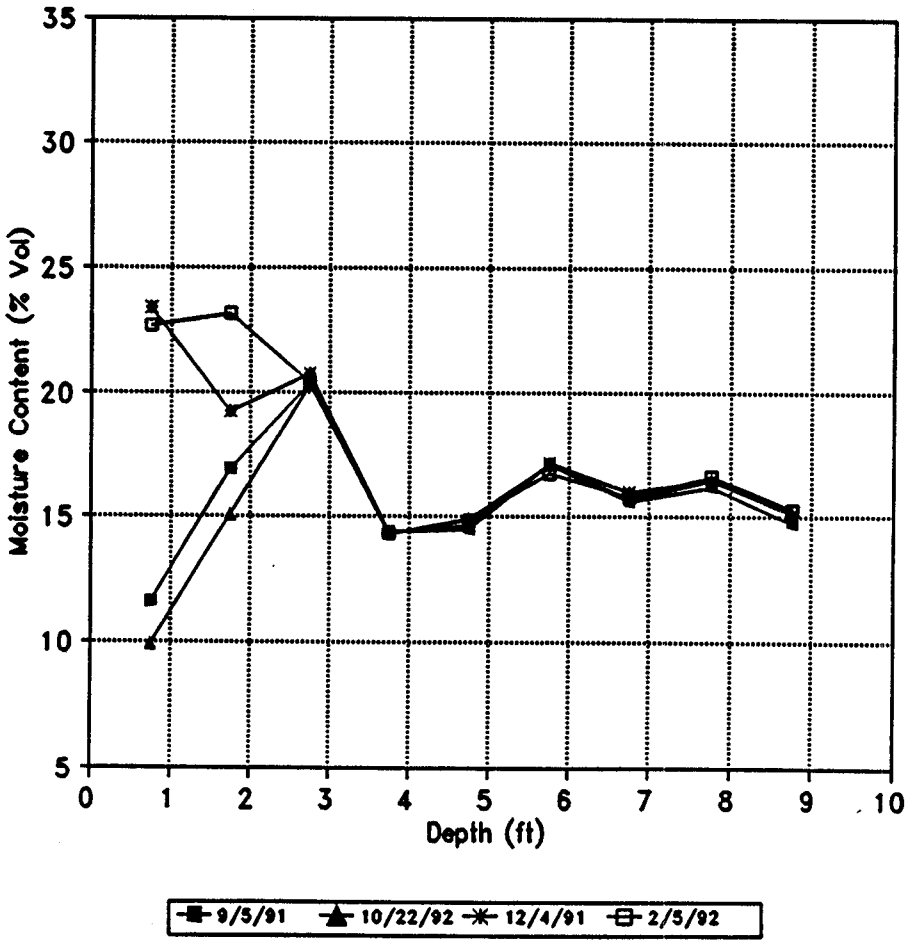

Figure 2.3 Moisture profile summary for hole #1 from September 1991 through February 1992.

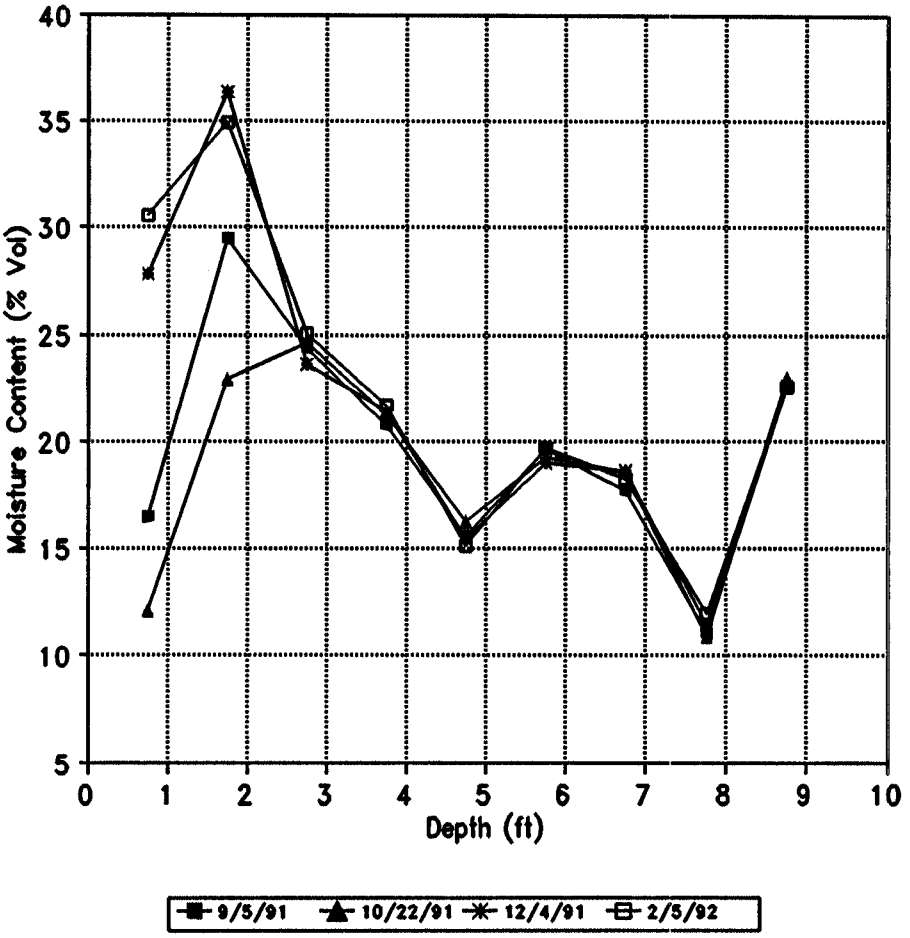

Figure 2.4 Moisture profile summary for hole #2 from September 1991 through February 1992

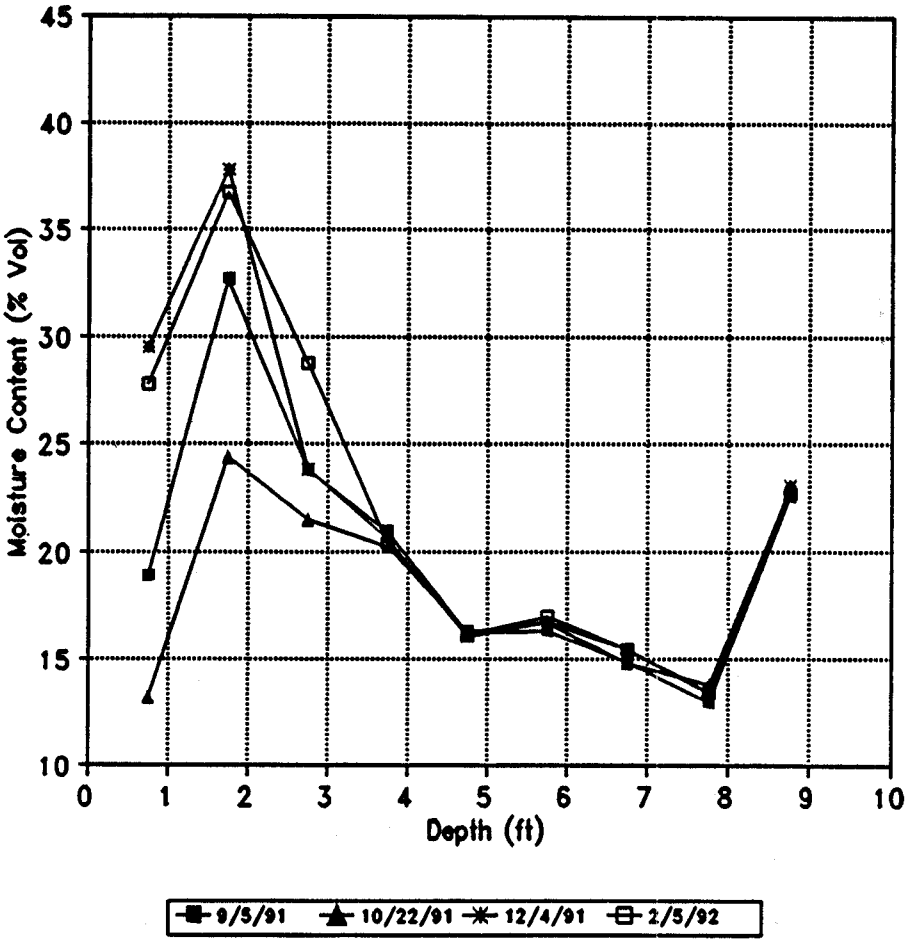

Figure 2.5 Moisture profile summary for hole #4 from September 1991 through February 1992

vertical distances during this period. However, it was apparently used to meet evapotranspiration demands since there was no increase in moisture content below 3.75 feet. From March through April, a wetting front moved through the soil to a depth of 6.75 feet (Figures 2.6 through 2.8). A lower hydraulic conductivity layer is present at 6.75 feet and the wetting front was not detected below this depth during the duration of this study. Figures 2.6 through 2.8 show an increase in moisture at 6.75 feet with no corresponding moisture increase below this depth. Apparent changes in moisture content at 7.75 and 8.75 feet are within the range of variation which results from the random radioactive decay of the neutron source and cannot be considered reliable. Throughout the remainder of the monitoring period, native grasses depleted the water in storage. Figures 2.9 through 2.11 show decreasing moisture contents above 6.75 feet due to moisture extraction by the grasses while there is no significant increase in moisture content below 6.75 feet, indicating there is no significant drainage from the root zone. These moisture profiles show the grasses can effectively extract water to depths of 6 feet. At the conclusion of this study, the study area had not returned to the moisture distribution from the previous year (Figure 2.12 through 2.14). This large increase in moisture over the year

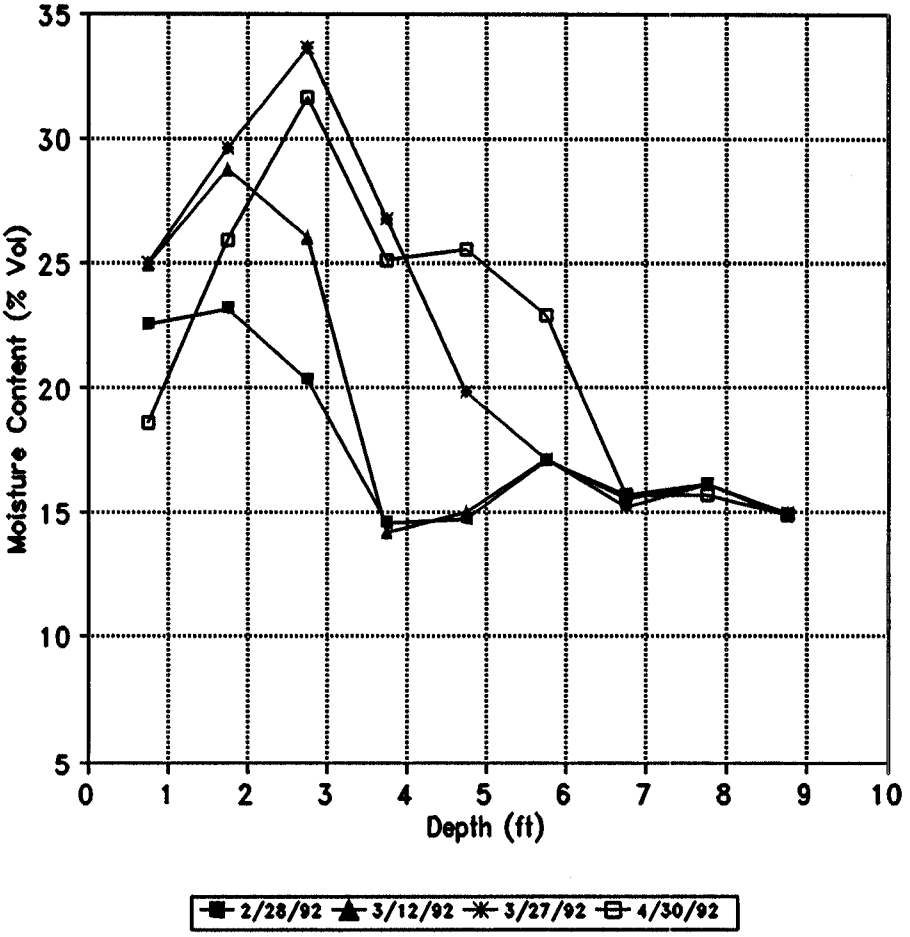

Figure 2.6 Moisture profile summary for hole #1 from February 1992 through April 1992

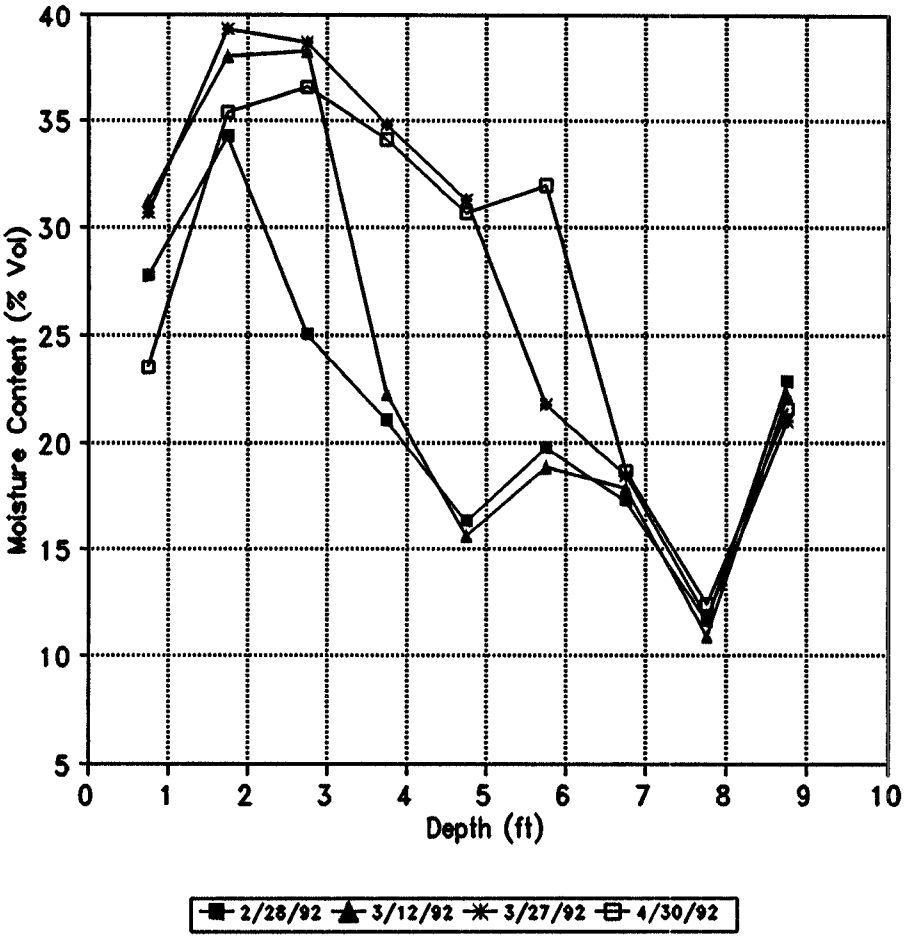

Figure 2.7 Moisture profile summary for hole #2 from February 1992 through April 1992

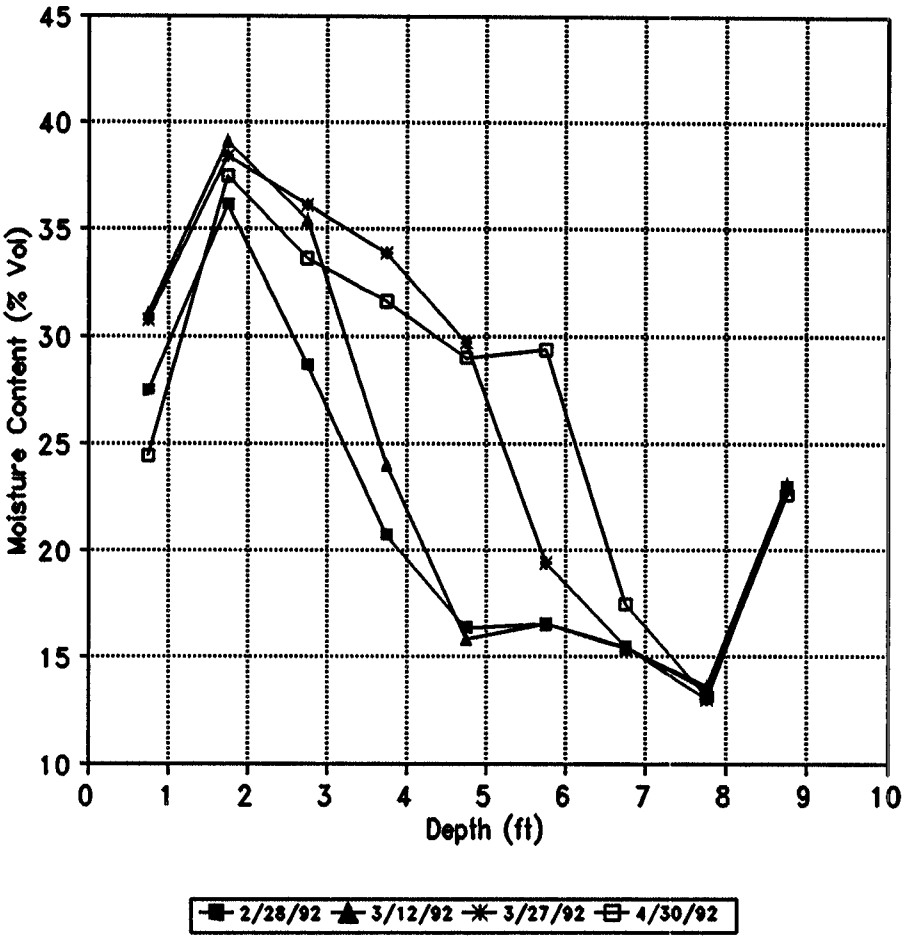

Figure 2.8 Moisture profile summary for hole #4 from February 1992 through April 1992

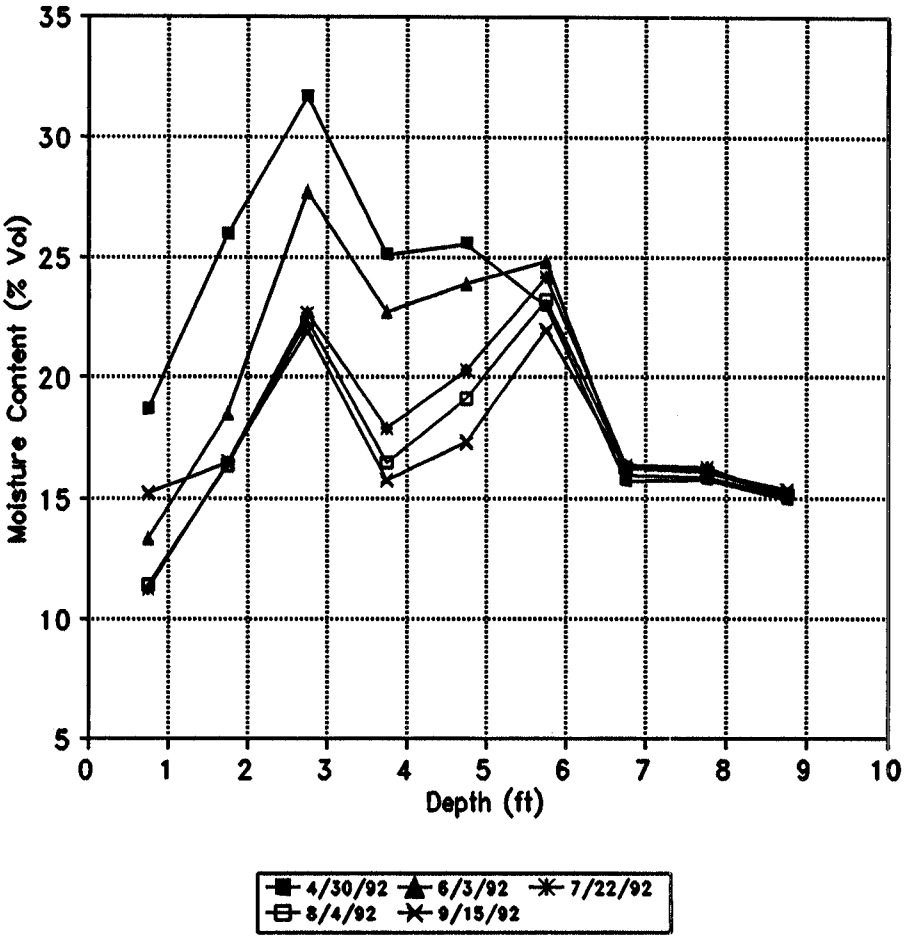

Figure 2.9 Moisture profile summary for hole #1 from March 1992 through September 1992

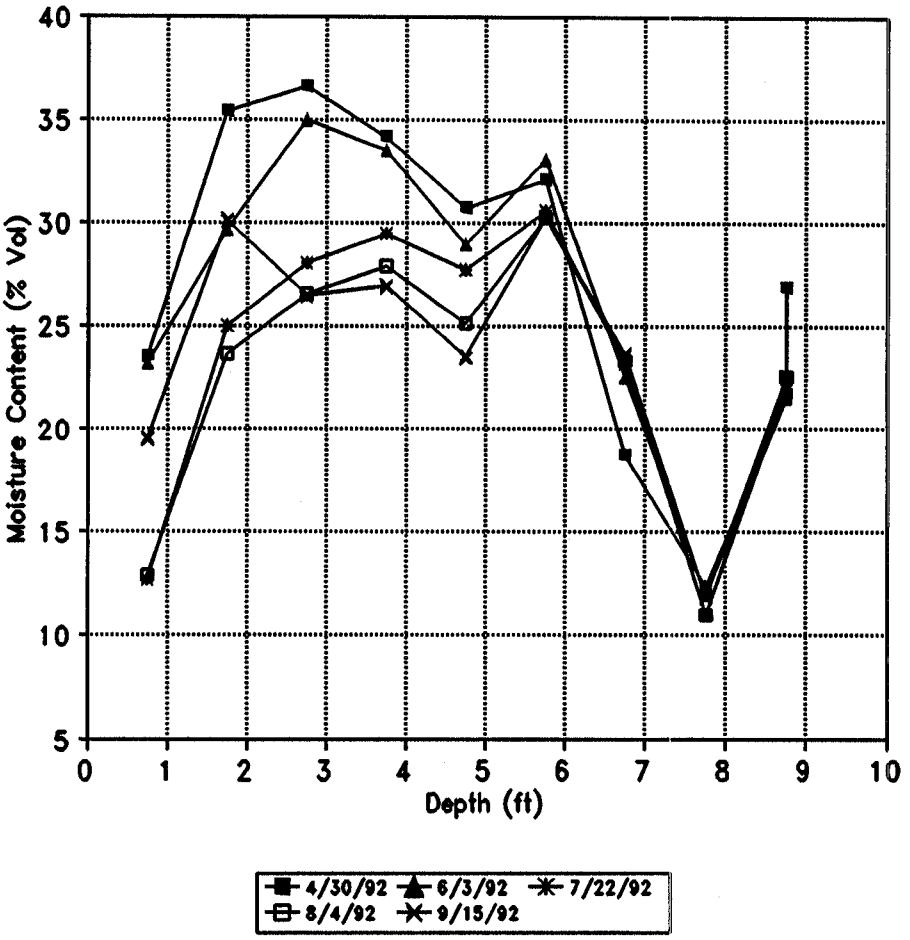

Figure 2.10 Moisture profile summary for hole #2 form March 1992 through September 1992

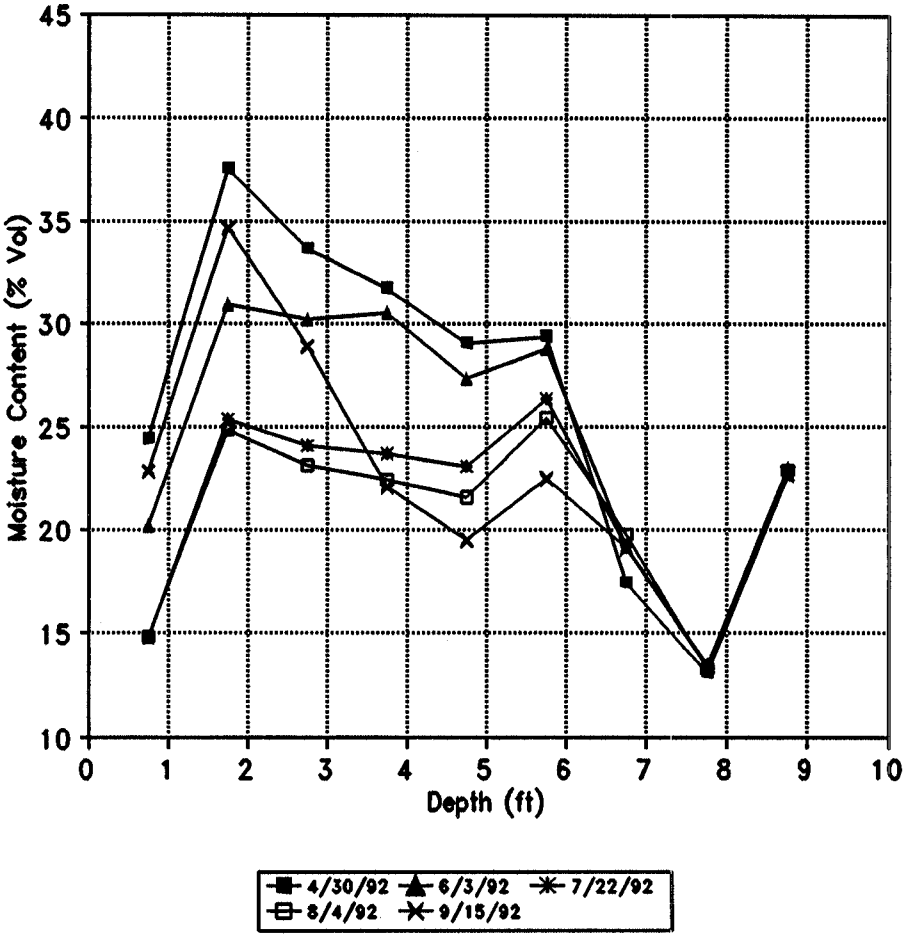

Figure 2.11 Moisture profile summary for hole #4 from March 1992 through September 1992

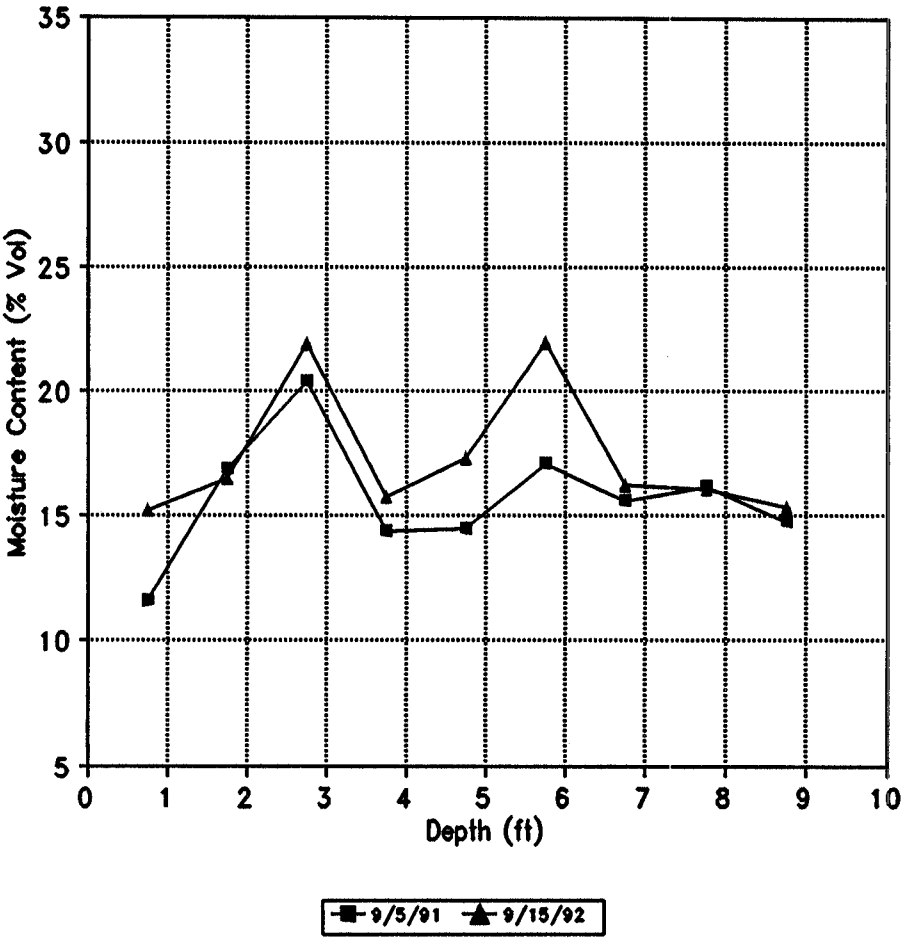

Figure 2.12 Moisture profile comparison for hole #1: September 1991 vs. September 1992

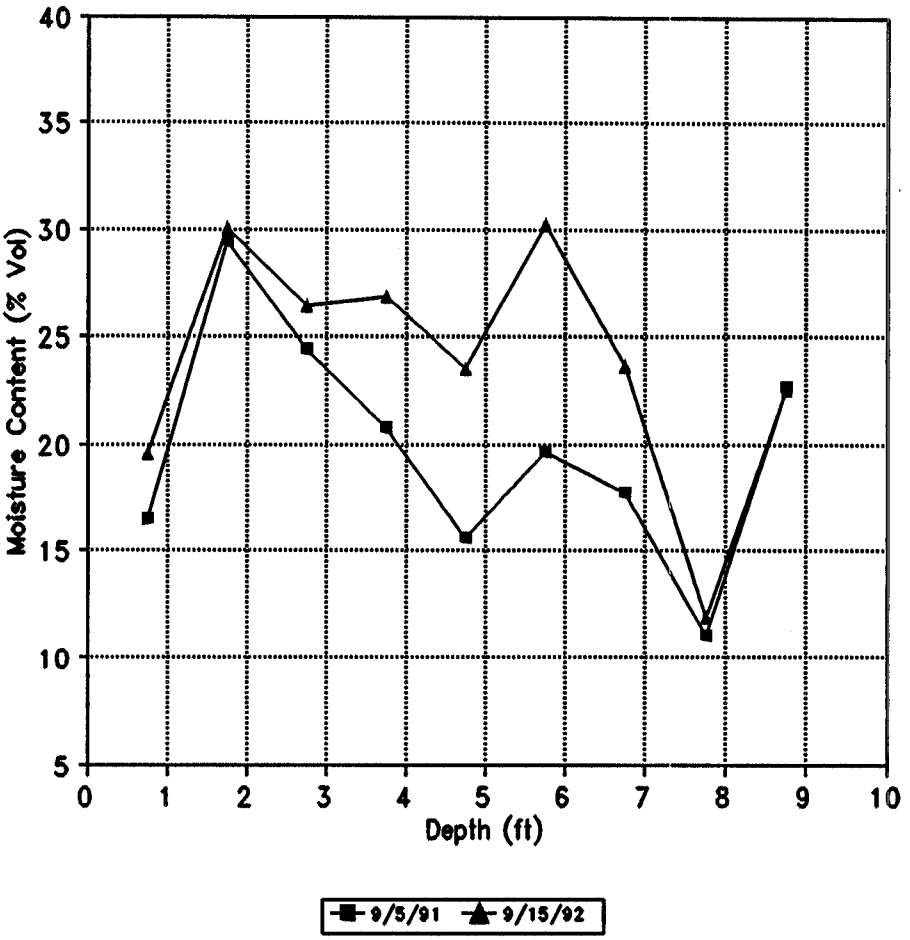

Figure 2.13 Moisture profile comparison for hole #2: September 1991 vs. September 1992

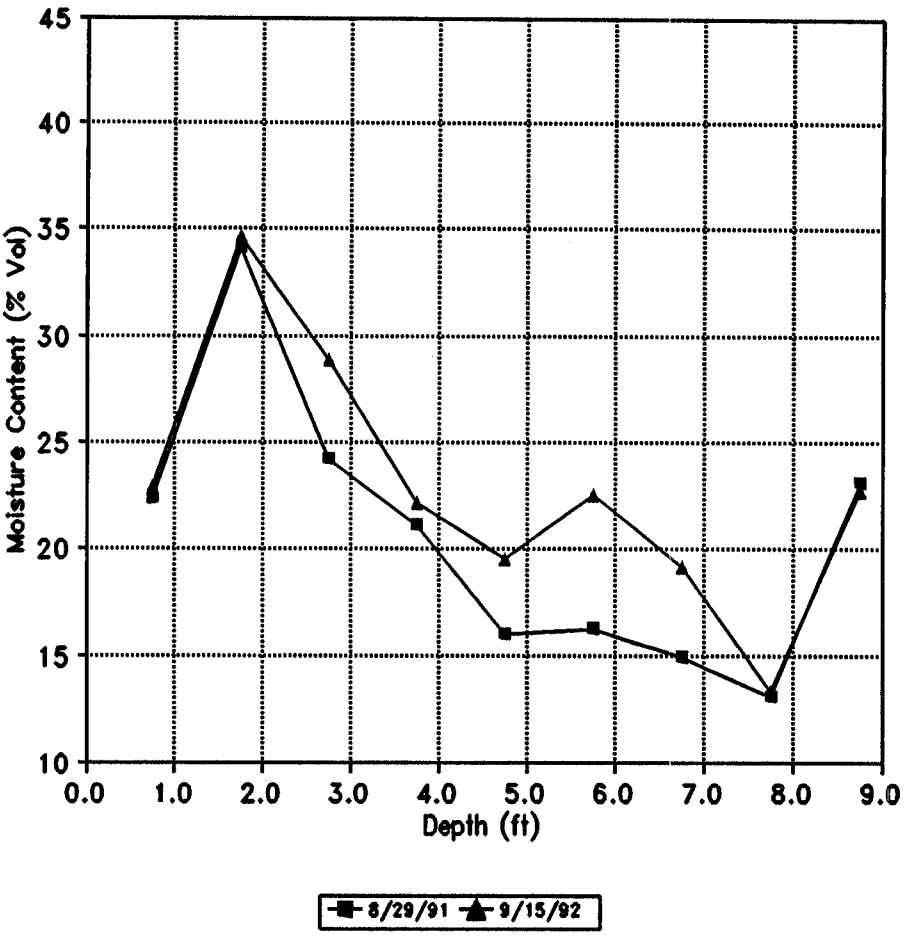

Figure 2.14 Moisture profile comparison for hole #4: September 1991 vs. September 1992

is believed to be due to an unusually wet March. Figures 2.15 and 2.16 provide a comparison of precipitation for the monitored year versus the yearly average for a site in Golden and a site at Rocky Flats approximately 10 miles North of the study area. Because the native grass at the site was dormant during this time and the sun is low in the sky, evapotranspiration demands are low. Therefore, this input of moisture could infiltrate the soil column before it could be used to meet evapotranspiration needs. Figures 2.17 through 2.19 illustrate changes in soil moisture storage for holes 1,2, and 4 throughout the duration of the study. A tabulated summary of moisture content versus depth for all holes throughout the duration of the study is provided in Appendix A.

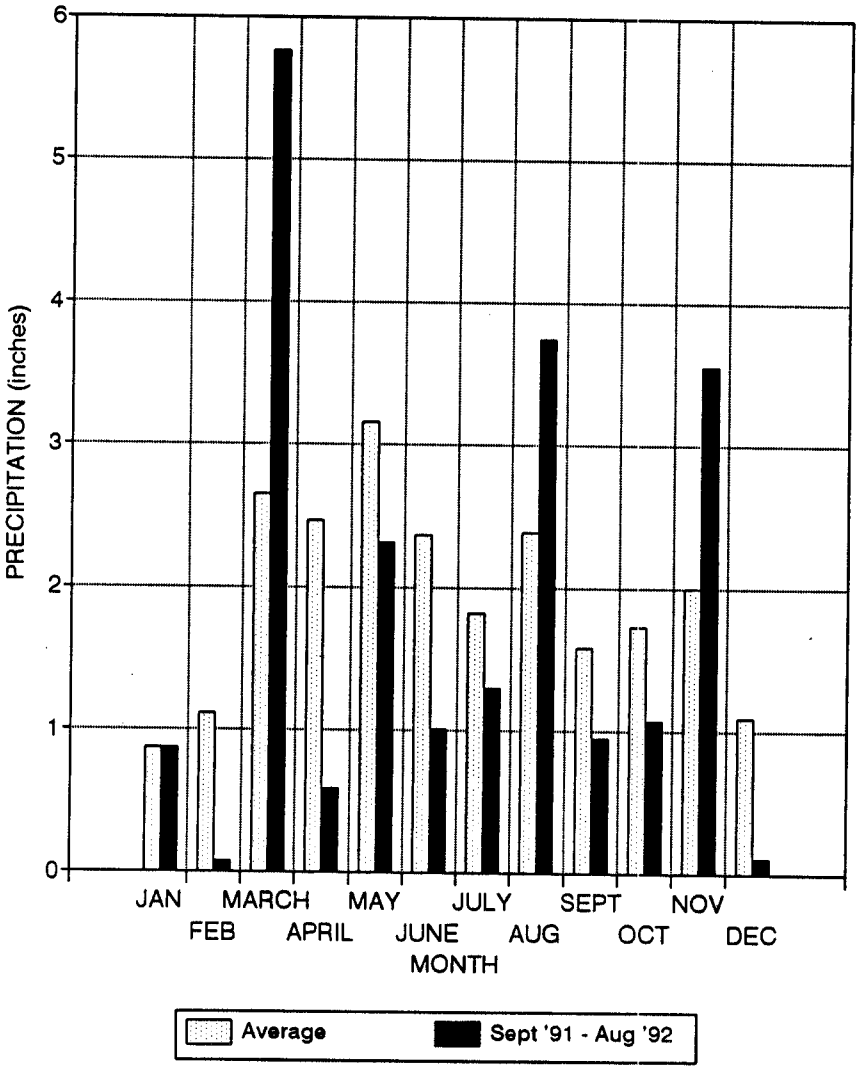

Figure 2.15 Precipitation data from Golden, Colorado

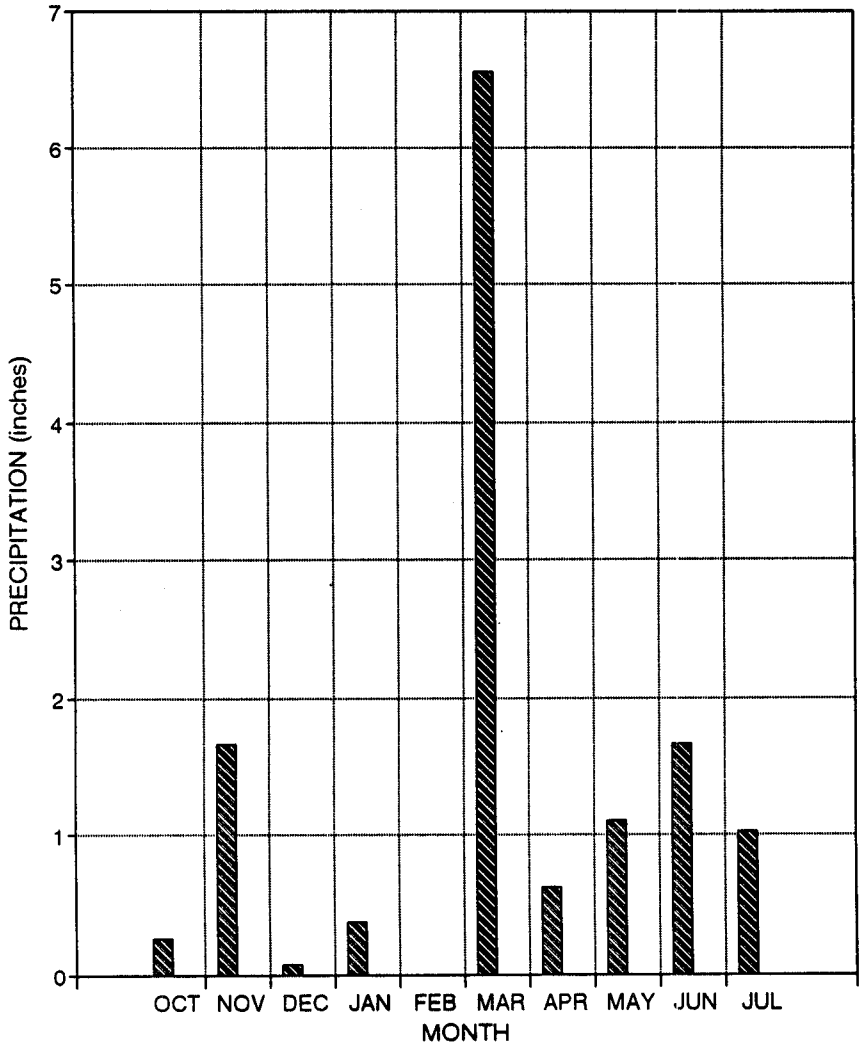

Figure 2.16 Precipitation data from Rocky Flats, Colorado

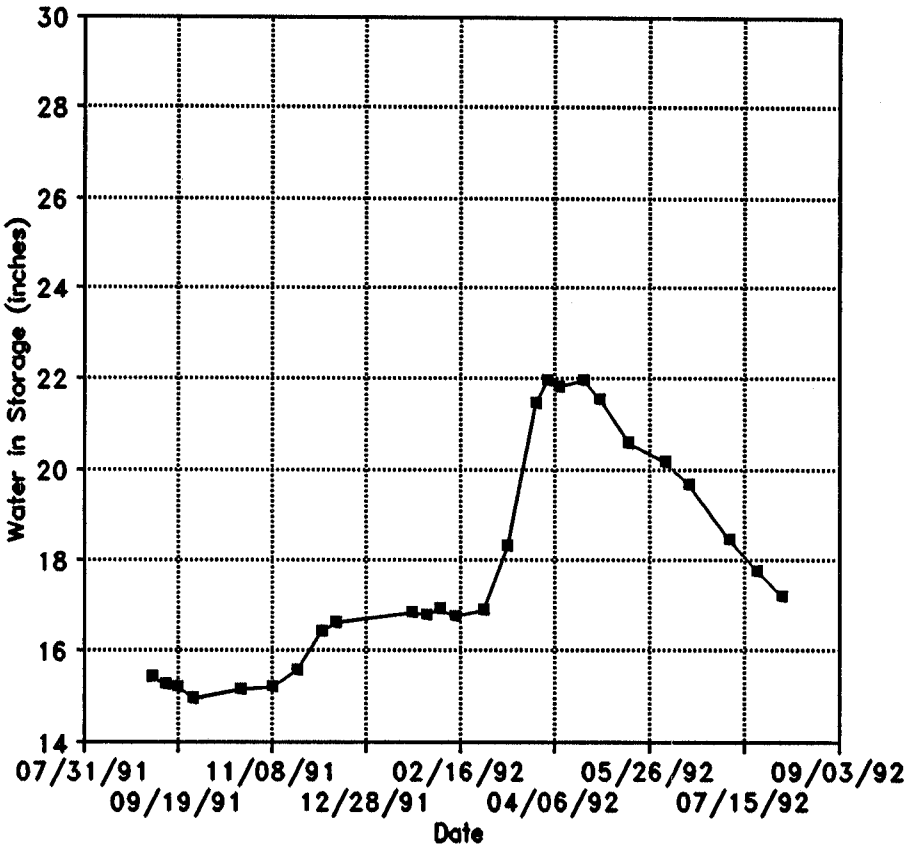

Figure 2.17 Summary of the amount of water in storage for hole 1.

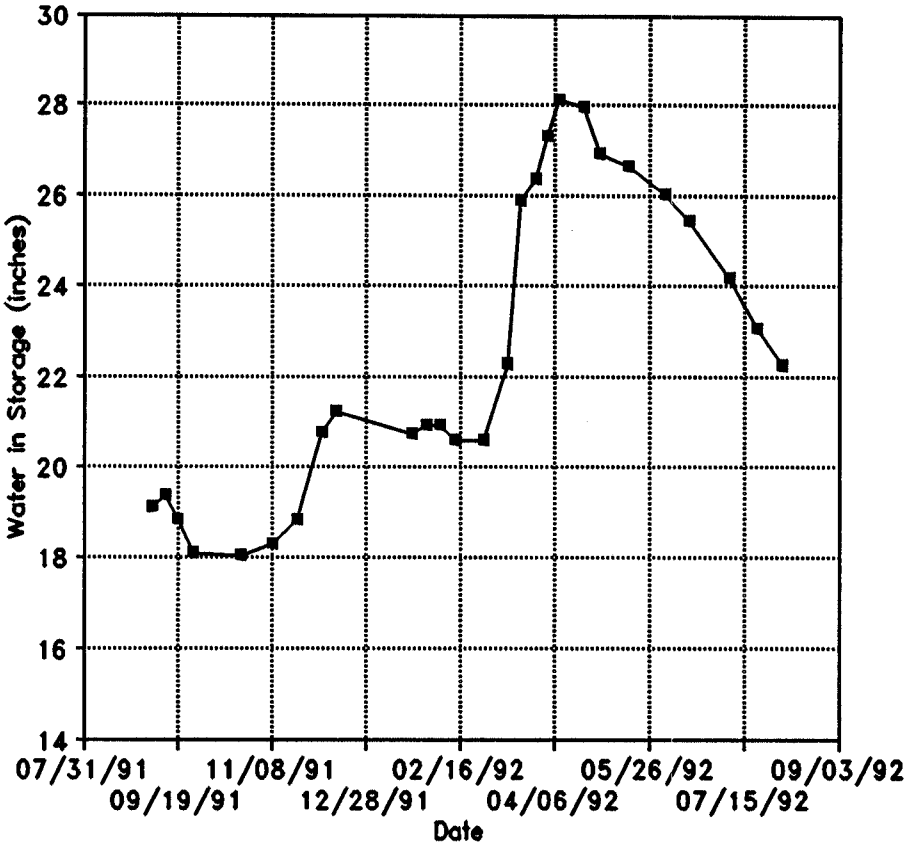

Figure 2.18 Summary of the amount of water in storage for hole 2.

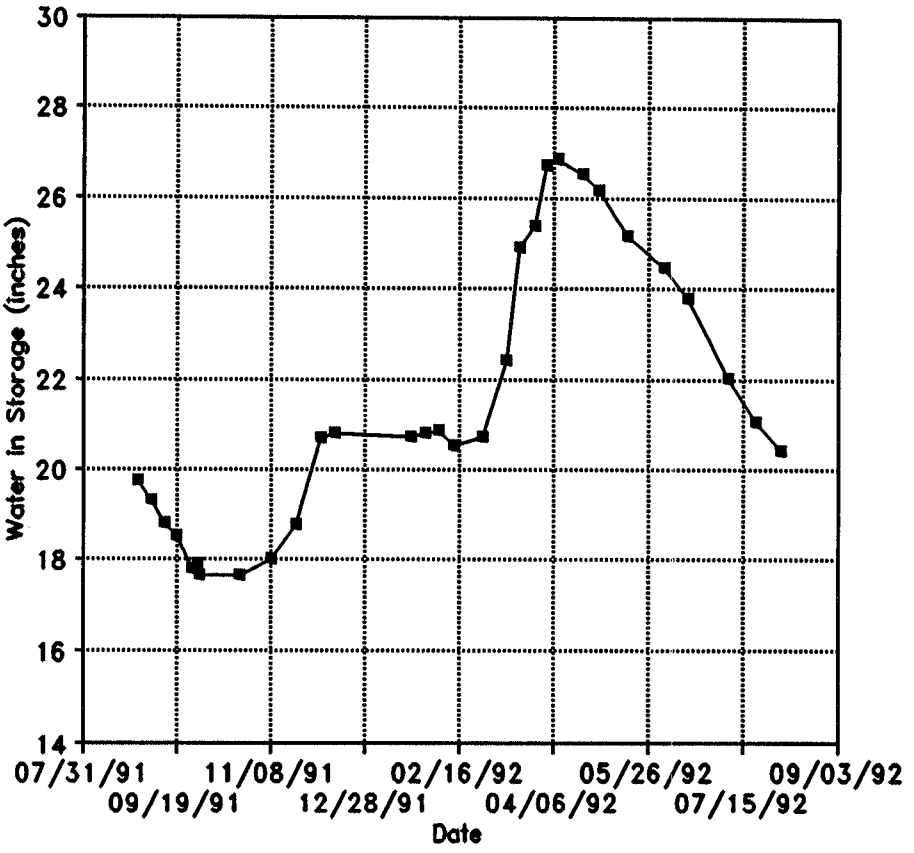

Figure 2.19 Summary of the amount of water in storage for hole 4.

3.0
VADOSE ZONE FLOW THEORY

3.1 Matric Potential

The vadose zone is defined as the area between the land surface and water table where water exists at less than atmospheric pressure (Lohman, 1988). The pressure differential across the liquid-gas interface results in a curved surface known as a meniscus. This pressure difference is defined as matric potential, and the radius of the meniscus is related to the surface tension of the liquid (Freeze and Cherry, 1979). Throughout this text, matric potential will be referred to as a positive quantity. Surface tension (σ) is a proportionality constant, with units of work per unit area, used to relate the amount of work (dW) necessary to increase the surface area of a liquid by an amount dA (eq. 3.1). This relationship

$$dW=\sigma dA \qquad [3.1]$$

can be used to relate matric potential to the radius of curvature of the meniscus (Remson and Randolph, 1962). Figure 3.1 shows a capillary tube inserted in a liquid. If the

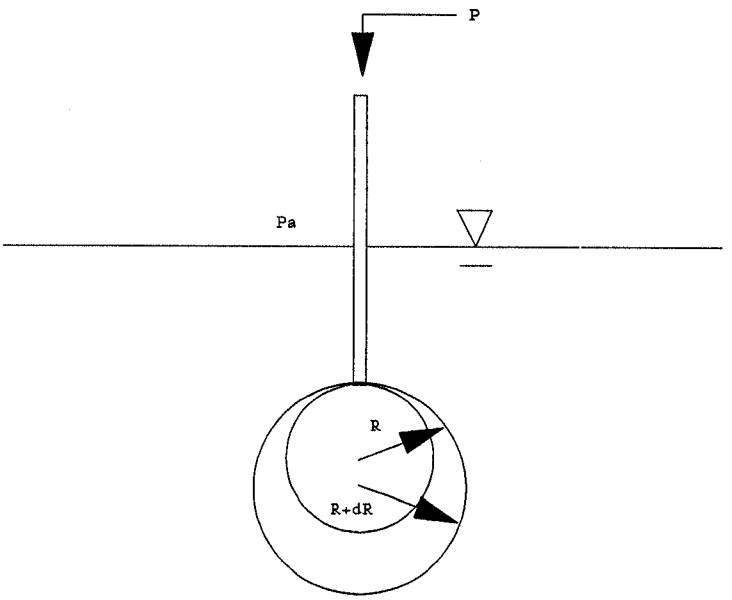

Figure 3.1 Capillary tube inserted in a liquid

effects of gravity are neglected, a spherical bubble will format the end of the capillary tube as the pressure, p, is increased above the atmospheric pressure, p_a. The surface area, A, of the bubble is:

$$A=4\pi R^2 \qquad [3.2]$$

where R is the radius of the bubble. As the radius is increased from R to R + dR, the increase in the surface area of the bubble is:

$$dA=8\pi RdR \qquad [3.3]$$

If this is substituted into eq. 3.1, the work required to increase the surface area of the bubble is:

$$dW=8\pi\sigma RdR \qquad [3.4]$$

This work is accomplished by the pressure differential across the liquid-gas interphase (Hillel, 1980). The net force on the bubble surface is:

$$F=(p-p_a)\,4\pi R^2 \qquad [3.5]$$

The surface of the bubble has been moved a distance dR. Thus, the work performed by the pressure difference is:

$$dW=(p-p_a)\,4\pi R^2 dR \qquad [3.6]$$

Equating and simplifying equations 3.4 and 3.6 yields:

$$(p-p_a)=\frac{2\sigma}{R} \qquad [3.7]$$

which states that the matric potential is inversely proportional to the radius of curvature of the meniscus.

Moisture content and matric potential are functionally related to each other which is known as the water characteristic (Bouwer, 1978). This relationship is commonly expressed graphically as a soil-moisture characteristic curve where matric potential is plotted versus soil moisture content (Figure 3.2). As shown, matric potential increases as the moisture content of the material decreases. However, the shape of the soil-moisture characteristic curve is not unique for each soil. The relationship is different for drainage of water (drying) than it is for imbition (wetting). At equilibrium, matric potential is greater for drainage than imbition at a given moisture content (Figure 3.3). This effect is known as hysteresis.

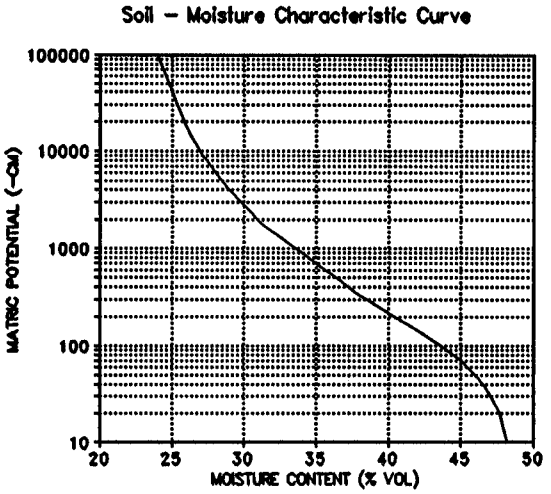

Figure 3.2 Matric Potential versus volumetric soil moisture content

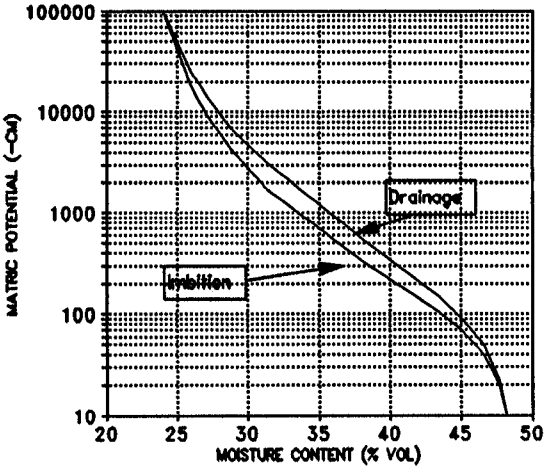

Figure 3.3 Moisture characteristic curve showing effect of hysteresis

3.2 Capillary Rise

A fluid is said to wet a solid if the solid liquid contact angle is less than 90 degrees (Figure 3.4). This occurs if the forces of adhesion between liquid and solid are greater than the forces of cohesion within the liquid and the attraction between the gas and solid (Hillel, 1980). If a capillary tube is inserted in water under these conditions a

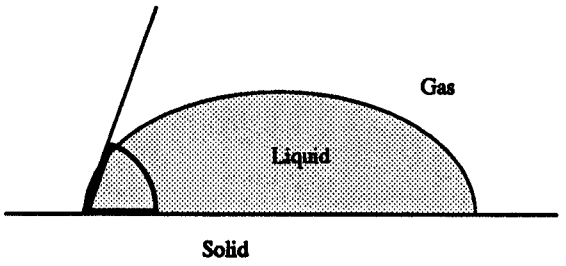

Figure 3.4 Fluid wetting a solid

concave upward meniscus will form. This results in a pressure difference across the water-gas interface and the water will rise in the capillary tube above it's initial position (Figure 3.5).

A relationship between capillary rise and meniscus curvature (or capillary tube radius) can be derived by applying Bernoulli's equation to points A and B of Figure 3.5. Bernoulli's equation is expressed as:

$$\frac{V_a^2}{2g}+\frac{P_a}{\rho g}+z_a=\frac{V_b^2}{2g}+\frac{P_b}{\rho g}+z_b \qquad [3.8]$$

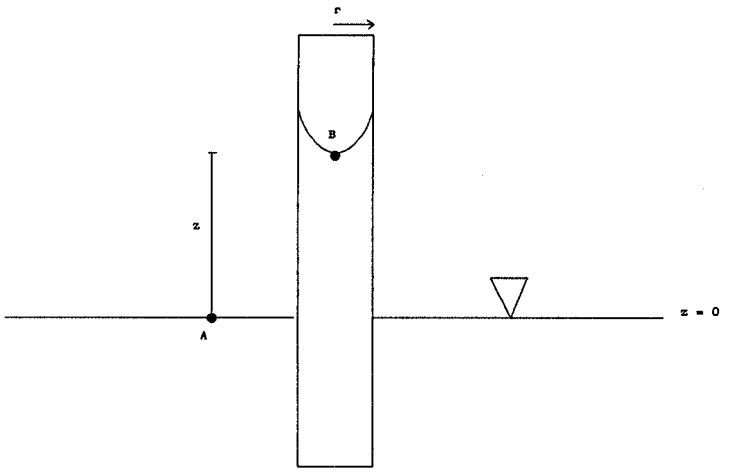

Figure 3.5 Rise of fluid in a capillary tube

where p is pressure, V is velocity, g is gravitational acceleration, ρ is fluid density, z is elevation, and subscripts 1 and 2 indicate any two points on a streamline. Because the water in Figure 3.5 has reached static equilibrium, the velocity terms in equation 3.8 are 0. Applying equation 3.8 to this problem results in

$$\frac{p_a}{\rho g}=\frac{p_b}{\rho g}+z \qquad [3.9]$$

rearranging equation 3.9 yields:

$$(p_a-p_b)=\rho g z \qquad [3.10]$$

equating equations 3.7 and 3.10 and solving for z results in

$$z=\frac{2\sigma}{\rho g R} \qquad [3.11]$$

or in terms of the capillary tube radius:

$$z=\frac{2\sigma\cos\alpha}{\rho g r} \qquad [3.12]$$

where r is the capillary tube radius and α is the wetting angle. The wetting angle is commonly assumed to be 0 degrees. Thus, equation 3.12 reduces to

$$z=\frac{2\sigma}{\rho g r} \qquad [3.13]$$

This states that the capillary rise is inversely proportional to the radius of the capillary tube.

3.3 Hydraulic Conductivity

Hydraulic conductivity of unsaturated porous media is a function of moisture content. As illustrated in Figure 3.6, hydraulic conductivity is at a maximum when the sample is saturated. As the sample desaturates, some pores become air filled. This decreases the effective cross section of the sample that is capable of transmitting fluid. Additionally, the first pores to de-water are the largest, most conductive pores. Therefore, desaturation is often accompanied by a rapid decrease in hydraulic conductivity. The unsaturated

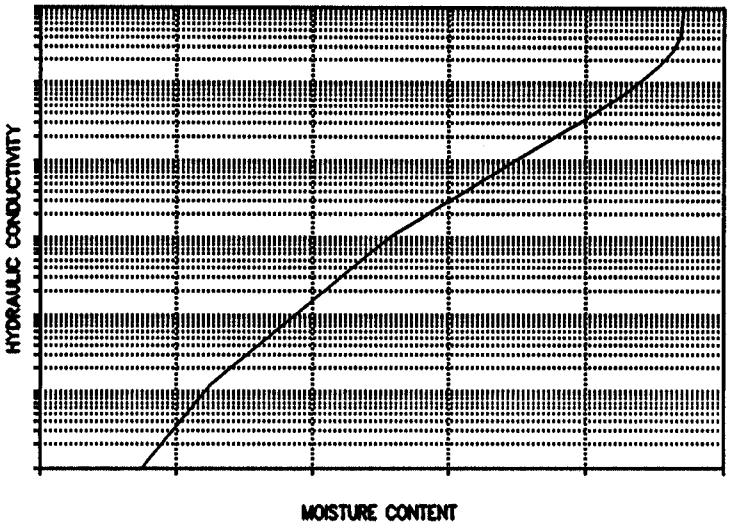

Figure 3.6 Hydraulic conductivity as a function of volumetric moisture content

hydraulic conductivity is commonly expressed as relative hydraulic conductivity which is defined as

$$K_r = \frac{K}{K_{sat}} \qquad [3.14]$$

where K is the unsaturated hydraulic conductivity at a given moisture content and K_{sat} is the saturated hydraulic conductivity.

3.4 Development of Richard's Equation

Total potential in the vadose zone is the sum of matric potential, gravitational potential, thermal potential, adsorption potential, and osmotic potential. In non-shrinking soils, the contribution of the later three to the total potential can be ignored as can thermal gradients (Remson and Randolph, 1962). Therefore, total potential is most commonly defined as

$$h=\psi+z \qquad [3.15]$$

where h is total potential, ψ is matric potential, and z is the gravitational potential.

Darcy's law and the continuity equation was first applied to unsaturated porous media by Richards (1931). Specific flux, q, is defined as

$$q=K\frac{dh}{dl} \qquad [3.16]$$

for saturated flow in porous media. Equation 3.16 can be re-written for unsaturated flow to include the dependence of the total potential and hydraulic conductivity on moisture content:

$$q=K(\theta)\frac{d[\psi(\theta)+z]}{dl} \qquad [3.17]$$

Substitution of equation 3.17 into the continuity equation for vertical flow,

$$\frac{d\theta}{dt}=\frac{dq}{dz} \qquad [3.18]$$

yields Richards' Equation:

$$\frac{d\theta}{dt}=\frac{d}{dz}\left[\frac{K(\theta)\,d\psi(\theta)}{dz}\right]+\frac{dK(\theta)}{dz} \qquad [3.19]$$

3.5 van Genuchten Functions

Determining the unsaturated hydraulic properties of porous materials can be time consuming and very expensive,

especially the hydraulic conductivity versus moisture content relationship. Over the past several decades many closed form analytical expressions have been presented to represent the moisture characteristic curve and the relative hydraulic conductivity-moisture content relationship. One very attractive group of expressions are based on "statistical models" and allow the prediction of relative hydraulic conductivity based on parameters determined in the laboratory or estimated, based on physical soil properties. These models are based on three assumptions (Mualem, 1986):

1. The porous medium can be viewed as a collection of interconnected pores that can be described by a length scale often taken as the pore radius (Mualem and Dagen, 1978).

2. The Hagen-Poiseuille equation can be applied to individual pores to estimate their hydraulic conductivity. The total hydraulic conductivity can be determined by integrating the contribution of all filled pores.

3. Based on the capillary law, the moisture characteristic curve can be considered analogous to the pore radii distribution function.

The expression chosen for this study is the van Genuchten function (van Genuchten, 1980) based on the theory of Mualem (1976). This equation allows the estimation of the hydraulic conductivity-moisture content relationship with knowledge of

the moisture characteristic curve. Moisture content as a function of matric potential is defined as

$$\theta=\theta_r+\frac{\theta_s-\theta_r}{[1+(\alpha h)^n]^m} \qquad [3.20]$$

where h is matric potential (expressed as equivalent water column height and assumed to be positive), θ is volumetric moisture content, θ_s is saturated moisture content, θ_r is residual moisture content (discussed later), and α, n and m are fitted parameters. Relative hydraulic conductivity as a function of matric potential is defined as

$$K_r(h)=\frac{[1-(\alpha h)^{n-1}[1+(\alpha h)^n]^{-m}]^2}{[1+(\alpha h)^n]^{m/2}} \qquad [3.21]$$

where m is:

$$m=1-\frac{1}{n} \qquad [3.22]$$

Alternatively, relative hydraulic conductivity can be expressed in terms of effective (or dimensionless) moisture content;

$$K_r(\theta) = \theta_e^{1/2}\left[1-(1-\theta_e^{1/m})^{m}\right]^2 \qquad [3.23]$$

where effective moisture, θ_e, content is defined as

$$\theta_e = \frac{\theta-\theta_r}{\theta_s-\theta_r} \qquad [3.24]$$

This equation is currently the most popular and produces relatively accurate results (Durner, 1989). The derivation of this expression and the theory of Mualem will not be discussed here. For further information the reader should refer to Mualem (1976, 1978, and 1986) and van Genuchten (1980, and 1986).

The computer code SOHYP (van Genuchten, 1986) was used to determine the parameters α and n for this work. This code uses a non-linear least squares regression to estimate these parameters. The code is discussed in more detail later.

4.0

VADOSE ZONE MONITORING EQUIPMENT

4.1 Neutron Probe

4.1.1 Theory

A neutron moisture probe utilizes the principal of neutron moderation, or slowing, to determine water content in soils. Neutron probes contain a radioactive source, commonly Americium/Beryllium, which emits high energy neutrons and a detector that senses slow (thermal) neutrons. Through collisions with atoms in the soil, the high energy neutrons are thermalized (slowed).

The volume of soil sampled by the neutron probe, sometimes known as the zone of thermalization, has been reported as a sphere with a radius of 5.9 to 7.1 inches (Shirazi and Isobe, 1976), 2.95 inches in wet soils and 9.8 inches in dry soils (Van Bavel, 1956), to approximately 6 inches (CPN Corp., Personal Communication). It requires an average of 17 collisions with a hydrogen atom for a neutron to become thermalized, compared to an average of 136 collisions with an oxygen atom (Stone, 1990). 70% of slowing is due to collisions with hydrogen atoms, 10% with oxygen, and 20% with other atoms (Dickey, 1990a). Because the primary source of hydrogen atoms in soil is water, a relationship can be derived

between water content and thermalized neutrons. This relationship is usually linear for moisture contents commonly encountered in soils.

4.1.2 Description

The neutron probe used in this study is a 503 DR Hydroprobe manufactured by CPN Corporation. It contains a 50 mCi Americium-241/Beryllium source (CPN Corp., 1984).

4.1.3 Standard Count

"The standard count is the most important test to determine if the probe's electronics and other components are functioning properly" (Dickey, 1990a). It is a series of neutron counts taken under a standard set of conditions: the average of these counts is the standard count. These readings are checked for a normality using a chi-squared test. A standard count is also compared to the previous standard count to determine if the probe is functioning correctly. The difference between the two standard counts should fall within 0.707 times the square root of their average 95% of the time (CPN Corporation, 1984).

The 503 DR takes 32 counts (each is 8 seconds long) and displays the chi-squared ratio of the counts to check for normality. This value should fall between 0.75 and 1.25 for

31 degrees of freedom and a 95% probability range (CPN Corp., 1984). However, even if the probe is functioning correctly, the chi-squared ratio will fall outside this range approximately 5% of the time. CPN recommends that the standard count is taken in the paraffin shield by placing the neutron probe on the carrying case. Because the shield is not 100% effective, the standard count is subject to surrounding conditions such as surface moisture and nearby objects. Therefore, this method requires standard counts be taken under identical conditions. Dickey (1990a) recommends that standard counts be taken 1 to 2 meters above the ground in access tube material identical to that used in the field. Because this method was not practical for this study and is believed to expose the worker to un-needed amounts of radiation, the previous method was used. Standard counts were not taken after precipitation events when excess surface moisture was present.

4.1.4 Factors Affecting Calibration

Not all hydrogen encountered in soils is in the form of water molecules. Natural soils contain different amounts of hydrogen in clay and other mineral structures. Thermal neutrons are also subject to capture by iron, potassium, chlorine, boron and other atoms. Therefore, the relationship

between moisture content and neutron thermalization must be determined separately for different soils.

Variations in soil bulk density may have different effects on neutron probe calibration. Increasing the bulk density of a soil may have two results. It can increase the concentration of capture elements. This will decrease the number of thermalized neutrons reaching the detector for a given moisture content (Olgaard and Haar, 1968). It may also increase the concentration of chemically bound hydrogen (Holmes, 1966) which will increase neutron thermalization. However, for most field situations, there is little effect on calibration resulting from bulk density variations (Stone, 1990). The effects of bulk density were not taken into consideration in this study when calibrating the neutron probe.

Access tube material, thickness, and size also influence neutron probe calibration (Allen and Segura, 1990). Access tubes constructed of materials such as PVC contain neutron capture elements (PVC contains chlorine). The presence of capture elements decreases the number of thermalized neutrons returning to the detector. This increases the slope of the calibration curve if moisture content is plotted on the Y axis and neutron count on the X axis (Dickey, 1990a). Access tubes made of steel or aluminum are fairly transparent to both fast

and slow neutrons. Allen and Segura (1990) reported higher coefficients of determination (R^2) and lower standard errors of estimate for calibrations in aluminum access tubes when compared to PVC. Keller, Everett, and Marks (1990) found a 2½-inch stainless steel access tube reduced neutron counts 13% with respect to readings without access tubes. A 2-inch schedule 40 PVC pipe resulted in a 29% reduction in neutron count. However, the masking effects of PVC do not render them useless for access tube material. The lower cost of PVC can make it an attractive alternative especially when the soil or soil moisture contains constituents that deteriorate aluminum or stainless steel.

Large diameter access tubes and air gaps between the tube and borehole produce similar effects on neutron probe calibrations. By moving the zone of thermalization farther from the detector, the number of thermalized neutrons returning to the detector is reduced (Allen and Segura, 1990). This increases the slope of the calibration curve and the sensitivity of moisture content on neutron count and results in larger errors in moisture content from smaller corresponding errors in neutron counts. Allen and Segura (1990) report a 5% increase in the calibration slope for a 10 mm air gap between schedule 40 PVC and the soil, and a

corresponding 1% increase for aluminum. Therefore, air gaps should be avoided especially when using PVC access tubes.

4.1.5 Improving Calibration Accuracy

The two primary sources of error from estimating soil moisture content with neutron probes are from the probe itself and the calibration. The calibration component is the largest individual source of error (Haverkamp *et al.*, 1984).

Calibration accuracy can be improved by plotting the data and eliminating outlying points before applying regression techniques (Dickey, 1990a). Neutron probes sample a spherical volume of soil but are calibrated to smaller physical samples. Outliers may be due to physical samples not corresponding to the moisture content of the volume sampled by the neutron probe. Dickey (1990a) reported significant improvements in correlation coefficients when using average moisture contents from an interval as opposed to moisture contents of discrete samples taken from the same depth as the neutron reading.

Because radioactive decay is a random process, there is some degree of uncertainty associated with count rates registered by neutron probes. This uncertainty can be reduced with longer count times or multiple readings at each point (Haverkamp *et al.*, 1984). The distribution of repeated neutron counts taken at a point may be approximated by a

normal distribution for a large population (CPN Corp., 1984). Therefore, normal statistical methods may be used to quantify the uncertainty associated with moisture readings. The use of count ratios instead of counts produces negligible errors (Haverkamp *et al*, 1984) especially if they fall within a narrow range.

4.1.6 Access Tube Installation and Calibration Procedure

The neutron probe was calibrated using a method similar to the Soil Conservation Service method outlined by Dickey (1990b) which is as follows:

1) Access tube diameter and air gaps were minimized by selecting access tubes with a slightly larger diameter than the smallest hand auger available. Three inch access tubes with outside diameters of 3.5 inches were used in conjunction with a 3¼-inch hand auger. The drill stem was marked at 1-foot intervals starting at 6 inches for soil sampling. One foot intervals were chosen to maximize the number of soil samples while minimizing soil compaction resulting from sample extraction using the slide hammer.

2) Two inch diameter, 6-inch long samples were taken at the designated intervals using a soil sampler and 8-pound slide

hammer to drive the sampling tube into the soil. Samples were immediately capped after removal and temporarily stored in a shaded area to prevent moisture loss. After the day's field activities, samples were stored in a humidity room on their side to reduce vertical redistribution of moisture due to gravity.

3) Each hole was drilled and sampled to a depth 2 inches less than the fully assembled access tube. The access tube was inserted into the hole and driven to the total depth using a sledge hammer and a 4 X 4 placed over the top of the access tube to prevent damage to the tube. Any depressions or void spaces surrounding the top of the access tube were filled with compacted soil to prevent channeling or ponding of water in the depressions.

4) The neutron probe cable was fitted with cable stops that would place the neutron source and detector in the center of each sample interval. The operating manual provides information on the location of the neutron source and detector with respect to the bottom of the probe. A standard count was taken according to CPN Corporation specifications and checked for accuracy using the previously mentioned tests.

5) The neutron probe was placed on the access tube and the probe lowed into the tube to the sampling intervals. Three, 64 second counts were taken at each interval and the average was used for calibration. The deepest measurement was taken at 8.75 ft to minimize influence of the PVC drive point on the reading.

6) Moisture content was determined as follows:

- Approximately ½-inch was removed from the ends of each sample using a horizontal extruder to extract the sample from the tube. The ends of the samples may have been compacted by using the slide hammer and would not represent natural soil conditions.
- One centimeter long samples were extruded from each end of the liner to determine moisture variation and the degree of heterogeneity for each 6-inch sample. Samples were trimmed flush with the liner using a flat edged knife and immediately placed in a soil moisture tin and weighed to the nearest 0.01 gram. Samples were oven dried at 100 degrees celsius for 24 hours and re-weighed to determine dry weight.
- Volumetric moisture content, dry bulk density and porosity were determined for each sample. Volumetric moisture content, θ, was determined by:

$$\theta = \frac{\Delta V_{water}(cm^3) * 100}{V_{sample}(cm^3)} \qquad [4.1]$$

where V_{water} and V_{sample} refer to the volume of water lost from oven drying and sample volume respectively. Dry bulk density was determined by:

$$BD_{dry} = \frac{W_{dry}(g)}{V_{sample}(cm^3)} \qquad [4.2]$$

where W_{dry} is the dry weight of the sample. Porosity was determined by assuming a particle specific gravity of 2.67 and using the formula:

$$POR = \frac{V_{sample}(cm^3) - \frac{W_{sample}(g)}{2.67}}{V_{sample}(cm^3)} \qquad [4.3]$$

where W_{sample} is the dry sample weight. Samples were then labeled and stored in a desiccator for further testing.

7) Average moisture content for each interval was plotted versus count ratio for each hole. After outliers were

eliminated, a least squares linear regression was used to determine the y intercept, slope, and the coefficient of determination (R^2).

4.1.7 Results

Moisture content, dry bulk density, porosity values and corresponding count ratios for all samples used in calibration are presented in Appendix B. It should be noted that porosity values determined in zones of high carbonate content will have higher errors due to the lower specific gravity of the carbonate. The resulting calibration curves for all holes are presented in Figures 4.1 through 4.6. Table 4.1 provides a summary of the calibrations for each hole.

Table 4.1 Neutron probe calibrations

Hole #	Material	Calibration Equation	R^2
1	SCH 80 AL	MOIST(%) = RAT * 28.82 - 5.56	.78
2	SCH 80 PVC	MOIST(%) = RAT * 106.24 - 28.35	.98
3	SCH 40 PVC	MOIST(%) = RAT * 54.08 - 7.39	.91
4	SCH 80 AL	MOIST(%) = RAT * 34.28 - 9.06	.92
5	SCH 80 AL	MOIST(%) = RAT * 26.65 - 5.29	.96
6	SCH 80 AL	MOIST(%) = RAT * 28.21 - 5.37	.94

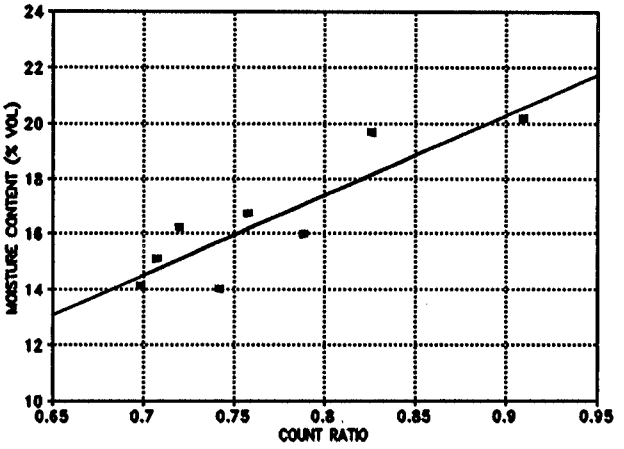

Figure 4.1 Neutron probe calibration for hole 1.

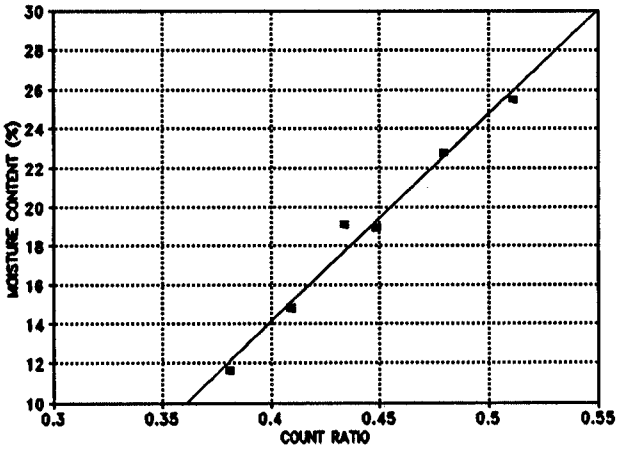

Figure 4.2 Neutron probe calibration for hole 2.

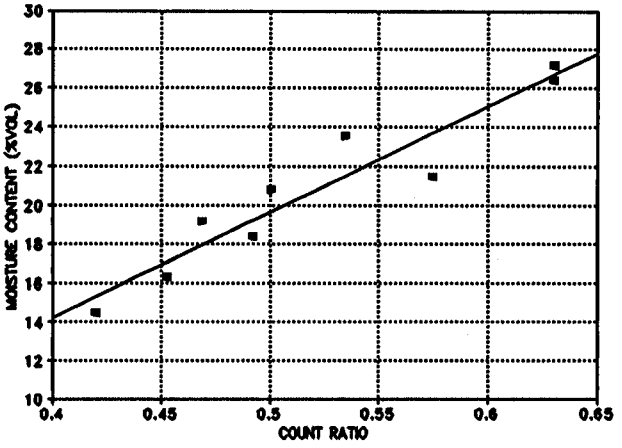

Figure 4.3 Neutron probe calibration for hole 3.

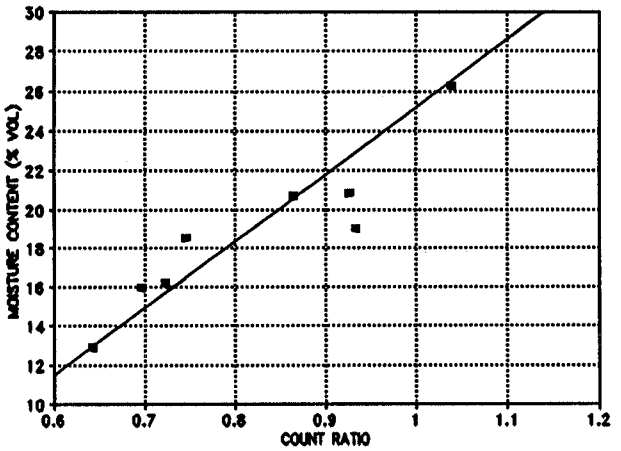

Figure 4.4 Neutron probe calibration for hole 4.

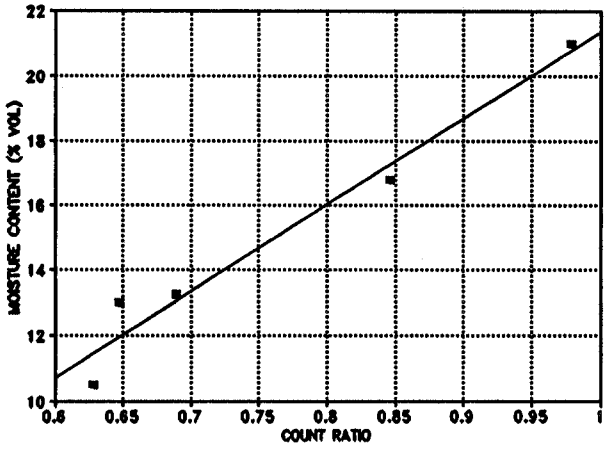

Figure 4.5 Neutron probe calibration for hole 5.

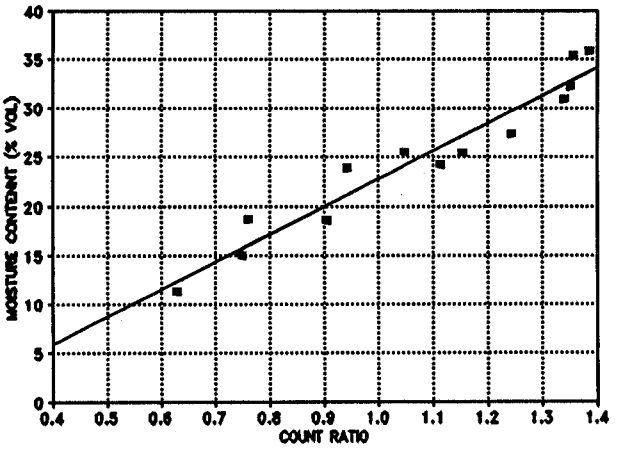

Figure 4.6 Neutron probe calibration for hole 6.

4.1.8 Hole 6 Installation

Hole 6 was installed on March 19th, 1992. This additional access tube was installed for three reasons: (1) to check the accuracy of the three adjacent access tube calibrations by comparing the moisture profiles, (2) to compare the moisture profile predicted by the neutron probe to the moisture profile obtained by laboratory analysis for moisture content, and (3) to provide additional samples for hydraulic property determination.

The same procedure was followed for the installation of neutron access tube 6 as the other holes. However, in addition to 6-inch samples taken every foot (starting at 6 inches), 2-inch samples were taken at 1-foot intervals from 1.33 feet to 5.33 feet. These additional samples allowed a more accurate representation of the wetting front geometry. Neutron counts were also taken at these locations to provide additional calibration points.

Care was taken to keep track of the orientation of the 6-inch soil samples. A 1 to 2-centimeter sample was taken at each end of the 6-inch samples and tested for moisture content. Moisture content was determined for the entire 2-inch samples.

4.1.9 Calculating the Amount of Water in Storage

An accurate prediction of the amount of water in storage is necessary to obtain reliable results when calculating recharge or evapotranspiration using water budget methods. The moisture profile determined by the laboratory method described in section 4.1.6 is compared to that predicted by the neutron probe in Figure 4.7. As expected, the moisture value predicted neutron probe is an average over the sphere of influence. This averaging is expected and is acceptable if the total amount of water in storage predicted by the neutron probe is in close agreement with that predicted by laboratory analysis. Simpson's rule was used to integrate the moisture profile estimated by the neutron probe. This method is most accurate for determining the amount of water in storage (Haverkamp *et al.*, 1984). It approximates the area under a curve as a series of parabolic arcs and is expressed as:

$$\int_a^b \theta d\theta = \left(\frac{b-a}{3n}\right)(\theta_0+4\theta_1+2\theta_2+4\theta_3+2\theta_4 \ldots 4\theta_{n-1}+\theta_n) \qquad [4.4]$$

where n is an even number of equally spaced intervals between

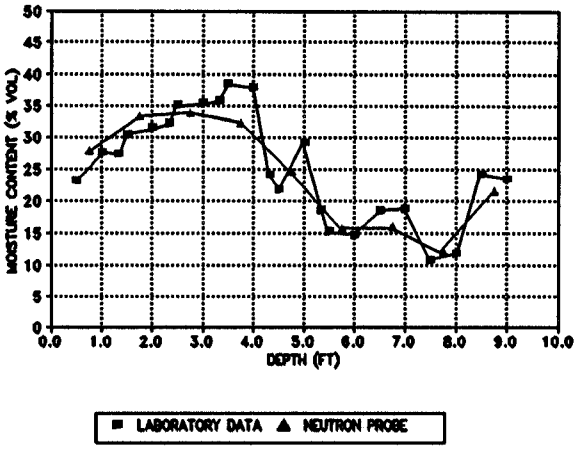

Figure 4.7 Hole 6 moisture profile determined in the laboratory versus moisture profile predicted by the neutron probe

a and b. This result is then converted to inches of water in storage, S_{inches}, by substituting it into equation 4.5;

$$S_{inches} = \int_a^b \theta d\theta * \frac{12}{100} \qquad [4.5]$$

Because Simpson's rule requires an even number of equally spaced intervals, it could not be applied to every neutron probe moisture reading from hole 6 used to calibrate the neutron probe. Instead, it was applied to 1-foot intervals

starting at 0.75 feet. This is the same reading interval used for monitoring.

For the same reasons stated above, it is not possible to apply Simpson's rule to the moisture profile determined in the laboratory. The data were integrated by dividing the area between each point into trapezoids. This method differs from Simpson's rule in that the data points are connected through a series of straight lines as opposed to parabolic arcs. Because the spacing of the laboratory data is smaller, it is believed that the resulting difference is minimal.

Laboratory data were available from 0.5 feet through 9.0 feet while hole 6 was only logged with the neutron probe from 0.75 feet through 8.75 feet. Linear interpolation between 0.5 to 1.0 feet, and 8.5 to 9.0 feet was used to allow comparison with neutron probe measurements. This resulted in 5.46% less water in storage predicted by the neutron probe. Integrating the laboratory data yielded 23.77 inches of water in storage compared to 22.47 inches from the neutron probe readings. This discrepancy is in part due to the method used to calibrate the neutron probe. Several anomalously high moisture values were outliers that were not used in calibration. These discarded points were not believed to be representative of the average moisture content in the neutron probe sphere of influence. Additionally, the moisture content

at 3.5 feet and 5.0 feet could not be used to predict *in situ* matric potentials as they yielded erroneous results (discussed in section 5).

4.1.10 Variance of Neutron Probe Readings at a Single Point

As mentioned in section 4.1.5, radioactive decay is a random process and a series of readings taken at a single point can be approximated by a normal distribution. Therefore it is necessary to quantify the degree of uncertainty associated with neutron probe moisture readings, or more importantly, be able to distinguish between a change in moisture content in the soil and random decay.

To accomplish this, 35 neutron probe readings were taken at a single point in hole 2 (sch 80 PVC), hole 3 (sch 40 PVC), and hole 4 (sch 80 aluminum). The variance and standard deviation of each population of neutron probe count ratios and corresponding moisture contents were calculated for each of the 3 holes. The log of the absolute value of the difference between sequential neutron probe readings were plotted on probability paper using a statistics program and a straight line was fit to the data (the data were found to have a log normal distribution). This line was used to determine the 95% probability value. The absolute value of the difference

between any two neutron probe readings from the same population have a 95% probability of being less than this value. There is only a 5% probability that the absolute value of the difference between any two neutron probe readings will be larger than this value if they were taken in soil that has the same moisture content. If the difference is larger, it is unlikely that the readings represent the same moisture content.

The 95% probability value was converted to moisture content and is presented in Table 4.2 with the variance of each population of neutron probe readings.

Table 4.2 95 % probability value, and variance of moisture content for neutron probe readings at a single point

Hole	Casing Material	95 % Probability Interval (count ratio)	95 % Probability Interval (moisture content)	Variance (moisture content)
2	SCH 80 PVC	± 0.0151	± 1.608%	0.2530%
3	SCH 40 PVC	± 0.0138	± 0.747%	0.0757%
4	SCH 80 Aluminum	± 0.0214	± 0.733%	0.0626%

It should be noted that moisture content is much more sensitive to neutron probe readings in sch 80 PVC than sch 40

PVC or sch 80 aluminum. Although the probability interval for count ratios in sch 40 PVC and sch 80 PVC are approximately the same, the probability interval is much larger for the moisture content in sch 80 PVC. This is due to the steeper slope of the calibration curve. Comparing the variance of these readings with a series of readings at a point throughout a time interval should indicate whether changes in moisture content constitute a trend or are expected fluctuations due to random decay.

4.2 Draining Lysimeter

4.2.1 Purpose

Weighing lysimeters provide a means of directly measuring vertical flux below the root zone and changes in soil-moisture storage within the root zone. Vertical flux is determined by measuring the amount of water that drains from the lysimeter over a period. Changes in storage can be determined by total weight changes through time. Problems related to draining lysimeters are soil and vegetation disturbance and alteration of the bottom boundary condition (Gee *et al.*, 1988). Both soil properties and vegetation directly affect vertical flux rates. Disturbing the soil structure can change hydraulic properties and damaging or destroying the vegetation can drastically alter evapotranspiration rates. Each of these

will affect vertical flux rates. For the lysimeter to drain, the bottom surface must be saturated. If this condition is not naturally present in the field, the moisture content at the bottom of the lysimeter must increase until it is saturated before it can drain. This artificial increase in moisture content (and corresponding decrease in matric potential) may influence moisture content and matric potentials throughout the lysimeter. Under these conditions, drainage from the lysimeter is not representative of natural conditions. An increase in moisture content in the root zone will increase growth and evapotranspiration rates of the native vegetation. This again is a deviation from natural conditions.

4.2.2 Description

The draining lysimeter used in this study consists of a 6-inch and 18-inch long segment of 12-inch diameter schedule 40 threaded flush joint PVC (Figure 4.8). The 18" segment contains undisturbed soil and vegetation. The 8-inch segment contains #8-12 Colorado Silica Sand. The purpose of the silica sand was to provide a good contact with the bottom of the soil, thus removing the need for the soil to saturate before it could drain. A section of landscape fabric was

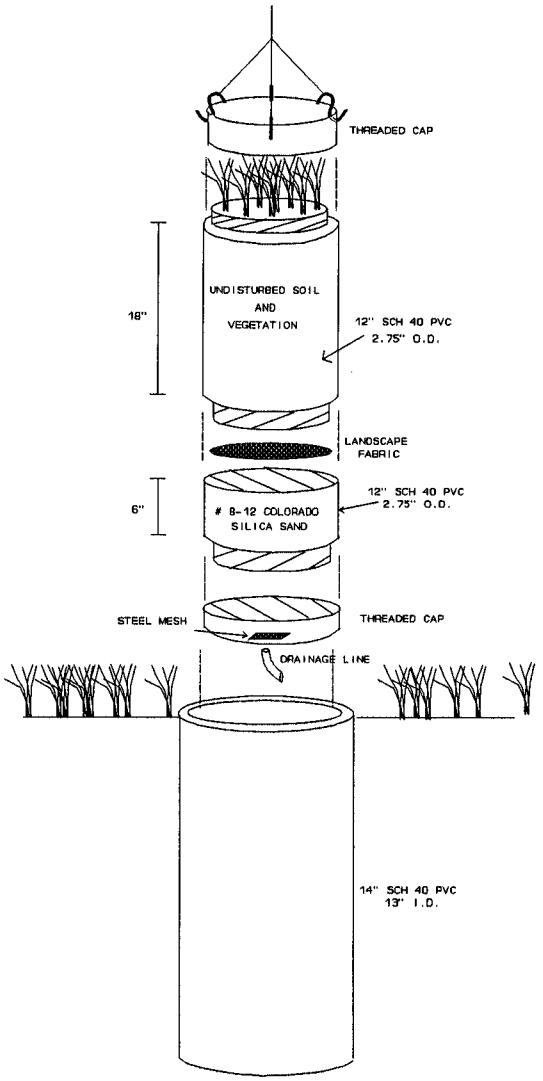

Figure 4.8 Draining Lysimeter Design

placed between the silica sand and soil. This material allows water to pass while preventing plant roots from extending below the soil. The assembled 12-inch diameter PVC sections were placed inside a section of 14-inch diameter schedule 40 PVC of equal length. This allowed easy removal of the lysimeter for weighing and provided stability to the excavation.

4.2.3 Installation

A pit was dug in the center of the study site just large enough to contain the 14-inch section of PVC. Care was taken to minimize disturbance to the site. After the PVC was placed in the excavation so the top was flush with the ground surface, the surrounding void space was filled and compacted.

An area outside the study site was selected that contained representative vegetation. A circular pit with an inside diameter larger than 12-inch was excavated to a depth of 2 feet. The 12-inch diameter PVC was placed vertically on the undisturbed soil column in the center of the pit. The soil column was carefully shaved to the outside diameter of the PVC in 4-inch increments with a shovel (Figure 4.8). By striking a 4X4 placed over the top of the PVC with a sledge hammer, the PVC was forced over the 4-inch section of the soil column. This procedure was followed until the entire 18-inch

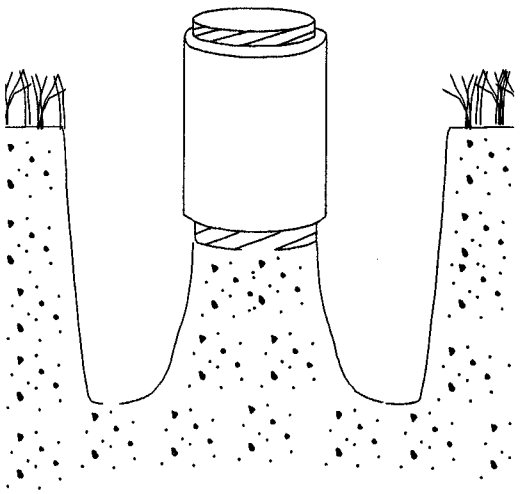

Figure 4.9 Lysimeter Installation

length of PVC was full and the ground surface was flush with the top of the PVC. This method was used for two reasons: (1) it reduced disturbance to the soil column and vegetation and, (2) it eliminated void space between the soil column which prevents water channelling around the soil. At this point, the soil column was sheared at the base by quickly twisting the PVC and removed from the pit.

The PVC containing the soil column was positioned upside down on the ground. The shorter PVC section was screwed on, filled with silica sand, and the PVC cap containing the drain was attached.

4.2.3 Monitoring

Field monitoring consisted of weighing and checking the lysimeter for drainage. A threaded PVC cap was screwed onto the top of the lysimeter (Figure 4.7). The cap was attached to a tripod hoist used to lift the lysimeter from the ground (Figure 4.9). The pinch clamp was removed from the drainage line and water was collected in a plastic bottle. The lysimeter was weighed using a force transducer attached to the tripod cable and a battery operated signal processor. The transducer has an operating range to 500 lbs, and an accuracy of ± 0.03 lbs.

4.2.4 Results

Attempts to obtain useful information from the draining lysimeter proved unsuccessful with drainage occurring only once, during March. At the time the lysimeter was installed, it was believed that the grass roots would not be effective below a depth of 1 to 2 feet. Moisture profiles presented in section 2 show that the grass effectively extracts water from

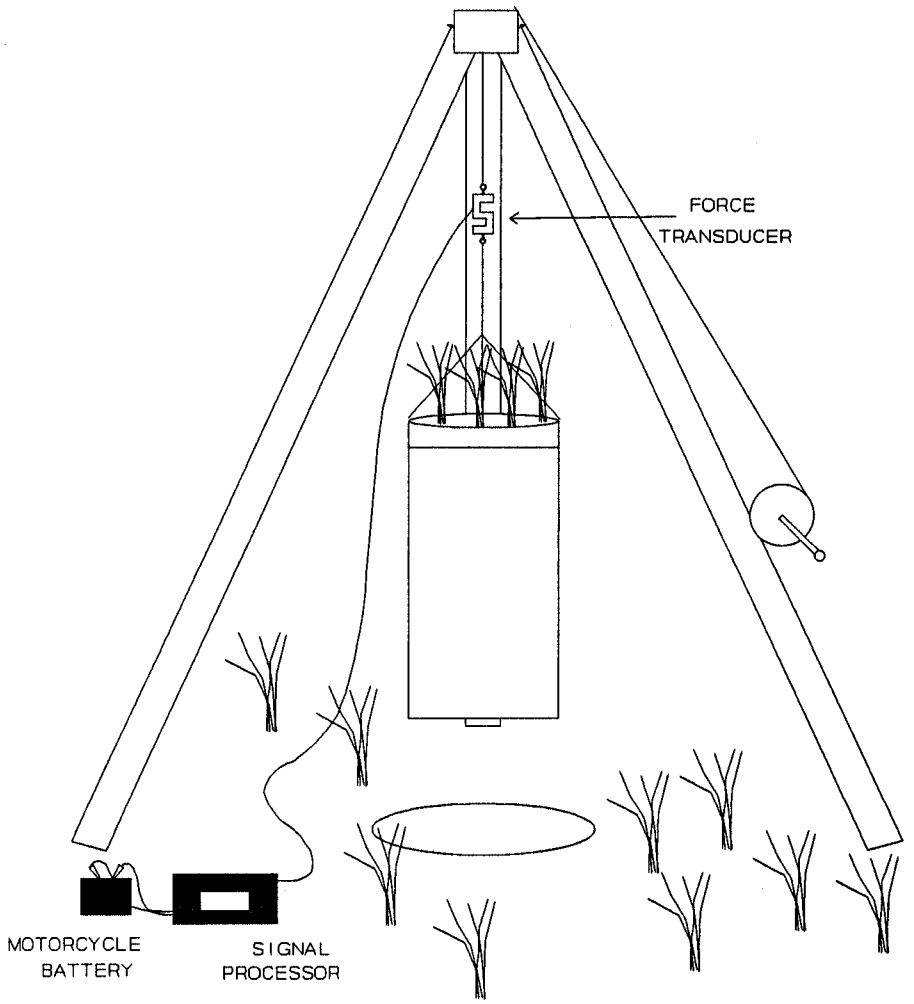

Figure 4.10 Lysimeter Monitoring Equipment

at least 5.75 feet. Field observations also provide evidence that the lysimeter was not deep enough. Water drainage from the lysimeter in March indicates that enough water had infiltrated to saturate the drainage surface. The grass in the lysimeter became green in early April, approximately 2 weeks before the rest of the grass. This was due to the lysimeter induced soil-moisture increase within the grass roots which was not available to the grass outside the lysimeter. By late May, the grass in the lysimeter had consumed all the available water and was brown. The surrounding grass was still green and extracting water from below the depth of the lysimeter.

5.0
SOIL PROPERTY DETERMINATION

5.1 Grain Size Distribution

5.1.1 Method

Grain size distribution was determined for samples used to calibrate the neutron probe for holes 2, 3, and 4 and samples tested for hydraulic properties. The following procedure was followed:

1) Oven dried samples were ground with a rubber tipped mortar and pestle for at least 4 minutes or until all visible clumps of soil were disaggregated.

2) The soil material was placed in a series of sieves and shaken for 5 minutes.

3) Before material was removed from the individual sieves, each sieve was shaken above a white piece of paper to make sure no additional material was still passing a particular sieve.

4) The material from each sieve was placed in a dish and weighed to the nearest 0.01 gram.

5) The percent passing was determined for each sieve size.

6) A 10% HCl solution was added to the dry soil to obtain a qualitative estimate of carbonate content.

5.1.2 Results and Analysis

The results of the sieve tests are presented in Appendix C. Although the soil is visually homogeneous, there is substantial variance in the sieve analyses even across a 6-inch sample. Figure 5.1 shows the average percent finer than a #200 sieve by weight for hole 4 and individual components that comprise the averages. There is a large variability in

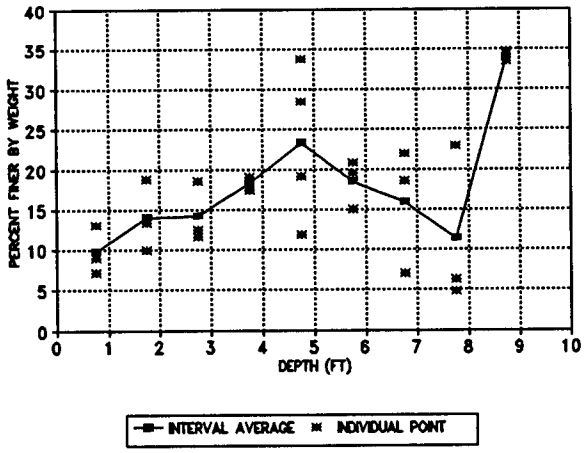

Figure 5.1 Percent of material passing a #200 sieve versus depth

the percent passing a #200 sieve, especially between 4 and 8 feet. This small scale heterogeneity makes it difficult to assign properties determined on a 1-centimeter sample to an interval of several inches.

As mentioned previously, a neutron probe moisture reading gives the average moisture content over a sphere of influence. Moisture content obtained from neutron probe and the average weight percent of soil passing a #200 sieve were plotted versus depth to see if there was a visible relationship. The results are presented in Figure 5.2. A good relationship can be seen at the lower depths where steady-state moisture conditions existed throughout most of

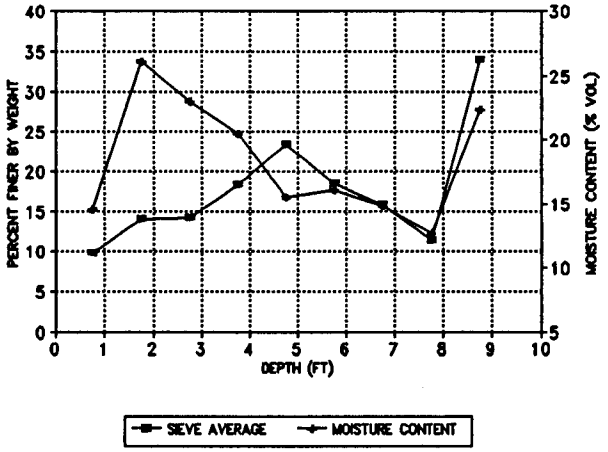

Figure 5.2 Average percent passing a #200 sieve versus depth and moisture content at steady state

the year. Since the average percent of soil particles finer than a #200 sieve in a 6-inch interval is a controlling factor influencing the steady-state moisture content, it is reasonable to assume that the same relationship exists for a 1-centimeter sample. Consequently, assigning matric potentials from moisture characteristic curves from point samples to neutron probe moisture readings can potentially lead to erroneous results. This is discussed in more detail later in this section. All additional attempts to correlate grain size distribution attributes to hydraulic properties were not successful.

5.2 Moisture Characteristic Curves

5.2.1 Method

Three separate tests were conducted to determine the moisture characteristic curves for soil samples from hole 2, 3, and 4. The procedure outlined in ASTM standard D 2325 was followed as closely as possible with the equipment available. A brief description of the equipment and procedure is presented here. For more information, the reader should refer to the ASTM book of standards.

5.2.2 Equipment

The equipment used in this test is illustrated in Figure 5.3. The testing apparatus consists of a pressure chamber (A) that is attached to an external source of air pressure (B) and a nitrogen tank (C). Air pressure to the cylinder is controlled through a pressure regulator. In this instance, two regulators were used; one with a 0 to 20 psi (0 to 1407 cm) (D) range and the other with a 5 to 150 psi range (352 to 10551 cm) (E). An interchangeable pressure gauge (F) was used to measure chamber pressure. Appropriate pressure gauges were used to provide proper resolution for different pressure ranges. Samples were placed on a ceramic plate (G) that is attached to an external drainage line (H). A 5-bar and 15-bar (5100 and 15299 cm) air-entry plate was used in this test. A two way valve (I) provided a means to switch between the air and nitrogen line and remove them from the chamber when the pressure was relieved using the bleed valve (J).

5.2.3 Theory

As mentioned in section 2, matric potential is defined as the difference between the soil water pressure and the surrounding atmospheric pressure. Samples are placed on a ceramic plate that is connected to a bleed line exposed to atmospheric pressure outside the chamber. Therefore

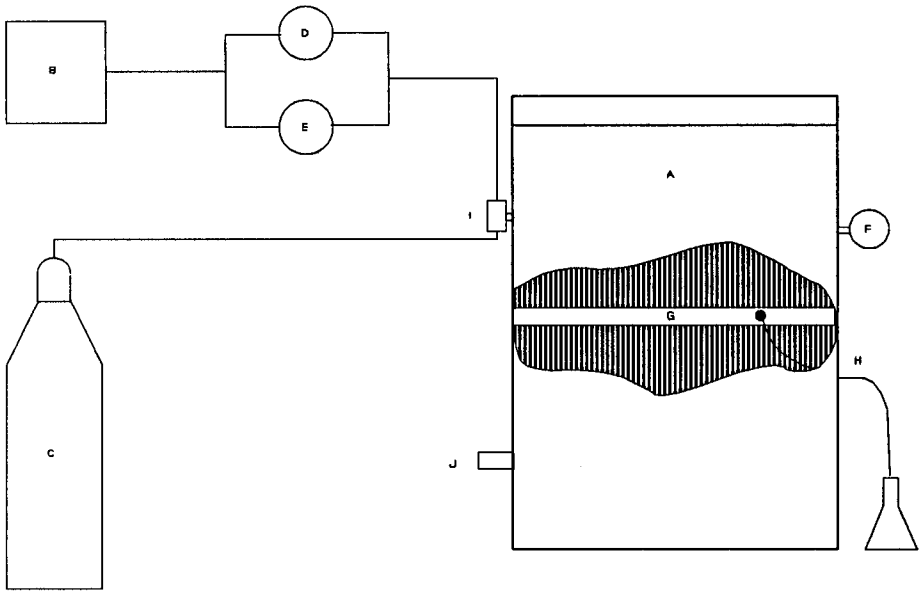

Figure 5.3 Pressure plate apparatus

the pressure in the ceramic plate is equal to atmospheric pressure. Consequently, a pressure difference can be created by raising the chamber pressure.

The pores in the ceramic plate are saturated with water and have a pore size that will allow them to remain saturated at the matric potential for that given test pressure. This pore size can be calculated using equation 3.13. The maximum pressure at which all pores will remain saturated is called the air-entry pressure. Applying Bernoulli's equation (3.8) to the water in the ceramic plate (Figure 5.4), the water pressure is equal to $P_a - z$, where P_a is atmospheric pressure

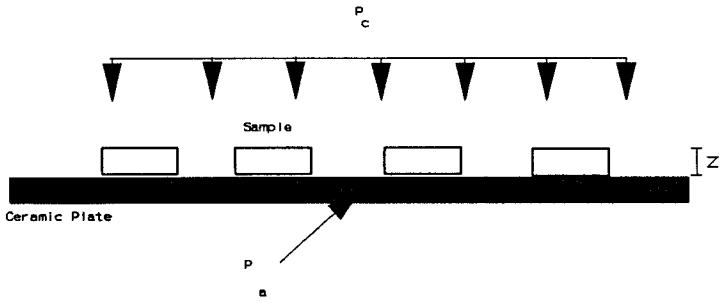

Figure 5.4 Pressures affecting matric potential during a pressure plate test

and z is the effective sample height above the base of the ceramic plate. Since z is negligible compared to the pressure difference between the pressure chamber and the atmosphere, the water pressure in the plate can be considered to be equal to P_a. The pressure difference across the water meniscus is equal to $P_c - P_a$ where P_c is the chamber pressure. Soil samples are placed on the ceramic plate and allowed to reach static equilibrium with the water in the plate. At equilibrium, the soil water has a matric potential of $P_c - P_a$. Atmospheric pressure is taken to be 0. Therefore, the matric potential in the soil sample is equal to the chamber pressure.

5.2.4 Test Procedure

Samples were prepared by cutting a 1 to 2-centimeter section from the 6-inch brass liner using a rock saw. Rough edges were removed with a file. This method was preferred over repacking the sample to its original bulk density in a brass liner as it preserved the soil structure. The samples were saturated by placing them on the filter paper on the 5-bar ceramic plate. The ceramic plate was allowed to saturate for several days before the samples were placed on it. The filter paper was used to prevent the samples from sticking to the plate and to establish and maintain the hydraulic contact throughout the test. The ceramic plate and samples were

placed in a tray of water deep enough to just cover the top of the samples. Surcharge weights approximately equal to field overburden pressure were placed on each sample for the duration of the saturation period.

After saturating for at least 72 hours, the plate and samples were placed in the chamber, the drainage line was attached, the chamber was closed, and air pressure was applied to the chamber.

Equilibrium was assumed to be achieved when there was no drainage for 24 hours. At this time, the pressure was removed, the chamber opened, and each sample was weighed to the nearest 0.01 gram. The used filter paper was discarded and new filter paper was placed on the plate. Enough water was applied to saturate the filter papers before the samples were placed on them. This ensured that the hydraulic contact between the ceramic plate and samples was re-established.

After the final pressure was reached, the samples were oven dried and weighed to the nearest 0.01 gram. The final pressure point is commonly 15 bars as this is generally accepted as the wilting point of most plants (the pressure at which plants can no longer extract moisture). The height of each sample and the liner weight was recorded. Samples were then placed in a desiccator until they were tested for grain size distribution.

Volumetric water content was determined using the formula

$$Moist\% = \frac{Weight_{wet}(g) - Weight_{dry}(g)}{Volume} \qquad [5.1]$$

The pressure(cm)-volumetric moisture content data pairs were used as input into the program SOHYP.

5.2.5 Analysis

SOHYP utilizes a non-linear least squares regression to fit experimental data to the van Genuchten analytical expression for the moisture characteristic curve. The code requires pressure - moisture content data pairs and effective porosity as input. Output includes the van Genuchten parameters α and n, and residuals between fitted and measured points.

A program option was used to estimate the residual moisture content. This is defined by the program as the moisture content at which $d\theta/dh$ is equal to zero. Residual moisture content is difficult to obtain in the laboratory and may become an "ill-defined parameter" (van Genuchten, 1980). However, a fairly accurate estimate of residual moisture content is required to reliably estimate unsaturated hydraulic conductivity.

Porosity was estimated by extrapolating the measured data points through the moisture axis. This value was used as input into SOHYP. Additional values of porosity that were slightly more and less than the extrapolated value were used in separate runs. The best fit was determined by examining the residuals of the function over the experimental data.

5.2.6 Results

Difficulties were encountered using the pressure plate data and neutron probe moisture readings to predict *in situ* matric potential. A recurring problem was that the residual moisture content calculated by SOHYP was greater than most of the corresponding field values measured using the neutron probe for the steady state period.

As shown in section 5.1.3, there is a good relationship between moisture content and the amount of soil finer than a #200 sieve. The variance in the percent passing a #200 sieve (Figure 5.1) in a 6-inch sample may make it invalid to compare a neutron probe reading to a moisture characteristic curve at high matric potentials because the discrete sample could be different from the average character within the neutron probe sphere of influence. This point is further illustrated in Figure 4.7 which compares the moisture profile determined by laboratory analysis to that predicted by the neutron probe.

Examination of moisture contents from 6.5 to 7.0 feet show the neutron probe moisture reading is approximately 4% lower than the laboratory measurement. Matric potentials predicted from the neutron probe moisture reading would be unrealistically large. The fact that the slope of the moisture characteristic curve ($dh/d\theta$) approaches infinity at large matric potentials compounds the problem. A small change in moisture content can result in an order of magnitude increase in matric potential, or, result in a neutron probe moisture reading lower than the residual moisture content for a point sample from the same interval.

To avoid these difficulties, a pressure plate test was conducted entirely on samples from hole 6. As mentioned previously, care was taken to record the orientation of each 6-inch sample when it was extracted in the field. Each of the 6-inch samples had 1 to 2-centimeters extruded from each end for volumetric moisture tests. Adjacent samples were used for determining moisture characteristic curves, and the centers were used for saturated hydraulic conductivity testing (Figure 5.7).

The samples were divided in this manner so moisture characteristic curves could be compared to volumetric moisture contents from adjacent samples, thus improving estimates of *in situ* matric potentials. Measurements were taken at matric

potentials of 106, 352, 1759, 4220, 9144, and 14771 centimeters to provide points for an accurate description of the full shape of the curve. Filter paper was not used for the 15-bar simulation. Instead, the hydraulic connection was re-established by slightly wetting the ceramic plate and placing the sample directly of the wet surface.

The resulting moisture characteristic curves and moisture content-matric potential data pairs are presented in Appendix D. This test produced more satisfactory results. However, adjustments had to be made for 2 samples in order to calculate *in situ* matric potential. The moisture content used to

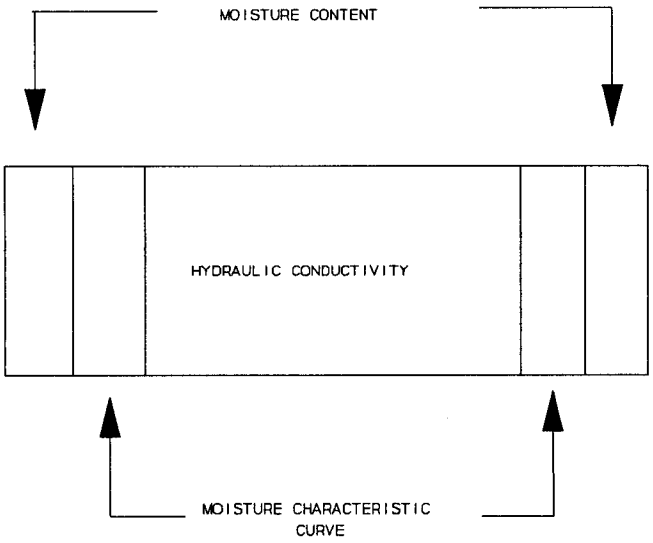

Figure 5.7 Sample division and use for hole 6

calculate the matric potential at 3.5 feet was taken from 3.33 feet opposed to the adjacent sample. The moisture content from 3.5 feet was higher than the porosity calculated in the neutron probe calibration procedure (see Appendix B) and higher than porosity used in the best fit from the SOHYP regression. In addition, this moisture content-neutron probe reading point was an outlier in the neutron probe calibration and was eliminated from the regression. Similarly, the moisture content used to calculate the matric potential at 5.0 feet came from 5.33 feet. The moisture content at 5.0 feet was approximately 10% higher than that for adjacent samples and is believed to be due to laboratory error.

Residual moisture contents predicted by SOHYP were less than the field moisture contents determined on the adjacent samples except the 6-foot sample. However, in-situ matric potentials were unreasonably high for all samples below 6 feet. Results are presented in Table 5.1. Sample compaction during field extraction is believed to be responsible for the high matric potentials.

Attempts were made to correct moisture characteristic curves for compaction. The most serious obstacles encountered were; (1) total compaction was not known for each sample, and (2) it was not known how initial pore size affects the deformation of each pore. It did not seem reasonable to make

unfounded assumptions about these unknowns to correct moisture characteristic curves, and apply the results to flow simulations.

5.3 Saturated Hydraulic Conductivity

Unsaturated hydraulic conductivity was estimated in this study using the van Genuchten function (equation 3.21). This

Table 5.1 Results from pressure plate test on samples from hole 6

Depth (ft)	θ_s	θ_r	α	N	Matric Pot. (cm)	Matric Pot. (bars)	Total Head (cm)
1.5	32.0	5.3	.00753	1.15357	85	.08	144
2.5	37.5	11.0	.00312	1.17178	290	.29	-92
3.0	37.5	2.8	.00092	1.16527	630	.62	-450
3.5	38.0	0.0	.00258	1.12933	270*	.27	-100
4.5	33.0	3.8	.01744	1.15155	1400	1.3	-1300
5.0	38.0	6.4	.01806	1.15367	2.6E+4**	26	-2.6E+4
5.5	36.0	14.0	.01359	1.52431	1.6E+4	15	-1.6E+4
6.0	40.0	15.8	.01200	1.56070	NA***	NA***	NA***
6.5	48.0	17.3	.01487	1.32425	1.8E+6	1800	-1.8E+6
7.0	48.0	16.8	.01673	1.43472	3.2E+4	32	-3.2E+4
8.5	48.5	21.4	.01145	1.33476	7.2E+4	71	-7.2E+4
9.0	51.0	18.7	.01407	1.25453	1.2E+5	120	-1.2E+5

* - Moisture content from 3.33 feet was used to calculate matric potential; ** - Moisture content from 5.33 feet was used to calculate moisture content; *** - Moisture content was less than the residual moisture content

function estimates the relative hydraulic conductivity as a function of moisture content or matric potential. Therefore, saturated hydraulic conductivity is required to calculate unsaturated hydraulic conductivity.

5.3.1 Methods

The method and equipment used to determine vertical saturated hydraulic conductivity is described by Olsen *et al.* (1991). A simplified diagram of the testing apparatus is presented in Figure 5.6. The test specimen is placed in a triaxial cylinder(A). A two way flow pump (B) produces a constant flow through the sample by simultaneously injecting water from the top and withdrawing form the bottom (or visa versa) while the gradient is measured with a differential transducer (C). Two bellowframs are used to control the pore water pressure (D) and the chamber pressure (E). The pressure difference between the two is the effective stress applied to the sample which is measure by a differential pressure transducer (F). Hydraulic conductivity is calculated using the measured gradient and the known flow rate.

5.3.2 Sample Preparation and Results

A rock saw was used to cut the test specimen to the desire length of 3.5 to 4.5 centimeters while still in the brass liner. This also produced a smooth flat surface at each end of the sample. The test specimen was removed from the liner by cutting the liner lengthwise with a small radial saw The sample was placed between two 0.1-inch thick porous disks with hydraulic conductivities of $1.45(10)^{-2}$ cm/sec. This

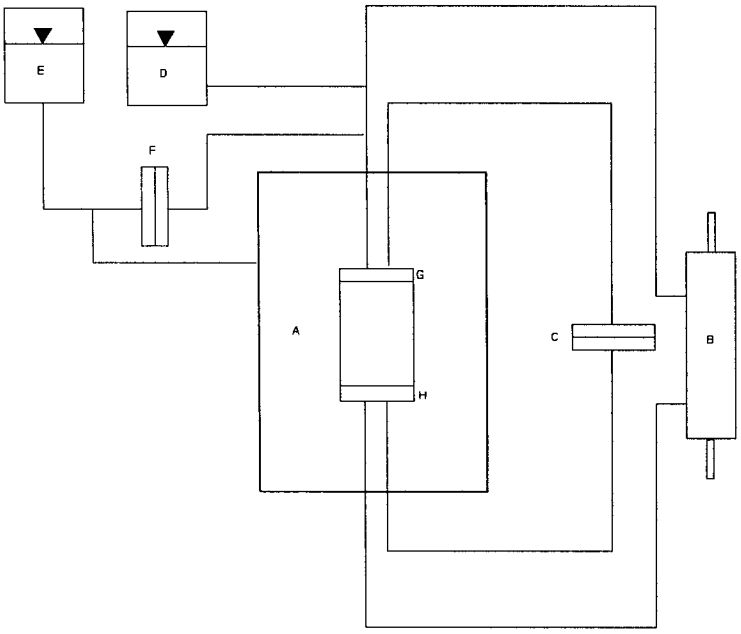

Figure 5.6 Triaxial system used for saturated hydraulic conductivity tests

configuration was in turn positioned between two plastic disks with numerous 1/8-inch holes drilled through it while a rubber membrane was stretched around the sample. The plastic disks made sample handling easier. Without them, it would be difficult to stretch the membrane over the end caps of the triaxial system (see G and H of Figure 5.8) without damaging the sample. The sample was then saturated in a vacuum desiccator for at least 24 hours.

After saturating, the sample was placed in the triaxial system. Hydraulic conductivity tests were conducted at effective stresses equal to the overburden pressure in the field and at pore pressures ranging from 20 to 35 psi (1400 to 2460 cm) to dissolve any entrapped air in the sample. The *in situ* effective stress is equivalent to the overburden pressure plus the matric potential (Das, 1990). However, at the moment a sample becomes saturated in the field, the matric potential is zero and the effective stress is equal to the overburden pressure only. Because the sample was saturated with no effective stress, it was necessary to let the sample re-equilibrate to the effective stress it experienced in the field. If the sample was not at equilibrium with the effective stress during the hydraulic conductivity test, a slow increase in the gradient was apparent due to sample

consolidation. If this was the case, the test was continued until the gradient was constant over time. Table 5.2 shows the data and results of the hydraulic conductivity tests.

Table 5.2 Saturated hydraulic conductivity test results

Interval (ft)	Flow Rate (cm^3/sec)	Sample Length (cm)	Pressure Difference across sample (cm)	Hydraulic Conductivity (cm/sec)
2.5 - 3	9.23E-4	4.9	31.7	7.6E-6
3.5 - 4	9.23E-5	3.2	24.6	1.6E-6
4.5 - 5	2.31E-2	4.2	39.4	1.3E-4
5.5 - 6	2.31E-2	5.5	33.8	2.0E-4
6.5 - 7	4.62E-4	5.0	35.9	2.6E-6
7.5 - 8	9.23E-4	3.8	11.3	1.7E-5
8.5 - 9	4.62E-4	4.6	40.8	2.8E-6

6.0
ANALYSIS

6.1 Steady-State Flow Analysis

Many methods have been presented in the literature for calculating vertical flux in the vadose zone. A good summary of methods is provided by Wilson (1982). However, many of the methods require data that are not available for this study or require conditions that were not satisfied. Of the methods available, the most appropriate for analyzing steady state vertical flow at this site are Darcy's law and numerical modeling.

Errors in the moisture characteristic curves due to sample compaction present the largest obstacle to an accurate estimation of vertical flux. Many of the calculated *in situ* matric potentials where static moisture profiles existed are not reasonable based on previous studies under similar climatic conditions. Additionally, because differential compaction within individual samples and between separate samples resulted in matric potentials that do not produce a consistent gradient (see table 5.1) it is not possible to determine if a downward gradient was present where static moisture profiles existed. To estimate downward vertical flux it is necessary to assume a downward gradient was present.

The intervals that show a downward gradient in Table 5.1 have unreasonably high matric potentials (8.5 to 9.0 feet for example). If data from this interval were used as input to Darcy's Law, the results would be insignificant because the gradient, matric potential and resulting hydraulic conductivity values are not reliable. It was decided the best way of evaluating vertical flux was by exploring the possible range of flux using a model.

Although some of the moisture characteristic curves are known to be imprecise, numerical modeling provides a means of determining the sensitivity of the flow system to changes in hydraulic parameters. Sample compaction must result in a decrease in pore size and consequently is believed to have changed the shape of the moisture characteristic curve. More specifically, a decrease in pore size yields higher matric potentials at low moisture contents. The effect at higher moisture contents is not known. When *in situ* moisture contents are input into the van Genuchten expressions that were fitted using data from compacted samples, it will result in higher matric potentials and lower hydraulic conductivities than exist in the field. By assigning more reasonable values of matric potential and hydraulic conductivity in the numerical model, it is possible to make a more accurate estimate of flux and determine how sensitive the system is to

changes in these parameters. No studies have been found in the literature to estimate the effect of compaction on moisture characteristic curves or to estimate the amount of compaction that occurred. Therefore, it is necessary to use the parameters predicted from some moisture characteristic curves that are known to be imprecise.

6.1.1 Conceptual Model

As shown previously, water infiltration and percolation at the site was limited to the top 3 feet throughout most of the study. This water was used to meet evapotranspiration demands. Heavy precipitation in March resulted a wetting front that penetrated to 6.75 feet. Saturated hydraulic conductivity is approximately 2 orders of magnitude lower for the 6.5 to 7.0-foot sample than the overlying sample (Table 5.2). Visual inspection of soil samples show similar material extending to 7.5 feet. Moisture profiles confirm that the wetting front did not progress beyond this relatively thick low hydraulic conductivity layer. Table 6.1 shows the variance of neutron probe moisture readings at 7.75 feet. Comparing these values to the variance due to the radioactive decay of the neutron source shows they are approximately equal (from Table 4.2). This suggests that fluctuations in moisture

readings at 7.75 feet are due to the radioactive decay process and not to changing moisture conditions.

It is believed that the majority of the water from the wetting front will be transpired and the moisture profile below 3 feet will return to its pre-March condition. Figures 2.8 through 2.10 illustrate the steady extraction of moisture by the native grasses to depths of 5.75 feet. If these trends continue, water should be extracted until the matric potential reaches the wilting point of the plants (approximately 15 bars). Moisture contents at 6.75 feet, which corresponds to a low hydraulic conductivity layer, and the amount of water

Table 6.1 Change in moisture content at 6.75 feet and change in storage below 6.75 feet from September 1991 to September 1992

	Hole			
	1	2	3	4
Moisture Content Change at 6.75 ft. (%)	-0.1	5.94	3.06	4.22
Increase in Storage Below 6.75 Feet (inches)	0.598	0.453	0.335	0.261
Moisture Content Variance at 7.75 Feet (%)	0.05140	0.2133	0.1108	0.0818
Moisture Content Variance due to Radioactive Decay of the Neutron Source (%) (from Table 4.2)	0.0626	0.2530	0.0757	0.0626

in storage below this depth have increased slightly since the wetting front reached this depth in April, 1992 (Table 6.1). Because of the limited accuracy of using neutron probe measurements to determine matric potential at high tensions, and the limited duration of this study, the fate of this water can only be speculated.

Moisture profiles show moisture is extracted much faster from 5.75 feet than the lower hydraulic conductivity layer below (6.75 feet). This does not necessarily imply that the grass roots do not extend to 6.75 feet. Comparison of the moisture profiles from August 1991 and September 1992 (Figure 2.11 to Figure 2.13), show significantly higher moisture contents at 5.75 feet at the conclusion of the study which correspond to lower matric potentials. The grass may preferentially remove water from this area where it is most easily obtained (due to a lower matric potential and higher hydraulic conductivity). As soil moisture at 5.75 feet is depleted, soil moisture storage at 6.75 feet may be lost via two mechanisms. The grass roots may begin to remove water from this zone at a higher rate, and a zero flux plane may develop where the residual moisture from the wetting front remains. This situation is illustrated in Figure 6.1. Higher matric potentials exist above and below the zero flux plane

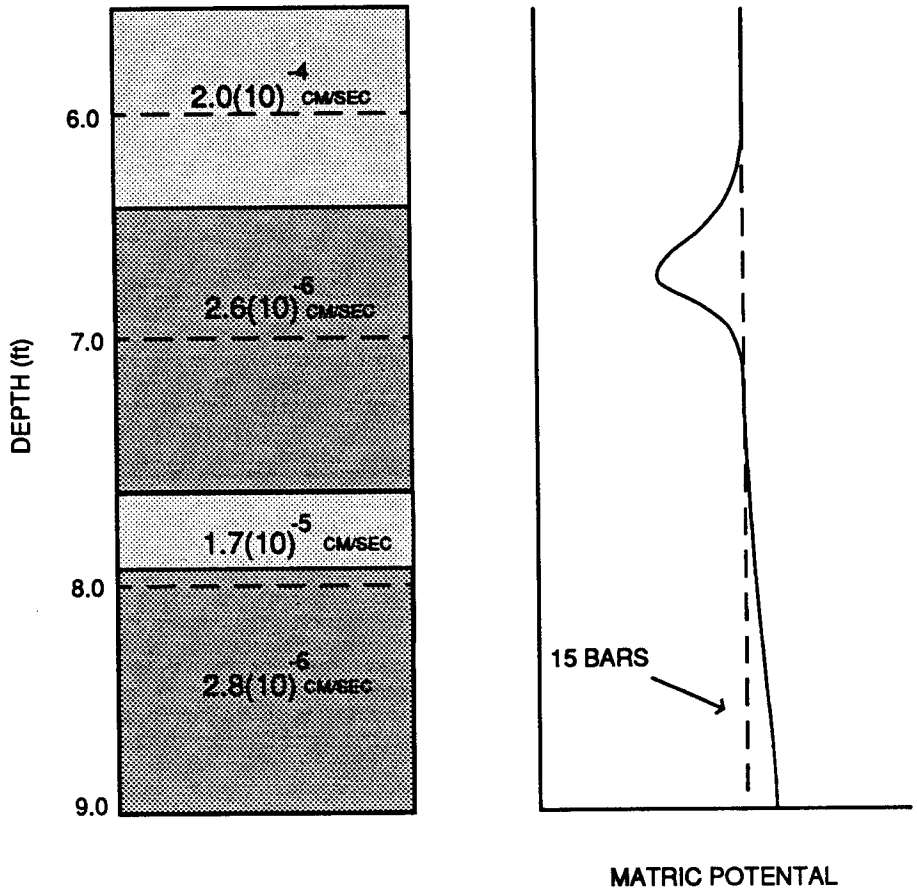

Figure 6.1 Conceptual flow system below 5 feet at the conclusion of the study

resulting an upward and downward gradient, above and below the zero flux plane respectively. Under these conditions, more water will flow upwards into higher hydraulic conductivity material where grass roots are productive.

Moisture contents show a very slow increase at the 6.75-foot measurement point for all holes (Appendix A) with an apparent trend towards decreasing moisture contents at the conclusion of the study. This indicates that the above process may have been taking place at this time. It is not believed that this water will contribute to groundwater recharge. If vertical flow below 6.75 feet does exist at this site, it most likely takes place under near steady state conditions. Due to the extremely low hydraulic conductivity of this soil at high matric potentials, changes in soil moisture storage occur very slowly. Therefore, the static moisture profiles may not represent true steady-state conditions, but transient conditions where changes in soil moisture occur too slowly to be detected during the span of this study.

To calculate vertical flux rates, it was assumed that the static moisture profiles that existed throughout most of the year represent steady state flow conditions with a downward vertical gradient to the water table. The lack of accurate matric potential data makes it impossible to

determine if a downward gradient is present. However, the hydraulic data can be used to make a reasonable estimate of vertical flux should a downward gradient exist. This is accomplished by assigning an overall gradient to the system within the numerical model.

6.1.2 VS2D/VS2DT

The model chosen for this study is VS2D\VS2DT (Healy, 1990), a U.S. Geological Survey finite difference code. This model was chosen for several reasons. It is public domain, and specifically intended for the analysis of unsaturated flow and transport. It is therefore capable of dealing with the non-linearities of unsaturated flow. It allows the user to use analytical expressions, specifically the van Genuchten function, to describe the unsaturated hydraulic relationships between moisture content, matric potential and hydraulic conductivity. And finally, the user can choose the method of determining intercell conductance. During unsaturated flow simulations, hydraulic conductivity can vary over several orders of magnitude across adjacent blocks. Consequently, different methods of determining conductance can produce very different results.

6.1.3 Intercell Conductance

The three most common methods for determining conductance between finite difference blocks are the arithmetic, harmonic, and geometric means. The Arithmetic mean of cells A and B is expressed as:

$$K=\frac{K_A+K_B}{2} \qquad [6.1]$$

The harmonic mean is:

$$K=\frac{2K_AK_B}{K_A+K_B} \qquad [6.2]$$

Stephens (1986) cites Mualem (1984) as recommending this method in unsaturated soils. It is also recommended by Apel (1976) for saturated conditions where conductance varies as a step function. The geometric mean is expressed as:

$$K=(K_AK_B)^{1/2} \qquad [6.3]$$

This method is recommended by Haverkamp and Vauclin (1979) who compared finite difference solutions using different weighting

methods to experimental data and analytical solutions. They found this method introduces the smallest weighting error.

VS2D/VS2DT determines intercell conductance, C, using equation 6.4, where A is the cell face area through which flow occurs, and z is the distance between the center of the cells. Equation 6.4 is separating it into a saturated ($\frac{K}{\Delta z}$) and unsaturated (K_r) component. The distance weighted harmonic

$$C_{n,j-\frac{1}{2}} = \left(\frac{\rho K K_r A}{\Delta z}\right)_{n,j-\frac{1}{2}} \qquad [6.4]$$

mean is used to determine the saturated hydraulic conductivity component of conductance. The user is given the option of a geometric mean or distance weighted arithmetic mean to calculate the unsaturated component of conductance. The geometric mean was used for this study.

6.1.4 Model Description

Steady-state analysis of vertical flux was performed using a one-dimensional model. The model was based entirely on hydraulic data from hole 6 below 4.5 feet. The most complete and reliable data were obtained from hole 6. Steady-state conditions were only present below 3.75 feet throughout

most of the year. Consequently, only the interval from 4.5 to 9 feet was modeled to estimate vertical flux for the steady state condition.

The hydraulic properties used in the simulation are listed in Table 5.1 and 5.2. Soil moisture characteristic curves and corresponding van Genuchten parameters were determined for samples at 6-inch intervals. These parameters were assigned to the material at each of these points and extended to the interval 3 inches above and below them. For example, the properties determined on a sample from 5 feet were assigned to the interval extending from 4.75 feet to 5.25 feet. Saturated hydraulic conductivity was determined in 1-foot increments. In a similar manner, these values were assigned to the adjacent material. The same hydraulic conductivity value obtained from a sample extracted from 5.5 to 6.0 feet was assigned to the interval from 5.25 to 6.25 feet. Therefore, two materials with different van Genuchten parameters were assigned the same hydraulic conductivity. Because a moisture characteristic curve could not be obtained from the 7.5 to 8.0-foot interval, hydraulic parameters from adjacent samples were extended to cover the missing interval.

The model domain was divided into cells with x and z dimensions of 1.0 and 1.905 centimeters respectively (An x dimension is required for one-dimensional simulations in the

code). Simulations were performed using a z spacing of 3.81 centimeters which resulted in flux rates within 3% of the simulation with the finer grid spacing. It was felt that a 3% change in flux due to changing grid dimensions was acceptable for this study due to the very low flux rates and potential errors associated with imprecise moisture characteristic curves.

Flow across the system was simulated through two fixed head (matric potential) cells at opposite ends of the model. Sensitivity to different gradients and corresponding hydraulic parameters was determined by changing the matric potential at the fixed head cells. Figure 6.2 shows the model geometry and material properties used as input.

Because VS2D/VS2DT does not have a steady-state option, a transient simulation was performed. Steady-state was assumed to have been reached when the difference between the flux into and out of the system was within 2%.

6.1.5 Results and Discussion

The results of the model simulations are presented in Table 6.2. Vertical flux rates range from $4.9(10)^{-4}$ to $9.7(10)^{-6}$ inches per year($1.2(10)^{-3}$ to $1.8(10)^{-3}$ cm per year). The highest flux was produced by a gradient of 74.4 cm/cm,

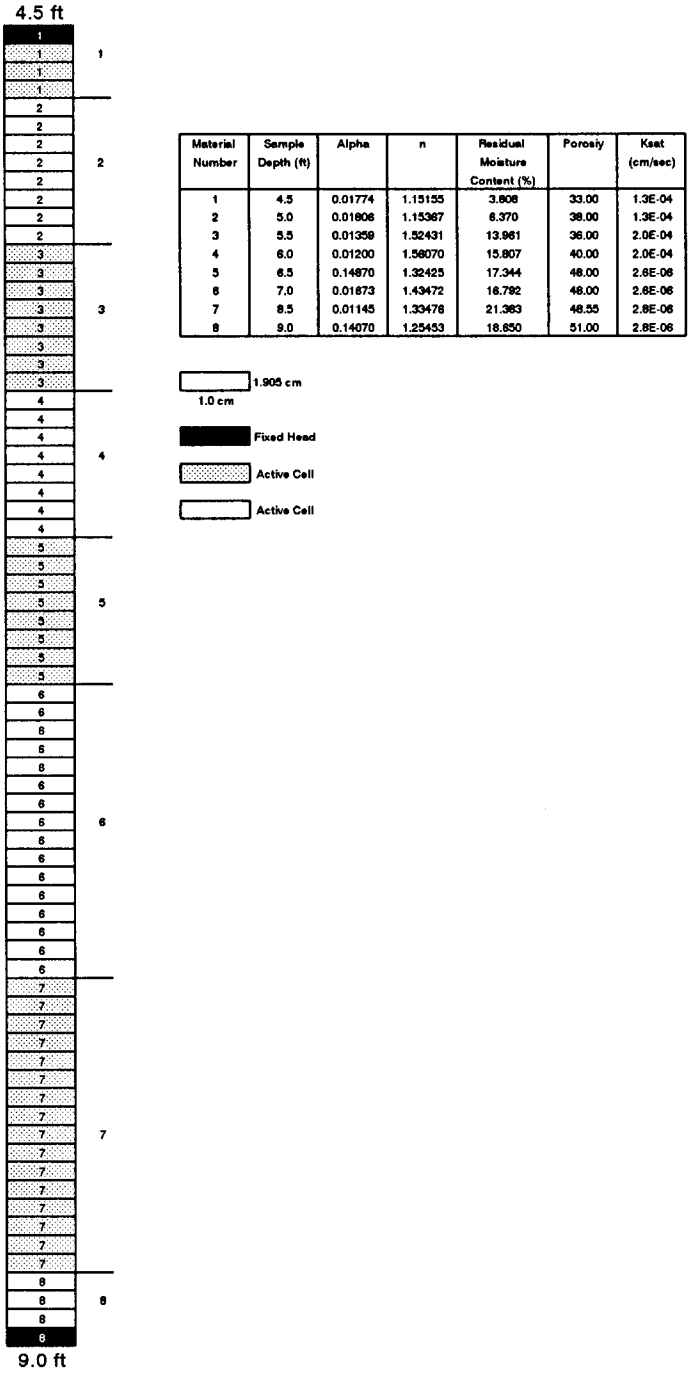

Material Number	Sample Depth (ft)	Alpha	n	Residual Moisture Content (%)	Porosity	Ksat (cm/sec)
1	4.5	0.01774	1.15155	3.808	33.00	1.3E-04
2	5.0	0.01808	1.15367	6.370	38.00	1.3E-04
3	5.5	0.01359	1.52431	13.961	36.00	2.0E-04
4	6.0	0.01200	1.58070	15.807	40.00	2.0E-04
5	6.5	0.14870	1.32425	17.344	48.00	2.6E-06
6	7.0	0.01873	1.43472	16.792	48.00	2.6E-06
7	8.5	0.01145	1.33476	21.383	48.55	2.6E-06
8	9.0	0.14070	1.25453	18.650	51.00	2.6E-06

Figure 6.2 Model geometry and material properties

ranging from 5 to 15 bars (5100 cm to 15300 cm) across the system. Klute *et al* (1971) reported matric potentials greater than 15 bars from moisture characteristic curves, and 10 to 20 bars from thermocouple psychrometers in Colorado rangeland. Using similar matric potentials (case 5 and 6) to simulate flow results in lower flux rates due to lower hydraulic conductivities at larger matric potentials. Although soil moisture characteristic curves are imprecise, calculated *in*

Table 6.2 Results of steady-state vertical flow simulations

Case #	Fixed Head (bars)*		Flux In (cm/day)	Flux Out (cm/day)	% Error	Average Vertical Flux	
	Top	Bottom				cm / sec	inches / year
1	5.0	7.0	7.371E-7	7.365E-7	0.08	8.5E-12	1.1E-4
2	5.0	10.0	1.091E-6	1.087E-6	0.37	1.3E-11	1.6E-4
3	5.0	15.0	1.284E-6	1.282E-6	0.16	1.5E-11	4.7E-4
4	5.0	20.0	1.354E-6	1.352E-6	0.15	1.6E-11	4.9E-4
5	10.0	15.0	2.145E-7	2.181E-7	1.65	2.5E-12	7.9E-5
6	15.0	20.0	6.879E-8	6.607E-8	4.08	7.8E-13	9.7E-6

* - multiply bars by 1020 to obtain centimeters

situ matric potentials indicate that it is unlikely that matric potentials of 5 bars exist at the top of the simulated

interval. Therefore cases 5 and 6 may provide a more realistic estimates of vertical flux.

These simulations show vertical flux, even with relatively high gradients, is negligible (eg. on the order of 10^{-5} to 10^{-4} cm/year) and did not contribute to groundwater recharge during the study. Additional simulations were performed with fixed head ranging from 1 to 5 bars (1020 cm to 5100 cm). The purpose of these simulations was to determine if it is possible to achieve 0.1 inches of vertical flux per year under unsaturated steady state conditions (the average value reported by Robson).

Table 6.3 Results of steady-state vertical flow simulations

Fixed Head (bars)		Flux In (cm/day)	Flux Out (cm/day)	% Error	Average Vertical Flux	
Top	Bottom				cm / sec	inches / year
1	2	3.216E-5	3.212E-5	0.12	3.72E-10	0.0117
1	3	3.679E-5	3.681E-5	0.05	4.26E-10	0.0134
1	5	3.937E-5	3.935E-5	0.05	4.56E-10	0.0144

Results, presented in Table 6.3, indicate that a steady state vertical flux of 0.1 inches per year is not possible at this site, even with matric potentials much smaller than are

likely to be sustained in the field. To achieve a yearly vertical flux on the order of 0.1 inches per year, it would be necessary to have a substantial wetting front progress through the soil column. However, vertical flux for this site is within the range reported by Robson.

The primary source of groundwater recharge occurring on a yearly basis near the study site may be localized, and found in depressions, creek beds or above shallow water tables. Additionally, this study has not investigated the possibility macropore flow along preferential pathways. It is likely that vertical movement of water through this mechanism would not be detected with the instrumentation used in this study.

6.2 Estimation of Evapotranspiration

6.2.1 Method

As a byproduct of monitoring soil moisture profiles, it is possible to estimate actual evapotranspiration rates. Evapotranspiration rates are a function of not only climate and vegetation, but water availability. Since the original purpose of this study was to estimate vertical flux, field site monitoring was not frequent enough to obtain a series of moisture profiles at regular intervals after precipitation events. Immediately after precipitation, evapotranspiration rates are usually highest due to the availability of water

(van Bavel *et al*, 1968). As soil moisture decreases through time, it becomes more difficult for plants to extract soil moisture and evapotranspiration rates decrease. With the data available, it is only possible to estimate an average evapotranspiration rate between monitoring intervals.

Evapotranspiration was estimated using a water budget equation. The water budget for the zone of thermalization surrounding each neutron access tube can be expressed as:

$$P=RO+\Delta S+Q_v+Q_l+ET \qquad [6.5]$$

where:

P = precipitation
RO = runoff
ΔS = change in soil moisture storage
Q_v = vertical flow out of the system
Q_l = lateral flow into or out of the system
ET = evapotranspiration

Each of the components of the water budget equation were determined as follows:

Precipitation (P)

Precipitation data were acquired from a site in Golden and at the intersection of state highway 93 and van Bibber creek (Figure 1.1). Precipitation data from these sites are presented in Appendix E. Figure 6.3 provides a comparison of

precipitation at van Bibber Creek and Golden sites between monitoring intervals. Precipitation was not monitored at van Bibber Creek during winter months.

Runoff (RO)

Runoff was assumed to be insignificant at this site. No runoff was visible during an August precipitation event where

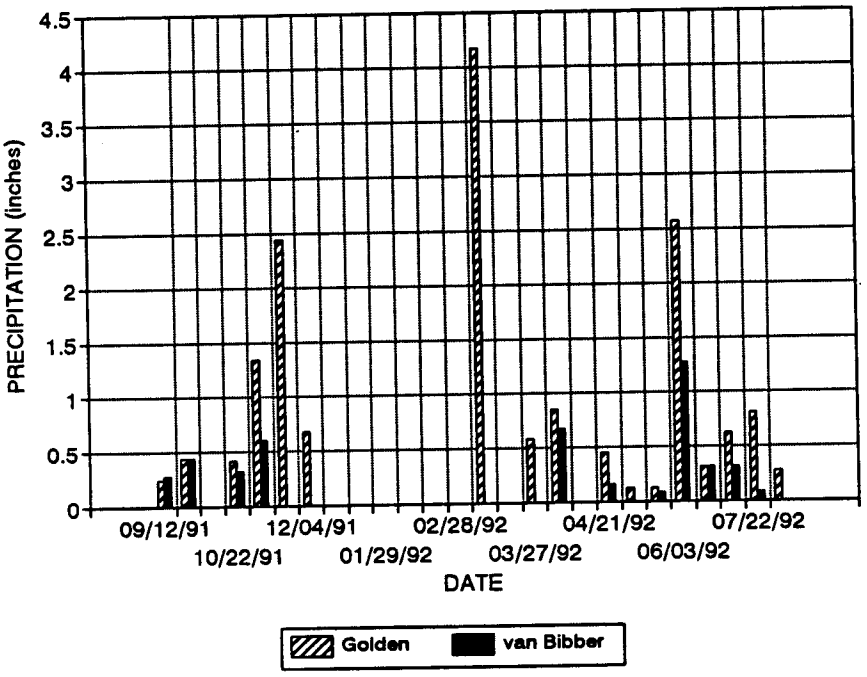

Figure 6.3 Precipitation at van Bibber Creek and Golden between monitoring intervals

approximately 2.8 inches of rain fell in 24 hours. Similar observations were made at a field site at the Rocky Flats Plant (M.Z. Litaor, 1992) which has a slope greater than the study area.

Change in Soil Moisture Storage (ΔS)

The amount of soil water in storage was obtained directly from integrating the moisture profile measured with the neutron probe using Simpson's Rule. The change in storage is equal to the difference in total storage between measurements. As discussed in section 1, neutron probes are limited by the depth at which readings can be taken. Readings above approximately 9 inches are subject to atmospheric effects. Neutrons are lost to the atmosphere yielding inaccurate readings. If neutron readings are taken several days after a precipitation event, it is reasonable to assume that water that has penetrated to 9 inches will be lost or has been lost to evapotranspiration. If readings are taken immediately after a precipitation event while water is above the neutron probe sphere of influence, it is incorporated into the ET component of equation 6.5. This is the case with snowfall events due to the lag between the snowfall event and subsequent melting and infiltration.

Vertical Flow (Q_v)

The calculated vertical flux rates presented in the previous section are 5 to 6 orders of magnitude lower than the amount of precipitation over the same period. Therefore,

vertical flow is assumed to be zero over the time periods which evapotranspiration is calculated.

Lateral Flow (Q_l))

The most uncertain term in this equation is lateral flow. If lateral flow occurs within the effective rooting depth of the vegetation, it is not possible to distinguish between lateral flow and evapotranspiration with the instrumentation used in this study. Lateral flow was assumed to be zero for evapotranspiration calculations.

Evapotranspiration (ET)

Evapotranspiration was calculated using equation 6.5.

6.2.2 Potential Evapotranspiration

Precipitation in the vicinity of the Colorado Front Range is often localized. Comparing precipitation from Golden and van Bibber Creek, reveals deviations that can significantly affect evapotranspiration calculations (Figure 6.3). To

assess the reliability of evapotranspiration calculations, potential evapotranspiration was calculated. If actual evapotranspiration is higher than potential evapotranspiration, results should be regarded with caution.

Potential evapotranspiration can be defined as "the amount of water transpired in unit time by a short green crop, completely shading the ground, of uniform height and never short of water", (Penman, 1956). Although these conditions are not met at the study site, estimation of potential evapotranspiration provides a useful estimate of the maximum amount of water that can be evapotranspirated. Many methods exist for estimating potential evapotranspiration including temperature, eddy correlation, statistical, energy balance and mass balance methods. A good review of these methods is provided by Jensen *et al.* (1990). The method chosen for this study is the FAO Penman equation (Doorenbos and Pruitt, 1977) which was derived for a grass reference crop. This is a combination energy balance, heat and mass transfer equation which is widely used in the agricultural industry. This equation is expressed as:

$$E=c\left[\frac{\Delta}{\Delta+\gamma}(R_n-G)+\frac{\gamma}{\Delta+\gamma}2.7W_f(e_{mean}-e_d)\right] \qquad [6.6]$$

where:

c = adjustment factor for differences between daytime and nighttime conditions

Δ = slope of the saturation vapor pressure-temperature curve = $\frac{4098e_{mean}}{(T_{mean}+237.3)^2}$ [kPa °C^{-1}]

e_{mean} = saturation vapor pressure at T_{mean} = $\exp\left[\frac{16.78T_{mean}-116.9}{T_{mean}+237.3}\right]$ [kPa]

T_{mean} = mean temperature [°C]

γ = Psychometric constant = $\frac{c_pP}{0.622\lambda}$ [kPa °C^{-1}]

c_p = specific heat of moist are at a constant pressure = 1.013 [kJ kg^{-1} °C]

λ = latent heat of vaporization of water = $2.501 - 2.316(10)^{-3}T_{mean}$ [kJ kg^{-1}]

R_n = Net Radiation = $(1-\alpha)R_s-R_b$ [mm]

α = $.29 + 0.6\sin[30(m+0.0333n + 22.5)]$

m = month (1-12)

n = day (1-31)

R_s = measured solar radiation [MJ m^{-2} d^{-1}]

R_b = net outgoing long-wave radiation

$$R_b = \left(a\frac{R_s}{R_{so}} + b\right) R_{bo} \quad [\text{MJ m}^{-2}\ \text{d}^{-1}]$$

a = if $\frac{R_s}{R_{so}} > 0.7$, a = 1.126, else a = 1.017

b = if $\frac{R_s}{R_{so}} > 0.7$, b = -0.07, else b = -0.06

R_{so} = solar radiation on a cloudless day = $A' + B' \cos\left[\frac{(2\pi d)}{365} - C\right]$ [MJ m^{-2} d^{-1}]

R_{bo} = net outgoing log-wave radiation on a cloudless day = $(a_1 + b_1\sqrt{e_d})\ \frac{4.90}{10^9}\ \frac{T_{kmax}^4 + T_{kmin}^4}{2}$ [MJ m^{-2} d^{-1}]

T_{kmax} = maximum temperature [°K]

T_{kmin} = minimum temperature [°K]

a_1 = $0.26 + 0.1\exp-[0.0154(30m + n - 207)]^2$

b_1 = -0.139

e_d = saturation vapor pressure at dewpoint temperature = $e_{mean}\frac{RH}{100}$ [kPa]

RH = relative humidity [%]

d = calendar day (1-365)

A' = 31.54 - .0273 Latitude° + 0.00078 E

E = Elevation [m]

B' = -0.30 + 0.268 Latitude° + 0.00041 E

C' = 2.93

G = Heat flux density to the ground (assumed 0 for daily periods) [MJ m^{-2} d^{-1}]

W_f = wind function = $(0.01\ u_2 + 1.0)$

u_2 = wind speed at 2 meters = $u_n[\frac{z_2}{z_n}]^{0.2}$ [km d^{-1}]

z_n = height at which wind speed (u_n) was measured [m]

A fortran program was written to compute potential evapotranspiration from hourly solar radiation, maximum and minimum temperature, wind speed, relative humidity, and barometric pressure measurements. The fortran source code is presented in Appendix F. Data were obtained from a meteorological station operated by the city of Aurora at Quincy Reservoir, approximately 30 miles east of the study area. Missing hourly data was inferred from neighboring days at the same time. Hourly data was missing for several entire days. These days were eliminated from calculations and evapotranspiration rates were taken as the average of the preceding and following day.

6.2.3 Results

Results of actual and potential evapotranspiration calculations are presented in Tables 6.3 through 6.7. Computation of actual evapotranspiration during winter months resulted in negative values. This problem was discussed in

section 6.2.1 and is caused by the lag between snowfall events and subsequent melting and infiltration. It is not possible to determine the timing of snowmelt water availability for infiltration with the instrumentation at this field site. Figure 6.4 provides a comparison between actual and potential evapotranspiration for hole 6 using van Bibber precipitation data.

Actual evapotranspiration calculated using the Golden data was higher than potential evapotranspiration for the 5/15/92 through 6/6/92 monitoring interval due to the higher precipitation recorded in Golden. This demonstrates the errors that occur as a result of extrapolating precipitation data over even moderate distances in this environment. Actual evapotranspiration calculations using the van Bibber precipitation station data are believed to be more reliable for the study site than those using Golden precipitation data. However, all evapotranspiration results should be regarded with caution due to the length of time between moisture profile measurements and the lack of accurate on-site precipitation data.

Total potential evapotranspiration calculated from September 1991 through September 1992 is 43.49 inches. This value is close to the yearly average of 39.19 inches reported by Koffer (1989). A daily summary of potential

evapotranspiration calculated for this study is presented in Appendix G.

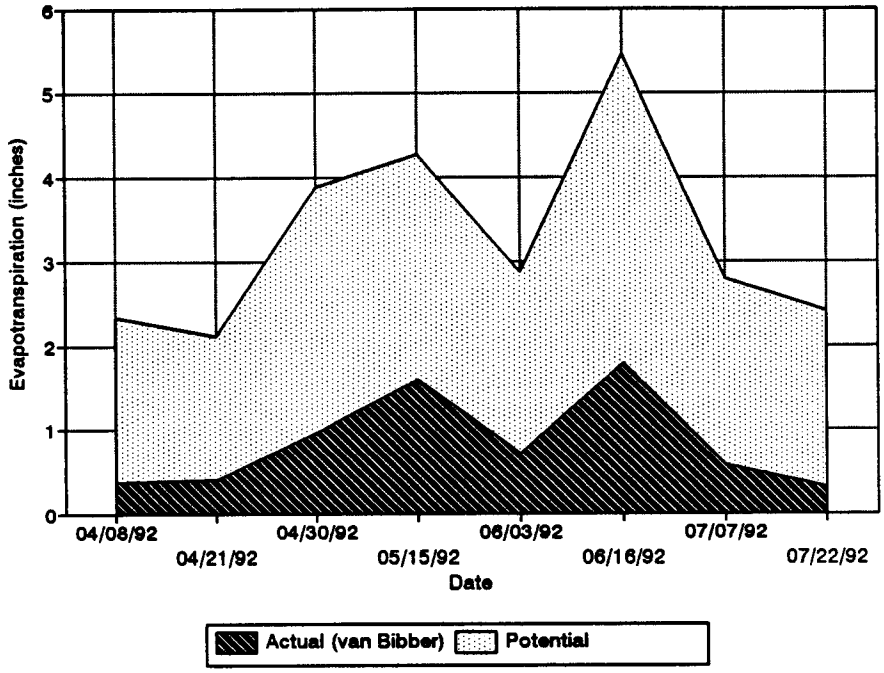

Figure 6.4 Actual versus potential evapotranspiration for hole 6 using van Bibber precipitation data

Table 6.4 Results of evapotranspiration calculations for hole 1.

Measurement Interval		Change in Storage	Golden Data			Van Bibbber Data			Potental ET
From	To	(inches)	Precipitation (inches)	Actual ET (inches)	Actual ET (inches/day)	Precipitation (inches)	Actual ET (inches)	Actual ET (inches/day)	(inches)
09/05/91	09/12/91	-0.16	0.24	0.40	0.058	0.28	0.44	0.063	1.393
09/12/91	09/19/91	-0.06	0.44	0.50	0.071	0.44	0.50	0.071	1.019
09/19/91	09/27/91	-0.25	0.00	0.25	0.031	0.00	0.25	0.031	1.474
09/27/91	10/22/91	0.20	0.42	0.22	0.009	0.32	0.12	0.005	3.652
10/22/91	11/08/91	0.04	1.34	1.30	0.076	0.60	0.56	0.033	1.470
11/08/91	11/21/91	0.35	2.44	2.09	0.160				0.958
11/21/91	12/04/91	0.87	0.68	-0.19	-0.014				0.740
12/04/91	12/12/91	0.21	0.00	-0.21	-0.026				0.679
12/12/91	01/21/92	0.21	0.00	-0.21	-0.005				2.489
01/21/92	01/29/92	-0.06	0.00	0.06	0.007				0.780
01/29/92	02/05/92	0.16	0.00	-0.16	-0.023				0.665
02/05/92	02/13/92	-0.19	0.00	0.19	0.024				0.613
02/13/92	02/28/92	0.16	0.00	-0.16	-0.011				1.596
02/28/92	03/12/92	1.41	4.16	2.75	0.212				1.180
03/12/92	03/27/92	3.12	0.75	-2.37	-0.158				1.801
03/27/92	04/02/92	0.52	0.85	0.33	0.055	0.67	0.15	0.025	0.694
04/02/92	04/08/92	-0.16	0.00	0.16	0.026	0.00	0.16	0.026	1.016
04/08/92	04/21/92	0.17	0.45	0.28	0.022	0.16	-0.01	-0.000	1.980
04/21/92	04/30/92	-0.44	0.13	0.57	0.063	0.00	0.44	0.049	1.722
04/30/92	05/15/92	-0.94	0.13	1.07	0.071	0.08	1.02	0.068	2.927
05/15/92	06/03/92	-0.43	2.57	3.00	0.158	1.27	1.70	0.090	2.685
06/03/92	06/16/92	-0.50	0.32	0.82	0.063	0.32	0.82	0.063	2.169
06/16/92	07/07/92	-1.18	0.63	1.81	0.086	0.32	1.50	0.072	3.672
07/07/92	07/22/92	-0.71	0.81	1.52	0.101	0.08	0.79	0.053	2.231
07/22/92	08/04/92	-0.54	0.28	0.82	0.063	0.00	0.54	0.041	2.112

Table 6.5 Results of evapotranspiration calculations for hole 2.

Measurement Interval		Change in Storage	Golden Data			Van Bibber Data			Potential ET
From	To	(inches)	Precipitation (inches)	Actual ET (inches)	Actual ET (inches/day)	Precipitation (inches)	Actual ET (inches)	Actual ET (inches/day)	(inches)
09/05/91	09/12/91	0.25	0.24	-0.01	-0.002	0.28	0.03	0.004	1.393
09/12/91	09/19/91	-0.54	0.44	0.98	0.140	0.44	0.98	0.140	1.019
09/19/91	09/27/91	-0.73	0.00	0.73	0.091	0.00	0.73	0.091	1.474
09/27/91	10/22/91	-0.06	0.42	0.48	0.019	0.32	0.38	0.015	3.652
10/22/91	11/08/91	0.25	1.34	1.09	0.064	0.60	0.35	0.021	1.470
11/08/91	11/21/91	0.54	2.44	1.90	0.147				0.958
11/21/91	12/04/91	1.94	0.68	-1.26	-0.097				0.740
12/04/91	12/12/91	0.48	0.00	-0.48	-0.059				0.679
12/12/91	01/21/92	-0.52	0.00	0.52	0.013				2.489
01/21/92	01/29/92	0.21	0.00	-0.21	-0.026				0.780
01/29/92	02/05/92	0.01	0.00	-0.01	-0.001				0.665
02/05/92	02/13/92	-0.34	0.00	0.34	0.042				0.613
02/13/92	02/28/92	-0.02	0.00	0.02	0.001				1.596
02/28/92	03/12/92	1.71	4.16	2.45	0.189				1.180
03/12/92	03/19/92	3.80	0.17	-3.43	-0.490				0.758
03/19/92	03/27/92	0.49	0.58	0.09	0.011				0.907
03/27/92	04/02/92	0.96	0.85	-0.10	-0.016	0.67	-0.26	-0.046	0.694
04/02/92	04/08/92	0.80	0.00	-0.80	-0.133	0.00	-0.80	-0.133	1.016
04/08/92	04/21/92	-0.16	0.45	0.61	0.047	0.16	0.32	0.025	1.980
04/21/92	04/30/92	-1.04	0.13	1.17	0.130	0.00	1.04	0.116	1.722
04/30/92	05/15/92	-0.28	0.13	0.41	0.027	0.08	0.36	0.024	2.927
05/15/92	06/03/92	-0.61	2.57	3.18	0.167	1.27	1.88	0.099	2.685
06/03/92	06/16/92	-0.59	0.32	0.91	0.070	0.32	0.91	0.070	2.169
06/16/92	07/07/92	-1.25	0.63	1.88	0.090	0.32	1.57	0.075	3.672
07/07/92	07/22/92	-1.12	0.81	1.93	0.128	0.08	1.20	0.080	2.231
07/22/92	08/04/92	-0.80	0.28	1.08	0.083	0.00	0.80	0.062	2.112

Table 6.6 Results of evapotranspiration calculations for hole 3.

Measurement interval		Change in Storage	Golden Data			Van Bibber Data			Potential ET
From	To	(inches)	Precipitation (inches)	Actual ET (inches)	Actual ET (inches/day)	Precipitation (inches)	Actual ET (inches)	Actual ET (inches/day)	(inches)
08/29/91	09/05/91	-0.41	0.00	0.41	0.058	0.00	0.41	0.058	1.452
09/05/91	09/12/91	-0.04	0.24	0.28	0.040	0.28	0.32	0.045	1.393
09/12/91	09/19/91	-0.26	0.44	0.70	0.101	0.44	0.70	0.101	1.019
09/19/91	09/27/91	-0.04	0.00	0.04	0.005	0.00	0.04	0.005	1.474
09/27/91	09/30/91	-0.06	0.26	0.32	0.105	0.20	0.26	0.085	0.593
09/30/91	10/01/91	-0.30	0.00	0.30	0.301	0.00	0.30	0.301	0.092
10/01/91	10/22/91	0.07	0.16	0.09	0.004	0.12	0.05	0.002	3.060
10/22/91	11/08/91	0.37	1.34	0.97	0.057	0.60	0.23	0.013	1.470
11/08/91	11/21/91	0.04	2.44	2.40	0.185				0.958
11/21/91	12/04/91	1.41	0.68	-0.73	-0.056				0.740
12/04/91	12/12/91	-0.01	0.00	0.01	0.001				0.679
12/12/91	01/21/92	-0.23	0.00	0.23	0.006				2.489
01/21/92	01/29/92	-0.01	0.00	0.01	0.001				0.780
01/29/92	02/05/92	-0.07	0.00	0.07	0.010				0.665
02/05/92	02/13/92	0.05	0.00	-0.05	-0.006				0.613
02/13/92	02/28/92	0.10	0.00	-0.10	-0.007				1.596
02/28/92	03/12/92	1.10	4.16	3.06	0.235				1.180
03/12/92	03/19/92	1.58	0.17	-1.41	-0.202				0.758
03/19/92	03/27/92	0.49	0.58	0.09	0.011				0.907
03/27/92	04/02/92	0.42	0.85	0.43	0.071	0.67	0.25	0.041	0.694
04/02/92	04/08/92	0.34	0.00	-0.34	-0.057	0.00	-0.34	-0.057	1.016
04/08/92	04/21/92	0.23	0.45	0.22	0.017	0.16	-0.07	-0.005	1.980
04/21/92	04/30/92	-0.38	0.13	0.51	0.056	0.00	0.38	0.042	1.722
04/30/92	05/15/92	-0.47	0.13	0.60	0.040	0.08	0.55	0.037	2.927
05/15/92	06/03/92	-0.53	2.57	3.10	0.163	1.27	1.80	0.095	2.685
06/03/92	06/16/92	-0.23	0.32	0.55	0.042	0.32	0.55	0.042	2.169
06/16/92	07/07/92	-0.82	0.63	1.45	0.069	0.32	1.14	0.054	3.672
07/07/92	07/22/92	-0.77	0.81	1.58	0.106	0.08	0.85	0.057	2.231
07/22/92	08/04/92	-0.33	0.28	0.61	0.047	0.00	0.33	0.026	2.112

Table 6.7 Results of evapotranspiration calculations for hole 4.

Measurement Interval		Change in Storage	Golden Data			Van Bibber Data			Potentail ET
From	To	(inches)	Precipitation (inches)	Actual ET (inches)	Actual ET (inches/day)	Precipitation (inches)	Actual ET (inches)	Actual ET (inches/day)	(inches)
08/29/91	09/05/91	-0.45	0.00	0.45	0.065	0.00	0.45	0.065	1.452
09/05/91	09/12/91	-0.50	0.24	0.74	0.105	0.28	0.78	0.111	1.393
09/12/91	09/19/91	-0.28	0.44	0.72	0.103	0.44	0.72	0.103	1.019
09/19/91	09/27/91	-0.73	0.00	0.73	0.091	0.00	0.73	0.091	1.474
09/27/91	09/30/91	0.12	0.26	0.14	0.047	0.20	0.08	0.027	0.593
09/30/91	10/01/91	-0.26	0.00	0.26	0.260	0.00	0.26	0.260	0.092
10/01/91	10/22/91	0.01	0.16	0.15	0.007	0.12	0.11	0.005	3.060
10/22/91	11/08/91	0.36	1.34	0.98	0.058	0.60	0.24	0.014	1.470
11/08/91	11/21/91	0.74	2.44	1.70	0.131				0.958
11/21/91	12/04/91	1.95	0.68	-1.27	-0.098				0.740
12/04/91	12/12/91	0.10	0.00	-0.10	-0.012				0.679
12/12/91	01/21/92	-0.09	0.00	0.09	0.002				2.489
01/21/92	01/29/92	0.09	0.00	-0.09	-0.011				0.780
01/29/92	02/05/92	0.06	0.00	-0.06	-0.009				0.665
02/05/92	02/13/92	-0.33	0.00	0.33	0.041				0.613
02/13/92	02/28/92	0.18	0.00	-0.18	-0.012				1.596
02/28/92	03/12/92	1.70	4.16	2.46	0.189				1.180
03/12/92	03/19/92	2.49	0.17	-2.32	-0.332				0.758
03/19/92	03/27/92	0.49	0.58	0.09	0.012				0.907
03/27/92	04/02/92	1.33	0.85	-0.48	-0.081	0.67	-0.66	-0.111	0.694
04/02/92	04/08/92	0.13	0.00	-0.13	-0.021	0.00	-0.13	-0.021	1.016
04/08/92	04/21/92	-0.33	0.45	0.78	0.060	0.16	0.49	0.038	1.980
04/21/92	04/30/92	-0.37	0.13	0.50	0.056	0.00	0.37	0.041	1.722
04/30/92	05/15/92	-0.98	0.13	1.11	0.074	0.08	1.06	0.071	2.927
05/15/92	06/03/92	-0.71	2.57	3.28	0.173	1.27	1.98	0.104	2.685
06/03/92	06/16/92	-0.66	0.32	0.98	0.076	0.32	0.98	0.076	2.169
06/16/92	07/07/92	-1.77	0.63	2.40	0.114	0.32	2.09	0.099	3.672
07/07/92	07/22/92	-0.99	0.81	1.80	0.120	0.08	1.07	0.071	2.231
07/22/92	08/04/92	-0.62	0.28	0.90	0.069	0.00	0.62	0.048	2.112

Table 6.8 Results of evapotranspiration calculations for hole 6.

Measurement Interval		Change in Storage	Golden Data			Van Bibber Data			Potential ET
From	To	(inches)	Precipitation (inches)	Actual ET (inches)	Actual ET (inches/day)	Precipitation (inches)	Actual ET (inches)	Actual ET (inches/day)	(inches)
03/19/92	03/27/92	0.70	0.58	-0.12	-0.015				0.907
03/27/92	04/02/92	0.77	0.85	0.08	0.014	0.67	-0.10	-0.016	0.694
04/02/92	04/08/92	0.12	0.00	-0.12	-0.020	0.00	-0.12	-0.020	1.016
04/08/92	04/21/92	-0.21	0.45	0.66	0.051	0.16	0.37	0.029	1.980
04/21/92	04/30/92	-0.41	0.13	0.54	0.060	0.00	0.41	0.045	1.722
04/30/92	05/15/92	-0.88	0.13	1.01	0.067	0.08	0.96	0.064	2.927
05/15/92	06/03/92	-0.33	2.57	2.90	0.153	1.27	1.60	0.084	2.685
06/03/92	06/16/92	-0.39	0.32	0.71	0.054	0.32	0.71	0.054	2.169
06/16/92	07/07/92	-1.48	0.63	2.11	0.100	0.32	1.80	0.086	3.672
07/07/92	07/22/92	-0.50	0.81	1.31	0.087	0.08	0.58	0.039	2.231
07/22/92	08/04/92	-0.31	0.28	0.59	0.045	0.00	0.31	0.024	2.112

7.0

CONCLUSIONS

This study has shown that a static moisture profile existed below 3 feet from September 1991 through February 1992. Corresponding matric potentials at this depth are believed to be greater than 15 bars. Although water did infiltrate short vertical distances, most of it was used to meet evapotranspiration demands. Significant infiltration below this depth occurred during March, when the highest precipitation for the 10 year record was recorded. Based on neutron probe moisture readings, this wetting front is not believed to have penetrated below 6.75 feet. At the conclusion of the study, the moisture profile below 3 feet had not returned to the condition that existed the previous year. It is hypothesized that the additional water will be consumed by the native grasses and not contribute to groundwater recharge. Monitoring will be continued to validate this hypothesis.

Numerical simulation of vertical flux based on steady state moisture profiles ranged from $9.7(10)^{-6}$ to $4.9(10)^{-4}$ inches per year. Although total precipitation in March was the highest recorded in 10 years, it did not provide enough water to penetrate below 6.75 feet. To produce a wetting

front capable of contributing to groundwater recharge or soil-moisture storage below 10 feet, it may require a series of wet months in early spring when evapotranspiration demands are low. Average recharge estimates of 0.1 inches per year for the Denver Basin and 0.8 inches per year reported by various authors for regions east of the Colorado Front Range are not reasonable for this site as a yearly average. However, the this site represents a small portion of the Denver Basin. Much higher recharge rates may occur in portions of the Denver Basin where different hydrogeologic properties are present. The primary contribution to groundwater recharge near the study site may occur through macropore flow or in limited areas where hydrogeologic conditions are more favorable such as creek beds, depressions, or areas with higher water tables or different hydraulic properties.

This study also revealed limitations of available soil sampling equipment and using neutron probe moisture readings to predict matric potential in dry soils. Neutron probes take readings over a sphere of influence. These readings were applied to moisture characteristic curves from samples representing a much smaller volume to determine matric potential. Heterogeneities within the neutron probe sphere of influence result in inaccurate matric potentials. This problem is compounded in dry soils due to the increased

sensitivity of matric potential to moisture content. Soil sampling using a slide hammer caused sample compaction. As a consequence of sample compaction, moisture characteristic curves were altered. Moisture contents determined in the laboratory were used to determine *in situ* matric potentials by comparing moisture contents to moisture characteristic curves developed on immediately adjacent samples from the same sample interval. This often resulted in unreasonably high matric potentials.

Despite these difficulties, using neutron probes to monitor vertical movement of soil-moisture in the vadose zone is cost effective and provides valuable information. Moisture profiles provide information on the existence and timing of transient moisture movent. Although it is difficult to use neutron probe readings to predict matric potentials in dry soils, reasonable estimates of vertical flux can be made. As shown in this study, little water moves under these conditions.

8.0

RECOMMENDATIONS

This study has shown that the contribution to groundwater recharge in bedrock aquifers was minimal from this study site during the period of this study. Monitoring at this site should be continued for several years to draw relationships between the timing and amount of precipitation and subsequent water movement. Although a wetting front may not penetrate below the depth of the neutron access tubes every year, it is important to determine if this does occur, and if it does, under what conditions. It is also recommended that deeper neutron access tubes are installed should a wetting front progress below 10 feet. These access tubes may also be used to determine if there is transient moisture movement due to lateral flow at greater depths.

Additionally, this site represents only a small portion of the Denver Basin. Larger recharge rates may occur in localized areas with different hydraulic, geomorphic, and vegetative properties. Future studies should be conducted to determine the presence or extent localized recharge. Possible areas to examine include creek beds, localized depressions, areas with coarse grained material and relatively shallow water tables. Through these types of studies, it may be

possible to develop relationships between geomorphology, vegetation, soil properties, and groundwater recharge.

Several improvements can be made on this study. Difficulties were encountered in trying to predict *in situ* matric potentials in the dry soils at this study site. These difficulties may be reduced by using sampling equipment that minimizes compaction, such as the Madera Soil Sampler (the design is available through the American Society of Agricultural Engineers - Irrigation and Drainage Division). Improved evapotranspiration estimates can be achieved through more regular monitoring and better estimates of moisture content near the ground surface. Matric potential readings from shallow tensiometers may be used to predict moisture content above the neutron probe measurements. And finally, an accurate rain gauge at the site would eliminate the need to extrapolate precipitation data.

9.0

REFERENCES CITED

Allen, R.G. and Segura, D., 1990. Access tube Characteristics and Neutron Meter Calibration: Proceedings of the National Conference on Irrigation and Drainage, ASCE, July 11 - 13, 1990 pp. 21-31.

Boettcher, A.J., 1966. Geology and Ground-Water Resources of Eastern Cheyenne and Kiowa Counties, Colorado: U.S. Geological Survey Water Supply Paper 1891-I

Bouwer, H., 1978. Groundwater Hydrology: New York, McGraw-Hill Book Company, 480p.

Balek, J., 1988. Groundwater Recharge Concepts: Estimation of Natural Groundwater Recharge. Ed. I. Simmers, Dordrecht, D. Reidel Publishing Co., pp. 3 - 9

Cardwell, W.D.E., and Jenkins, E.D., 1963. Geology of Ground-Water Resources of the Frenchman Creek Basin of Colorado and Nebraska above Palisade, Nebraska: U.S. Geological Survey Water Supply Paper 1577

CPN Corporation, 1984-1985. 503 DR Hydroprobe Operating Manual: Martinez, CPN Corporation, 104 p.

Daas, B.M., 1990. Principles of Geotechnical Engineering, 2nd Edition: Boston, RWS - KENT Publishing Company, 665 p.

Davis, L.C., and Pittman, J.R., 1990. Hydrological, Meteorological, and Geohydrological Data for an Unsaturated Zone Study near the Radioactive Waste Management Complex, Idaho National Engineering Laboratory, Idaho - 1987: U.S. Geological Survey Open File Report 90-114., 189 p.(check)

Dickey, G.L., 1990a. Factors Affecting Neutron Meter Calibration: Proceedings of the National Conference on Irrigation and Drainage, ASCE, July 11 - 13, 1990 pp. 9-20

Dickey, G.L., 1990b. Field Calibration of Neutron Gauges: SCS Method: Proceedings of the National Conference on Irrigation and Drainage, ASCE, July 11 - 13, 1990, pp. 192-201

Doorenbos, J., and Pruitt, W.O., 1977. Guidelines for Predicting Crop Water Requirements: FAO Irrigation and Drainage Paper No. 24, 2nd ed., FAO Rome, Italy. 156 p.

Durner, W., 1989. Predicting the Unsaturated Hydraulic Conductivity Using Multiporosity Water Retention Curves: Program and Abstracts of the International Workshop on Indirect Methods for Estimating the Hydraulic Properties of Unsaturated Soils, October 11 - 13, 1989 pp. 26.

Enfield, C.G., Hsiesh, J.J.C., and Warwick, A.W., 1973. Evaluation of Water Flux above a Deep Water Table using Thermocouple Psychrometers: Soil Sci. Soc. Am. Proc., 37, pp. 968-970

Freeze, R.A. and Cherry, J.A. 1979. Groundwater: Englewood Cliffs, Pretence-Hall Inc., 604p.

Gee, G.W., and Hillel, D., 1988. Groundwater Recharge in Arid Regions: Review and Critique of Estimation Methods: Hydrological Processes, V. 2, pp. 255 -266.

Hammermeister, D.P., Blout, D.O., and McDaniel, J.C., 1985 Drilling and Coring Methods that Minimize the Disturbance of Cuttings, Core, and Rock Formation in the Unsaturated Zone, Yucca Mountain, Nevada. Proceedings of the NWWA Conference on Characterization and Monitoring of the Vadose (Unsaturated) Zone, November 19 - 21, 1985, pp. 507 - 563.

Haverkamp, R., and Vauclin, M., 1979. A Note on Estimating Finite Difference Interblock Hydraulic Conductivity Values for Transient Unsaturated Flow Problems: Water Resources Research, V. 15, No. 1, pp. 181-187

Haverkamp, R., Vauclin, M., and Vachaud, G., 1984. Error Analysis in Estimating Soil Water Content from Neutron Probe Measurements: 1. Local Standpoint: Soil Science, V. 137, No. 2, pp. 78-90

Healy, R.W, 1990. Simulation of Solute Transport In Variably Saturated Porous Media with Supplemental Information on Modifications to the U.S. Geological Survey's Computer Program VS2D: U.S. Geological Survey Water Resources Investigation Report 90-4025

Hillel, D., 1980. Fundamentals of Soil Physics: San Diego, Academic Press Inc., 413p.

Holmes, J.W., 1966. Influence of Bulk Density of the Soil on Neutron Moisture Meter Calibration: Soil Science, V. 102, no. 6, pp. 355-360.

Jackson, R.D., Reginato, and van Bavel, C.H.M., 1965. Comparison of Measured and Calculated Hydraulic Conductivities of Unsaturated Soils: Water Resources Research, V. 1, pp. 375-380.

Jensen, M.E., Burman, R.D., and Allen, R.G., Ed., 1990. Evapotranspiration and Irrigation Water Requirements: New York, American Society of Civil Engineers., 332p.

Keller, B.R., Everett, L.G., and Marks, R.J., 1990. Effects of Access Tube Material and Grout on Neutron Probe Measurements in the Vadose Zone: Ground Water Monitoring Review. Winter 1990, p 96-100

Klute, A., Danielson R.E., Linden, D.R., and Hamaker, P., 1972. Ground Water Recharge as Affected by Surface Vegetation and Management: Colorado Water Resources Institute, Completion Report No. 41

Koffer, J.P., 1989. Investigation of the Surface and Groundwater Flow Mechanics of an Evaporation Spray Field at the Rocky Flats Nuclear Weapons Plant, Jefferson County, Colorado: Colorado School of Mines, Master of Engineering Report ER-3728

Litaor, M.Z., 1992. Personal Communication: EG&G Rocky Flats Inc., Golden, Co.

Lohman, S.W. 1972. Definitions of Selected Ground-Water Terms - Revisions and Conceptual Refinements: U. S. Geological Survey Water-Supply Paper 1988, 21p.

McGovern, H.E., 1964. Geology and Ground Water Resources of Washington County, Colorado: U.S. Geological Survey Water Supply Paper 1777

Mualem, Y., 1976. A New Model for Predicting the Hydraulic Conductivity of Unsaturated Porous Media: Water Resources Research, V. 12, pp. 513 - 522.

Mualem, Y., and Dagan, G., 1978. Hydraulic Conductivity of Soils: Unified approach to the Statistical Models: Soil Sci. Soc. Am. J., V. 42 pp. 392 - 395.

Mualem. Y., 1984. Anisotropy of Unsaturated Soils: Soil Sci. Soc. Am. J., V. 48, pp. 505-509.

Mualem, Y., 1986. Hydraulic Conductivity of Unsaturated Soils: Prediction and Formulations: Methods of Soil Analysis, Part 1, Physical and Mineralogical Methods, Ed. A. Klute, Madison, American Society of Agronomy. pp. 799 - 823.

Nixon, P.R.. Lawless, G.P., and McOrmick, R.L., 1972. Soil Hydrology in a Semiarid Watershed: Transactions of the American Society of Agricultural Engineers, Vol. 15, No. 5., pp. 985-991

Olgaard, P.L. and Haar, V., 1968. On the Sensitivity of Subsurface Neutron Moisture Gauges to Variations in Bulk Density: Soil Science, V. 127, no. 1, pp. 62-64.

Olsen, H.W., Gill, J.D., Wilden, A.T, and Nelson K.R. 1991. Innovations in Hydraulic-Conductivity Measurements: Transportation Research Record, No. 1309, pp. 9 - 17.

Penman, H.L., 1956. Evaporation: An Introductory Survey: Netherlands J. Agric. Sci., Vol. 1, pp. 9-29, 87-97, 151-153.

Price, A.B., and Amen, A.E., 1983. Soil Survey of the Golden Area, Colorado: U. S. Department of Agriculture Soil Conservation Service

Reddell, D.W., 1967. Distribution of Ground Water Recharge: Technical Report No. AER 66-67 DLR 91, Agricultural Engineering Department, Colorado State University, Fort Collins, Colorado

Remson, I., and Randolph, J.R. 1962. Review of Some Elements of Soil-Moisture Theory: U. S. Geological Survey Professional Paper 411-D. 38p.

Richards, L.A., 1931. Capillary conduction of liquids through porous mediums: Physics, v. 1, pp. 318-333.

Robson, S.G., 1987. Bedrock Aquifers in the Denver Basin, Colorado; A Quantitative Water-Resources Appraisal: U.S. Geological Survey Proffesional Paper 1257, 73p.

Rushton, K.R., 1988. Numerical and Conceptual Models for Recharge Estimation in Arid and Semi-Arid Zones: Estimation of Natural Groundwater Recharge. Ed. I. Simmers, Dordrecht, D. Reidel Publishing Co., pp. 223-238

Shirazi, G.A., and Isobe, M., 1976. Calibration of Neutron Probe in some Selected Hawaiian Soils: Soil Science, V. 122, no. 3., pp. 165-170.

Stephens, D. B., and Knowlton, R. Jr., 1986. Soil Water Movement and Recharge Through Sand at a Semiarid Site in New Mexico: Water Resources Research, V. 22, No. 6., pp. 881-889

Stephens, D. B., and McOrd, J. T., 1987. Infiltration and Recharge on a Sandy Hillslope in and Arid Climate: Proceedings of the International Conference on Infiltration Development and Application, January 6 - 9, 1987 pp. 351-360

Stone, J.F., 1990. Relationship of Soil Type and Chemicals to the Calibration of Neutron Meters: Proceedings of the National Conference on Irrigation and Drainage, ASCE, July 11 - 13, 1990 pp. 32-38

van Bavel, C.M., 1956. Neutron and Gamma Radiation as Applied to Measuring Physical Properties of Soils in its Natural State: Transactions of the 6th International Congress of Soil Science, Paris, France, pp. 355-360

van Bavel, C.H.M., Brust, K.J., and Stirk, G.B., 1968. Hydraulic Properties of a Clay Loam and the Field Measurement of Water Uptake by Roots: II. The Water Balance of the Root Zone: Soil Sci. Amer. Proc., Vol. 32

Van Horn, R., 1957. Bedrock Geology of the Golden Quadrangle, Colorado: U. S. Geological Survey Quadrangle Map GQ-103

van Genuchten, M. Th., 1980. A Closed-Form Equation for Predicting the Hydraulic Conductivity of Unsaturated Soils: Soil Society of America Journal. V. 44, pp. 892 - 898.

van Genuchten, M. Th., 1986. SOHYP An Analytical Model for the Calculation of the Unsaturated Hydraulic Conductivity Function: Golden, International Ground Water Modeling Center / Institute for Ground-Water Research and Education, 63 p.

Van Tonder, G.J., and Kirchner, J., 1990. Estimation of Natural Groundwater Recharge in the Karoo Aquifers of South Africa: Journal of Hydrology, V. 121, pp. 395 - 419.

Weist, W.G., Jr, 1964. Geology and Ground-Water Resources of Yuma County, Colorado: U.S. Geological Survey Water Supply Papers 1539-J

Wilson, L.G., 1982. Monitoring in the Vadose Zone: Part II: Ground Water Monitoring Review, Winter, 1982, pp. 34-42.

Appendix A

SOIL-MOISTURE CONTENT MEASUREMENTS

HOLE #1

Date	Depth (ft)									Water in Storage (inches)
	0.75	1.75	2.75	3.75	4.73	5.75	6.75	7.75	8.75	
	Moisture Content (% Vol)									.75 to 8.75 ft
9/5/91	11.60	16.86	20.37	14.34	14.46	17.06	15.62	16.20	14.74	15.41
9/12/91	10.49	15.69	20.35	14.26	14.67	17.40	15.68	16.24	14.80	15.25
9/19/91	10.65	15.31	20.64	14.27	14.73	17.39	15.89	15.94	14.85	15.19
9/27/91	9.83	14.94	20.54	14.19	14.64	16.84	15.39	15.96	14.66	14.94
10/22/91	9.93	15.09	20.30	14.29	14.89	17.08	15.68	16.48	15.12	15.14
11/8/91	12.03	14.89	20.56	14.56	14.96	17.03	15.38	16.11	15.41	15.18
11/21/91	17.26	15.43	20.22	14.56	14.93	16.81	16.12	16.56	15.19	15.54
12/4/91	23.38	19.27	20.75	14.38	14.61	17.15	15.95	16.44	15.13	16.40
12/12/91	23.61	20.96	20.35	14.25	14.93	16.99	15.96	16.22	15.61	16.62
1/21/92	21.64	22.95	20.37	14.60	15.23	16.89	15.46	16.06	14.89	16.83
1/29/92	21.31	22.76	20.12	14.24	15.31	16.95	15.60	16.37	14.66	16.77
2/5/92	22.67	23.17	20.40	14.31	14.83	16.72	15.75	16.63	15.29	16.93
2/13/92	21.93	22.58	20.37	13.85	14.91	17.17	15.46	16.50	14.73	16.74
2/28/92	22.52	23.15	20.33	14.56	14.73	17.09	15.71	16.13	14.83	16.90
3/12/92	24.94	26.75	26.03	14.16	15.02	17.14	15.52	16.12	14.90	18.31
3/27/92	24.97	29.61	33.61	26.74	19.82	17.15	15.25	16.11	14.96	21.43
4/2/92	24.99	28.93	33.94	26.83	25.20	17.62	16.02	16.18	15.14	21.95
4/8/92	24.40	27.96	33.21	26.96	26.20	17.88	15.84	15.90	15.02	21.79
4/21/92	21.92	27.27	32.79	25.43	26.37	21.59	15.73	16.17	15.35	21.96
4/30/92	18.61	25.90	31.66	25.09	25.55	22.90	15.70	15.73	14.92	21.52
5/15/92	14.00	20.68	30.63	24.24	24.97	24.60	15.98	16.14	14.70	20.58
6/3/92	15.11	19.57	29.23	23.29	24.22	24.85	16.08	15.84	15.32	20.14
6/16/92	13.29	18.50	27.69	22.71	23.86	24.83	15.99	15.86	15.05	19.64
7/7/92	11.40	16.89	23.71	20.12	22.11	24.80	16.33	15.90	14.95	18.46
7/22/92	11.19	16.49	22.64	17.85	20.24	24.15	16.36	16.23	15.10	17.75
8/4/92	11.36	16.35	22.32	16.45	19.07	23.22	16.24	16.09	15.15	17.21
8/26/92	22.86	14.76	21.79	15.94	17.57	21.96	16.20	15.87	15.16	16.93
9/15/92	15.20	16.49	21.88	15.76	17.29	21.92	16.24	16.10	15.31	16.90

HOLE #2

Date	Depth (ft)									Water in Storage (Inches)
	0.75	1.75	2.75	3.75	4.75	5.75	6.75	7.75	8.75	.75 to 8.75 ft
	Moisture Content (% Vol)									
9/5/91	16.44	29.45	24.36	20.76	15.54	19.59	17.69	11.00	22.62	19.10
9/12/91	16.12	28.08	25.64	21.89	16.13	19.86	18.41	11.57	21.75	19.35
9/19/91	14.76	26.34	25.88	22.33	15.16	19.17	18.00	10.89	22.56	18.81
9/27/91	12.00	24.08	23.55	20.39	14.89	20.23	17.61	11.95	21.42	18.08
10/22/91	12.02	22.93	24.61	21.22	16.25	19.26	18.53	10.83	22.97	18.03
11/8/91	16.83	22.57	24.16	21.23	15.46	19.79	18.46	11.57	23.20	18.27
11/21/91	27.83	22.49	23.72	21.70	15.82	19.94	17.97	12.20	22.06	18.81
12/4/91	27.80	36.42	23.60	21.42	15.43	18.99	18.61	11.42	22.56	20.75
12/12/91	28.98	37.98	25.24	21.76	15.27	19.07	18.12	11.72	22.15	21.22
1/21/92	28.23	34.60	25.65	21.18	15.89	18.94	18.68	11.78	22.93	20.71
1/29/92	31.47	35.16	25.15	21.98	14.63	19.38	19.21	11.24	22.30	20.91
2/5/92	30.56	34.98	25.04	21.70	15.14	19.70	18.22	11.89	22.58	20.92
2/13/92	30.23	34.35	24.01	21.71	16.03	19.17	18.99	11.85	22.00	20.58
2/28/92	27.75	34.30	24.99	21.01	16.30	19.76	17.21	11.57	22.81	20.56
3/12/92	31.24	38.00	38.25	22.25	15.63	18.85	17.84	10.88	22.17	22.27
3/19/92	32.35	39.02	39.25	35.98	26.86	19.38	17.54	12.20	20.73	25.87
3/27/92	30.72	39.28	38.67	34.84	31.32	21.76	18.50	11.71	20.99	26.36
4/2/92	31.03	38.25	39.07	35.17	32.97	27.65	17.61	11.63	21.24	27.31
4/8/92	29.05	39.25	37.60	36.21	31.91	31.19	18.17	12.46	21.84	28.11
4/21/92	27.80	38.18	37.96	35.91	30.80	32.94	18.67	11.59	21.52	27.95
4/30/92	23.48	35.39	36.58	34.12	30.68	32.04	18.71	12.35	21.58	26.90
5/15/92	16.29	33.41	36.10	34.77	30.24	33.07	20.91	11.89	22.14	26.62
6/3/92	23.17	29.67	34.99	33.50	28.92	33.04	22.53	11.99	21.48	26.01
6/16/92	15.76	29.88	33.84	32.36	29.13	32.65	22.29	12.14	21.27	25.43
7/7/92	12.89	25.41	30.85	31.50	28.21	31.96	23.72	12.20	21.60	24.17
7/22/92	12.69	24.98	28.02	29.48	27.70	30.56	23.20	10.97	21.92	23.06
8/4/92	12.87	23.63	26.57	27.93	25.14	30.23	23.31	10.97	22.51	22.26
8/26/92	30.22	30.47	26.35	27.03	23.37	29.84	23.60	11.52	22.28	24.67
9/15/92	19.53	30.10	26.47	26.91	23.52	30.27	23.63	11.85	22.53	24.01

HOLE #3

Date	Depth (ft)									Water In Storage (Inches)
	0.75	1.75	2.75	3.75	4.75	5.75	6.75	7.75	8.75	
	Moisture Content (% Vol)									.75 to 8.75 ft
8/29/91	21.90	27.26	24.22	19.31	17.61	18.09	20.01	15.52	21.92	19.53
9/5/91	19.08	26.39	23.67	19.06	17.23	18.40	19.19	15.33	22.03	19.12
9/12/91	18.14	25.19	23.38	19.81	17.24	18.37	19.51	15.83	21.87	19.08
9/19/91	17.63	24.75	23.34	19.38	17.53	18.28	19.36	15.25	21.69	18.82
9/27/91	18.42	23.88	23.43	18.98	17.36	18.23	20.03	16.25	22.01	18.78
9/30/91	16.87	23.71	23.07	19.61	17.39	18.38	19.16	15.86	21.75	18.72
10/1/91	16.53	22.65	23.33	19.18	17.24	18.20	19.46	15.39	22.25	18.42
10/22/91	16.27	22.54	23.11	19.29	17.41	18.45	19.95	15.50	22.00	18.50
11/8/91	23.04	22.86	23.41	19.11	17.07	18.25	20.20	15.91	22.75	18.87
11/21/91	27.11	22.91	22.67	18.82	17.93	17.80	19.80	16.01	22.63	18.91
12/4/91	26.56	31.22	23.20	19.41	17.65	18.30	20.04	15.49	21.93	20.32
12/12/91	26.36	31.22	22.98	19.50	17.25	18.10	19.63	16.09	22.00	20.31
1/21/92	25.16	29.99	23.61	19.40	17.19	18.24	19.95	15.82	21.61	20.08
1/29/92	25.40	29.98	24.01	19.43	17.27	17.90	19.61	15.95	21.72	20.08
2/5/92	25.00	29.92	23.79	19.32	16.63	17.94	20.12	15.78	22.25	20.01
2/13/92	25.22	30.20	23.58	19.17	17.74	18.59	19.57	15.10	22.05	20.05
2/28/92	26.20	30.14	24.24	19.29	17.72	18.23	19.76	15.50	21.54	20.15
3/12/92	28.05	32.04	32.74	19.60	17.03	18.18	19.76	15.80	21.76	21.26
3/19/92	27.56	32.48	32.36	28.64	19.38	18.48	18.72	15.55	21.91	22.84
3/27/92	27.56	32.50	32.03	28.77	24.85	18.00	19.43	15.96	22.18	23.33
4/2/92	28.05	31.86	32.92	28.51	25.96	20.12	20.00	16.17	21.37	23.75
4/8/92	26.65	31.94	32.18	28.00	26.01	23.54	19.65	15.92	22.12	24.10
4/21/92	24.86	34.17	30.99	26.77	25.64	25.78	19.30	15.83	21.16	24.32
4/30/92	23.09	30.99	30.66	27.27	25.46	26.56	20.15	15.39	22.19	23.95
5/15/92	19.48	28.55	30.57	26.93	25.13	26.45	21.93	15.65	21.94	23.48
6/3/92	20.31	27.36	29.42	25.63	24.76	25.56	22.11	16.15	21.94	22.95
6/16/92	18.79	26.68	28.46	25.30	24.31	25.47	23.12	16.23	22.68	22.72
7/7/92	16.65	24.69	26.44	24.04	23.97	24.96	23.63	16.55	21.70	21.90
7/22/92	16.81	23.64	25.58	22.97	22.19	24.35	23.47	15.76	21.87	21.13
8/4/92	16.85	23.54	24.74	22.06	21.35	24.06	23.87	15.62	21.96	20.79
8/26/92	27.31	30.53	25.30	21.24	20.55	23.45	23.77	15.96	21.54	20.79
9/15/92	23.56	28.65	24.33	20.69	21.08	22.86	23.07	16.33	22.83	20.79

HOLE #4

Date	Depth (ft)									Water in Storage (inches)
	0.75	1.75	2.75	3.75	4.75	5.75	6.75	7.75	8.75	
	Moisture Content (% Vol)									.75 - 8.75 ft
8/29/91	22.29	34.16	24.18	21.05	16.00	16.21	14.90	13.11	23.03	19.74
9/5/91	18.87	32.71	23.76	20.92	16.20	16.26	14.83	12.93	22.53	19.29
9/12/91	16.42	30.31	24.20	20.23	16.33	16.32	15.22	13.03	22.39	18.79
9/19/91	15.28	28.65	23.60	20.67	16.15	16.29	14.60	13.29	22.82	18.51
9/27/91	14.55	26.09	22.99	20.47	15.53	16.05	14.83	12.65	22.34	17.78
9/30/91	13.91	26.25	22.29	20.26	16.12	16.30	14.73	13.50	22.17	17.90
10/1/91	14.59	25.33	22.75	20.17	15.75	16.36	14.79	12.61	21.99	17.64
10/22/91	13.14	24.34	21.52	20.21	16.23	16.70	14.77	13.76	22.98	17.65
11/8/91	21.21	24.14	22.12	20.02	16.12	16.95	15.53	13.58	22.74	18.01
11/21/91	29.26	26.96	21.91	20.25	15.89	16.83	15.13	13.57	23.07	18.75
12/4/91	29.48	37.83	23.81	20.61	16.07	16.74	15.42	13.40	23.02	20.70
12/12/91	29.45	38.19	24.32	20.53	16.14	16.54	15.01	13.71	23.60	20.79
1/21/92	26.71	36.63	27.81	20.35	16.11	16.74	15.40	13.49	23.47	20.71
1/29/92	27.32	36.43	28.11	20.67	16.32	17.05	15.32	13.41	22.87	20.80
2/5/92	27.74	36.79	28.78	20.45	16.13	16.96	15.44	13.36	22.71	20.86
2/13/92	27.17	35.35	28.61	20.51	15.88	16.55	15.63	13.24	23.28	20.53
2/28/92	27.41	36.14	28.65	20.67	16.29	16.45	15.40	13.40	22.96	20.71
3/12/92	31.07	39.15	35.44	23.99	15.80	16.49	15.38	13.57	23.13	22.41
3/19/92	30.83	38.61	36.03	34.25	27.00	16.53	15.05	13.80	22.85	24.90
3/27/92	30.78	38.46	36.13	33.67	29.68	19.39	15.44	12.95	22.79	25.39
4/2/92	31.12	39.96	35.79	34.03	30.62	25.74	15.18	13.06	22.74	26.73
4/8/92	30.02	38.50	35.42	33.41	30.79	28.62	15.01	13.35	23.29	26.85
4/21/92	28.05	37.86	33.93	32.32	29.68	29.47	16.17	13.51	22.78	26.52
4/30/92	24.43	37.54	33.65	31.65	29.02	29.37	17.40	13.09	22.63	26.15
5/15/92	18.86	33.84	31.52	31.43	28.41	29.04	18.41	13.37	22.91	25.17
6/3/92	20.23	30.92	30.18	30.53	27.37	28.78	19.16	13.44	23.02	24.45
6/16/92	16.98	29.90	29.18	29.61	28.01	28.05	19.50	12.94	22.45	23.79
7/7/92	15.04	26.35	25.52	25.73	25.35	27.71	19.30	13.32	22.78	22.03
7/22/92	14.79	25.42	24.12	23.71	23.05	26.37	19.16	13.44	22.79	21.04
8/4/92	14.81	24.87	23.15	22.44	21.54	25.43	19.73	13.25	22.84	20.42
8/26/92	30.50	38.52	30.19	21.43	19.80	22.90	19.29	13.47	22.67	23.06
9/15/92	22.88	34.65	28.88	22.11	19.51	22.48	19.12	13.37	22.66	22.04

HOLE #6

Date	Depth (ft)									Water in Storage (inches)
	0.75	1.75	2.75	3.75	4.75	5.75	6.75	7.75	8.75	
	Moisture Content (% Vol)									.75 to 8.75 ft
3/19/92	27.18	32.39	32.85	31.33	24.15	15.73	16.06	12.34	21.21	22.47
3/27/92	27.56	33.30	33.70	31.73	25.20	17.69	16.17	12.30	21.33	23.16
4/2/92	27.44	33.00	33.64	31.81	25.62	22.29	16.31	12.47	21.33	23.93
4/8/92	26.81	32.67	32.97	31.03	25.53	24.88	15.89	12.51	21.33	24.05
4/21/92	25.00	32.10	32.09	30.89	24.77	25.29	16.91	12.23	21.39	23.84
4/30/92	22.92	31.31	31.77	30.63	24.41	25.02	16.48	12.13	21.18	23.43
5/5/92	17.00	28.33	30.91	29.77	24.02	24.98	17.41	12.19	21.07	22.55
6/3/92	17.75	26.93	30.42	29.50	22.84	24.52	16.48	12.31	21.21	22.22
6/16/92	15.71	25.77	29.27	29.06	22.67	24.36	19.01	12.60	21.02	21.83
7/7/92	13.66	22.02	25.77	27.23	21.67	23.71	19.25	12.17	21.37	20.36
7/22/92	13.37	21.19	24.97	25.01	21.71	23.56	19.77	12.46	21.23	19.86
8/4/92	14.34	21.53	24.30	24.01	21.06	22.91	19.69	12.33	21.12	19.55
08/26/92	26.14	29.50	24.12	22.32	20.15	22.32	19.53	12.28	21.17	20.82
09/15/92	22.02	28.88	25.43	21.98	20.26	22.08	19.62	12.46	20.99	20.61

Appendix B

SIEVE ANALYSIS RESULTS

HOLE #2

Depth (ft)	Seive #						Reaction with 10% HCl
	#10	#16	#30	#50	#100	#200	
	% Finer by Weight						
0.75	95.70	87.33	69.50	44.42	20.52	5.94	none
0.75	89.34	75.08	54.15	33.22	15.10	4.77	none
1.75	99.74	95.83	82.63	53.89	25.12	8.63	none
1.75	99.93	98.91	87.37	51.46	24.17	9.58	none
2.75	99.06	97.04	86.32	60.11	29.87	8.70	none
2.75	99.35	98.24	87.65	57.07	28.06	8.93	none
3.75	100.00	99.86	97.30	74.48	35.60	10.58	weak
3.75	99.13	97.75	86.66	57.16	31.43	9.19	moderate
4.75	98.39	94.99	72.14	49.49	24.55	10.00	moderate
4.75	97.89	95.63	84.14	57.24	29.86	10.94	strong
5.75	100.00	99.92	99.10	87.20	48.58	16.62	strong
5.75	100.00	99.25	92.32	68.31	42.56	11.77	strong
6.75	99.80	99.25	92.78	68.75	46.19	24.35	moderate
6.75	97.53	96.89	89.73	63.77	38.19	16.90	weak
7.75	96.92	91.53	77.66	53.94	32.19	13.07	weak
7.75	95.72	84.50	61.80	36.20	17.19	5.33	weak
8.75	98.03	97.37	92.96	74.27	50.33	24.07	weak
8.75	95.53	91.41	79.57	56.44	36.92	19.16	weak

HOLE #3

Depth (ft)	Sieve #							Reaction with 10% HCl
	#4	#10	#16	#30	#50	#100	#200	
	% Finer by Weight							
0.75	100.00	94.61	87.05	68.51	44.13	21.20	6.93	none
1.75	100.00	98.53	94.72	76.89	48.92	23.75	7.89	none
2.75	100.00	96.91	89.85	73.94	50.18	26.12	7.60	none
3.75	100.00	99.75	96.94	84.70	59.21	32.44	8.36	weak
4.75	100.00	97.93	95.20	85.35	63.00	36.09	11.87	strong
5.75	100.00	99.82	99.26	93.60	75.51	51.07	21.65	strong
6.75	100.00	99.17	96.21	85.80	67.53	46.38	18.55	moderate
7.75	100.00	94.45	89.43	75.29	48.00	24.04	8.70	moderate
8.75	100.00	98.21	95.06	85.17	72.11	54.81	20.55	weak

HOLE #4

Depth (ft)	Sieve #					Reaction with 10% HCl
	#10	#40	#60	#100	#200	
	% Finer by Weight					
0.75	99.53	68.80	48.09	25.59	13.11	none
0.75	98.39	62.51	39.98	18.33	7.18	none
0.75	96.91	56.07	37.81	18.67	9.03	none
1.75	99.20	68.38	45.62	22.21	9.96	none
1.75	100.00	80.39	60.14	35.89	18.78	none
1.75	99.57	74.30	54.06	29.18	13.34	none
2.75	100.00	79.30	53.91	27.31	12.47	none
2.75	100.00	87.06	65.53	37.35	18.56	none
2.75	98.28	80.24	56.82	27.46	11.58	none
3.75	99.77	71.10	51.11	31.54	17.91	weak
3.75	100.00	75.57	54.97	33.67	19.06	weak
3.75	100.00	75.57	54.97	33.67	19.06	moderate
3.75	99.92	75.95	55.36	33.16	17.35	moderate
4.75	99.82	83.09	64.30	38.74	19.15	strong
4.75	100.00	93.77	81.93	61.10	33.73	moderate
4.75	100.00	95.74	84.31	56.92	28.48	strong
4.75	98.85	76.79	55.03	28.39	11.81	strong
5.75	100.00	81.67	61.35	40.33	19.54	strong
5.75	100.00	79.69	59.75	38.87	20.88	strong
5.75	99.65	72.79	53.89	31.87	14.99	strong
6.75	96.85	77.23	58.82	40.44	21.99	moderate
6.75	97.28	73.81	56.78	35.42	18.57	moderate
6.75	96.79	52.36	30.95	14.92	7.05	moderate
7.75	98.78	74.23	37.40	11.77	4.91	weak
7.75	96.91	66.61	39.04	16.43	6.29	weak
7.75	99.48	76.95	59.20	40.23	22.92	weak
8.75	97.49	89.21	81.24	63.85	34.74	weak
8.75	99.25	82.80	70.24	53.87	33.78	weak
8.75	99.19	89.18	79.49	61.73	33.39	weak

Appendix C

NEUTRON PROBE CALIBRATION DATA

HOLE #1

Depth (ft)	Moisture (%)	Dry Bulk Density (g/cc)	Porosity (%)	Relative Saturation	Count Ratio
0.75	32.81	1.74	34.65	94.68	0.9548
0.75	30.52	1.65	38.13	80.05	0.9548
0.75	29.72	1.67	37.59	79.07	0.9548
1.75	15.44	1.61	39.54	39.05	0.8258
1.75	15.50	1.62	39.24	39.50	0.8258
1.75	28.01	1.95	27.04	103.61	0.8258
1.75	26.04	1.92	28.23	92.24	0.8258
2.75	19.28	1.58	40.74	47.33	0.9091
2.75	19.97	1.59	40.38	49.46	0.9091
2.75	21.25	1.64	38.50	55.19	0.9091
3.75	13.69	1.44	46.00	29.76	0.6983
3.75	13.47	1.45	45.59	29.55	0.6983
3.75	15.28	1.61	39.84	38.35	0.6983
3.75	14.01	1.47	44.99	31.14	0.6983
4.75	18.59	1.46	45.37	40.98	0.7069
4.75	12.78	1.57	41.10	31.10	0.7069
4.75	13.90	1.56	41.58	33.43	0.7069
5.75	15.66	1.48	44.41	35.26	0.7881
5.75	16.67	1.48	44.57	37.40	0.7881
5.75	15.60	1.62	39.18	39.81	0.7881
6.75	14.86	1.52	43.13	34.45	0.7418
6.75	15.23	1.44	45.88	33.19	0.7418
6.75	11.93	1.74	34.77	34.31	0.7418
7.75	18.00	1.45	45.57	39.50	0.7574
7.75	18.00	1.36	49.18	36.60	0.7574
7.75	14.17	1.51	43.33	32.70	0.7574
8.75	15.82	1.56	41.42	38.20	0.7196
8.75	15.50	1.58	40.82	37.97	0.7196
8.75	17.26	1.60	40.22	42.91	0.7196

HOLE #2

Depth (ft)	Moisture (%)	Dry Bulk Density (g/cc)	Porosity (%)	Relative Saturation	Count Ratio
0.75	26.42	1.63	38.78	68.11	0.5111
0.75	26.36	1.64	38.72	68.07	0.5111
0.75	23.70	1.78	33.32	71.13	0.5111
1.75	17.57	1.47	44.77	39.26	0.5045
1.75	15.60	1.50	43.77	35.65	0.5045
1.75	16.87	1.49	44.29	38.09	0.5045
2.75	22.90	1.61	39.86	57.45	0.5101
2.75	21.94	1.65	38.05	57.67	0.5101
2.75	18.85	1.57	41.18	45.78	0.5101
2.75	18.43	1.52	43.05	42.81	0.5101
2.75	23.43	1.64	38.54	60.79	0.5101
3.75	14.22	1.49	44.09	32.25	0.4668
3.75	14.81	1.52	43.23	34.26	0.4668
3.75	17.95	1.62	39.28	45.69	0.4668
3.75	18.43	1.47	44.81	41.13	0.4668
4.75	15.02	1.48	44.59	33.68	0.4089
4.75	12.52	1.49	44.33	28.23	0.4089
4.75	16.62	1.49	44.19	37.60	0.4089
4.75	14.97	1.44	46.10	32.47	0.4089
5.75	20.40	1.36	49.02	41.61	0.4483
5.75	16.88	1.39	48.12	35.08	0.4483
6.75	23.27	1.54	42.37	54.92	0.4337
6.75	19.97	1.37	48.60	41.09	0.4337
6.75	14.65	1.59	40.54	36.14	0.4337
6.75	18.48	1.77	33.58	55.04	0.4337
7.75	11.82	1.51	43.29	27.31	0.3087
7.75	16.62	1.53	42.53	39.07	0.3087
7.75	9.21	1.47	45.03	20.46	0.3087
7.75	8.89	1.41	47.34	18.78	0.3087
8.75	25.46	1.23	54.06	47.09	0.4792
8.75	19.60	1.48	44.41	44.13	0.4792
8.75	22.21	1.42	46.98	47.27	0.4792
8.75	23.68	1.21	54.78	43.23	0.4792

HOLE #3

Depth (ft)	Moisture (%)	Dry Bulk Density (g/cc)	Porosity (%)	Relative Saturation	Count Ratio
0.75	28.44	1.70	36.27	78.41	0.6303
0.75	25.88	1.68	36.97	70.01	0.6303
1.75	21.20	1.49	44.37	47.78	0.6299
1.75	31.58	1.72	35.59	88.73	0.6299
2.75	14.54	1.65	38.21	38.06	0.5745
2.75	28.44	1.77	33.62	84.60	0.5745
3.75	17.26	1.45	45.83	37.67	0.4916
3.75	19.71	1.52	42.99	45.85	0.4916
3.75	18.21	1.48	44.45	40.97	0.4916
4.75	15.55	1.54	42.35	36.71	0.4524
4.75	17.04	1.55	41.90	40.67	0.4524
5.75	19.17	1.46	45.29	42.33	0.4684
6.75	20.56	1.29	51.81	39.68	0.5005
6.75	21.04	1.44	46.00	45.73	0.5005
7.75	11.13	1.67	37.55	29.64	0.4195
7.75	17.47	1.46	45.27	38.59	0.4195
7.75	14.91	1.46	45.29	32.92	0.4195
8.75	21.25	1.39	47.78	44.47	0.5344
8.75	26.58	1.42	46.68	56.94	0.5344
8.75	22.79	1.30	51.15	44.55	0.5344

HOLE #4

Depth (ft)	Moisture (%)	Dry Bulk Density (g/cc)	Porosity (%)	Relative Saturation	Count Ratio
0.75	26.90	1.69	36.75	73.20	1.0381
0.75	25.88	1.59	40.54	63.84	1.0381
0.75	26.04	1.75	34.47	75.54	1.0381
1.75	35.10	1.59	40.28	87.14	1.2624
1.75	37.60	1.69	36.75	102.32	1.2624
1.75	36.85	1.80	32.46	113.53	1.2624
2.75	19.44	1.57	41.26	47.12	0.9328
2.75	16.88	1.52	43.25	39.03	0.9328
2.75	20.66	1.62	39.30	52.57	0.9328
3.75	17.47	1.38	48.48	36.04	0.8636
3.75	21.36	1.46	45.17	47.29	0.8636
3.75	20.98	1.36	48.92	42.89	0.8636
3.75	22.79	1.47	44.91	50.75	0.8636
4.75	16.40	1.38	48.40	33.89	0.7225
4.75	19.01	1.36	48.88	38.89	0.7225
4.75	15.92	1.47	45.07	35.33	0.7225
4.75	13.42	1.62	39.50	33.97	0.7225
5.75	14.65	1.35	49.53	29.58	0.7453
5.75	21.41	1.32	50.67	42.25	0.7453
5.75	16.19	1.25	53.08	30.50	0.7453
5.75	18.27	1.31	50.87	35.92	0.7453
5.75	22.10	1.36	49.19	44.92	0.7453
6.75	12.14	1.61	39.80	30.50	0.6957
6.75	19.81	1.49	44.11	44.91	0.6957
6.75	15.87	1.53	42.81	37.07	0.6957
7.75	8.20	1.54	42.45	19.32	0.6418
7.75	18.64	1.26	52.65	35.41	0.6418
7.75	11.77	1.51	43.53	27.04	0.6418
8.75	18.43	1.32	50.55	36.46	0.9261
8.75	20.29	1.24	53.40	37.99	0.9261
8.75	23.70	1.31	50.77	46.68	0.9261

HOLE #5

Depth (ft)	Moisture (%)	Dry Bulk Density (g/cc)	Porosity (%)	Relative Saturation	Count Ratio
0.75	24.13	1.59	40.28	59.91	0.9051
0.75	25.30	1.70	36.45	69.41	0.9051
1.75	18.21	1.40	47.54	38.30	0.9779
1.75	23.75	1.78	33.42	71.07	0.9779
2.75	15.92	1.47	45.09	35.31	0.8456
2.75	17.63	1.60	40.22	43.83	0.8456
3.75	12.99	1.66	37.87	34.30	0.6471
3.75	12.99	1.66	37.75	34.41	0.6471
4.75	13.26	1.59	40.56	32.69	0.6888
5.75	10.49	1.33	50.31	20.85	0.6276

HOLE #6

Depth (ft)	Moisture (%)	Dry Bulk Desity (g/cc)	Porosity (%)	Relative Saturation	Count Ratio
0.50	23.22	1.33	50.19	46.27	1.1540
1.00	27.59	1.47	45.12	61.14	1.1540
1.33	27.42	1.40	47.63	57.57	1.2433
1.50	30.38	1.49	44.01	69.04	1.3385
2.00	31.56	1.56	41.54	75.97	1.3385
2.33	32.18	1.52	43.11	74.66	1.3506
2.50	35.12	1.65	38.14	92.10	1.3549
3.00	35.47	1.52	43.21	82.08	1.3549
3.33	35.83	1.48	44.46	80.60	1.3844
3.50	38.56	1.66	37.89	101.77	1.3008
4.00	37.95	1.46	45.47	83.46	1.3008
4.33	24.22	1.40	47.44	51.06	1.1122
4.50	21.84	1.80	32.62	66.94	1.0465
5.00	29.16	1.57	41.37	70.49	1.0465
5.33	18.63	1.35	49.48	37.65	0.9039
5.50	15.28	1.36	48.94	31.23	0.7479
6.00	14.73	1.37	48.58	30.31	0.7479
6.50	18.46	1.26	52.97	34.86	0.7598
7.00	18.81	1.27	52.30	35.97	0.7598
7.50	10.78	1.60	40.02	26.93	0.6279
8.00	11.75	1.60	39.95	29.42	0.6279
8.50	24.25	1.35	49.47	49.02	0.9422
9.00	23.51	1.32	50.71	46.37	0.9422

Appendix D

PRESSURE PLATE TEST RESULTS
AND
HOLE 6 MOISTURE CHARACTERISTIC CURVES

TEST #1

Hole	Interval (ft)	Matric Potential (-cm)								
		70	141	246	352	563	844	1547	4924	9847
		Moisture Content (% vol)								
4	2.5-3	37.39	35.48	33.49	32.44	30.87	29.29	27.23	24.79	24.19
3	4.5-5	43.71	38.35	34.05	32.26	29.71	27.81	25.56	23.21	21.46
4	4.5-5	42.53	38.38	34.52	33.13	30.86	29.27	27.04	24.55	24.32
3	6.5-7	44.00	39.61	35.89	34.19	31.83	29.93	27.81	25.15	24.09
3	2.5-3	40.01	38.29	36.06	35.02	33.25	31.79	29.77	27.05	25.20
5	6.5-7	48.53	46.17	42.79	40.84	37.99	35.14	32.29	30.34	28.54
4	6.5-7	51.55	49.27	45.74	43.70	40.33	37.65	34.52	31.10	29.11
5	5.5-6	39.62	36.81	33.65	32.28	29.98	28.25	26.27	23.53	21.55

TEST #2

Hole	Interval (ft)	Matric Potential (-cm)				
		352	703	2110	4924	9847
		Moisture Content (% vol)				
5	7.5-8	23.72	21.79	19.67	18.41	16.37
3	8.5-9	40.56	37.03	33.66	31.79	28.60
5	8.5-9	36.35	33.57	30.62	29.37	26.27
4	8.5-9	37.70	34.09	31.33	29.73	26.92
4	8.5-9	39.39	36.97	35.21	33.37	30.53
2	8.5-9	39.39	36.97	35.21	33.37	30.53

TEST #3

Depth (ft)	Matric Potential (-cm)					
	106	352	1759	4220	9144	14771
	Moisture Content (% vol)					
1.5	29.88	27.40	24.03	21.47	19.03	17.97
2.5	36.51	34.67	31.38	28.28	25.59	24.71
3.0	37.08	36.09	33.35	29.93	27.22	24.88
3.5	37.13	34.60	31.15	28.01	25.17	23.26
4.5	29.10	25.24	21.70	19.13	17.28	16.04
5.0	33.70	29.28	25.52	22.89	20.61	19.41
5.5	29.78	22.92	18.62	18.38		15.11
6.0	33.62	25.89	20.75	20.49		16.87
6.5	41.32	34.48	28.23	27.43		22.59
7.0	39.00	30.07	24.79	24.01		19.30
8.5	43.75	37.36	31.65	42.53		26.13
9.0	45.40	39.33	33.13	32.43		26.89

1.5 FEET

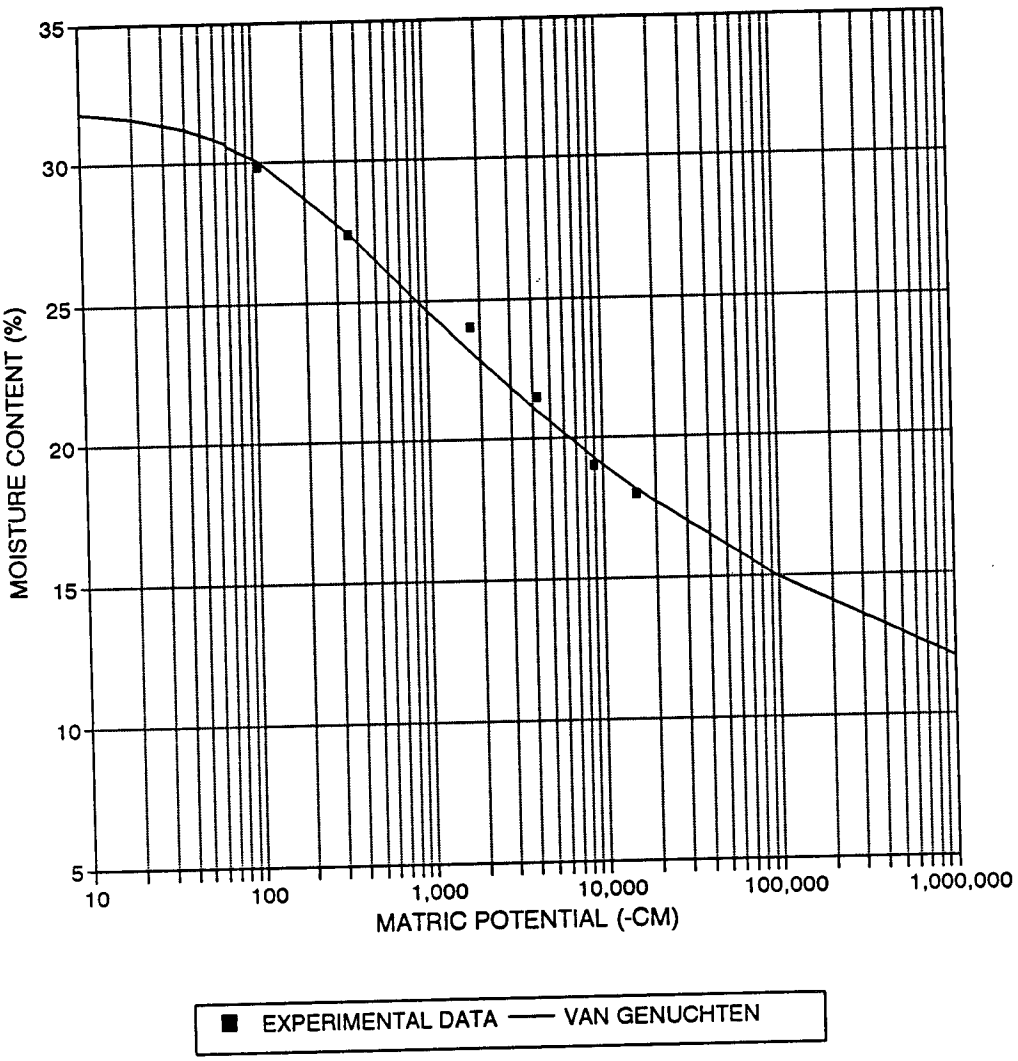
35
30
25
20
15
10
5
MOISTURE CONTENT (%)
10
100
1,000
10,000
100,000
1,000,000
MATRIC POTENTIAL (-CM)
EXPERIMENTAL DATA
VAN GENUCHTEN

2.5 FEET

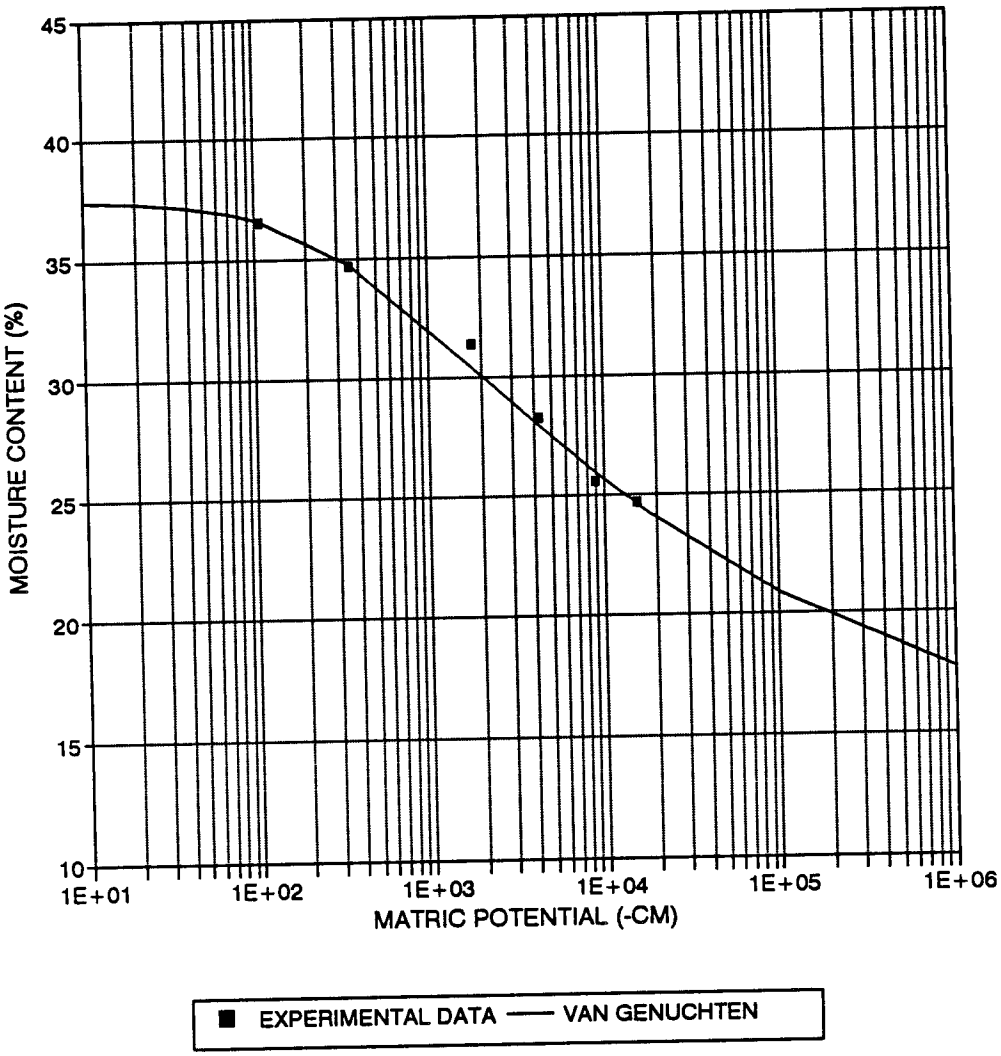
45
40
35
30
25
20
15
10
MOISTURE CONTENT (%)
1E+01
1E+02
1E+03
1E+04
1E+05
1E+06
MATRIC POTENTIAL (-CM)
EXPERIMENTAL DATA
VAN GENUCHTEN

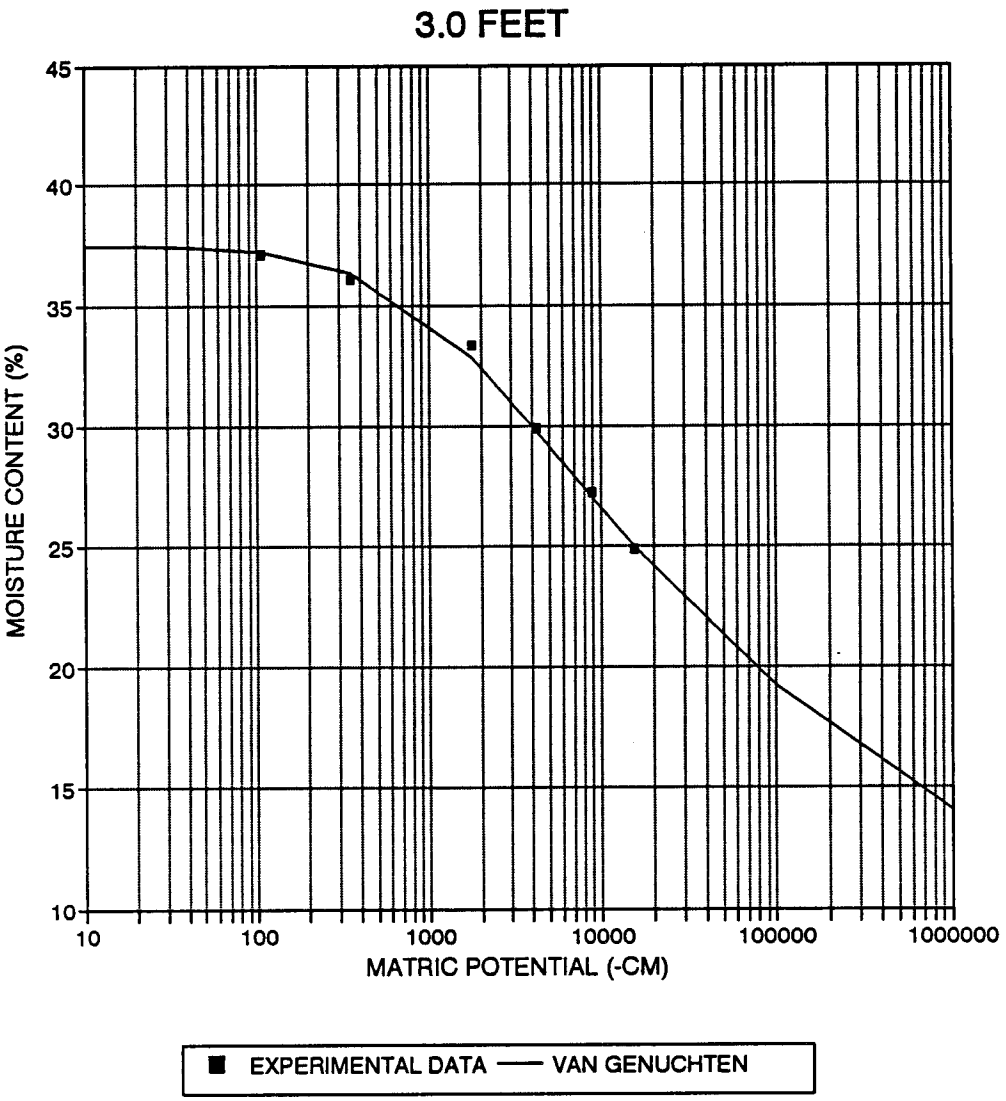
3.0 FEET
45
40
35
30
25
20
15
10
MOISTURE CONTENT (%)
10
100
1000
10000
100000
1000000
MATRIC POTENTIAL (-CM)
EXPERIMENTAL DATA
VAN GENUCHTEN

3.5 FEET

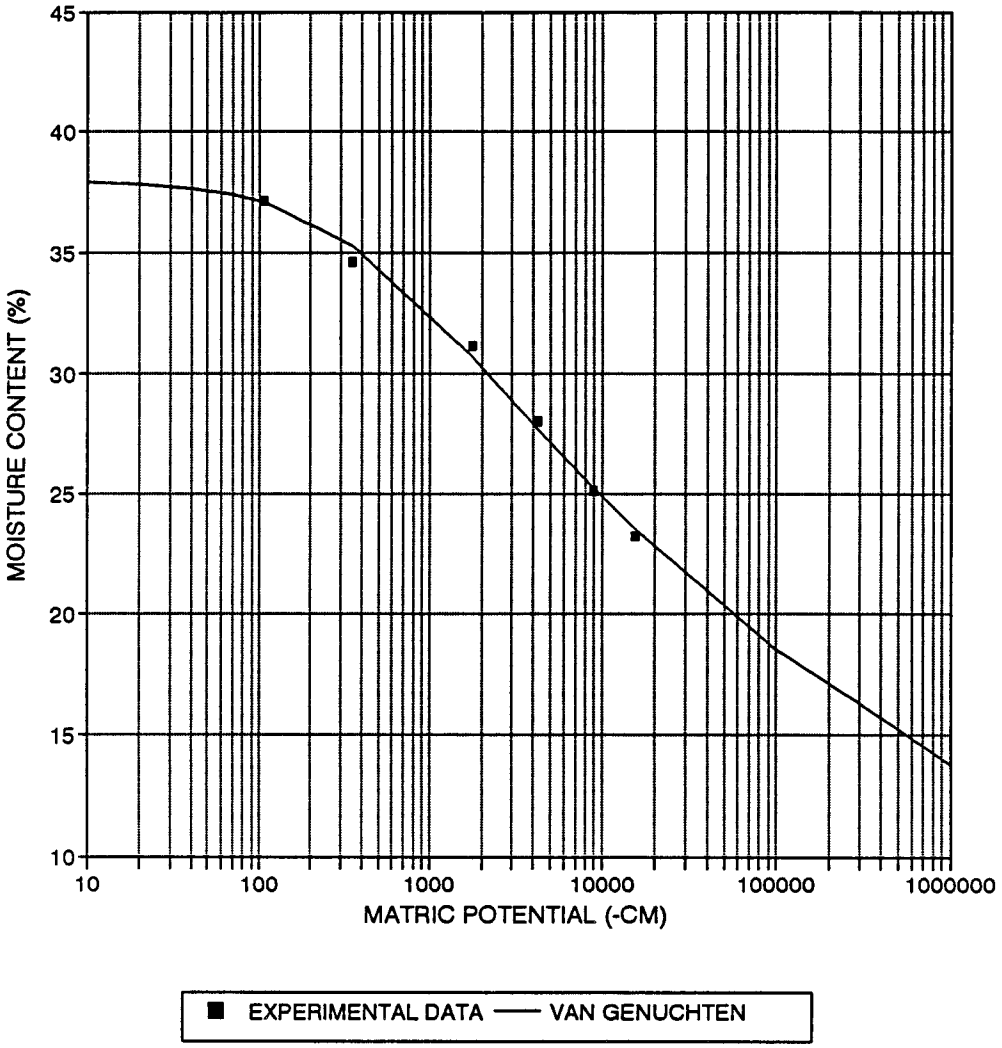
45
40
35
30
25
20
15
10
MOISTURE CONTENT (%)
10
100
1000
10000
100000
1000000
MATRIC POTENTIAL (-CM)
EXPERIMENTAL DATA
VAN GENUCHTEN

4.5 FEET

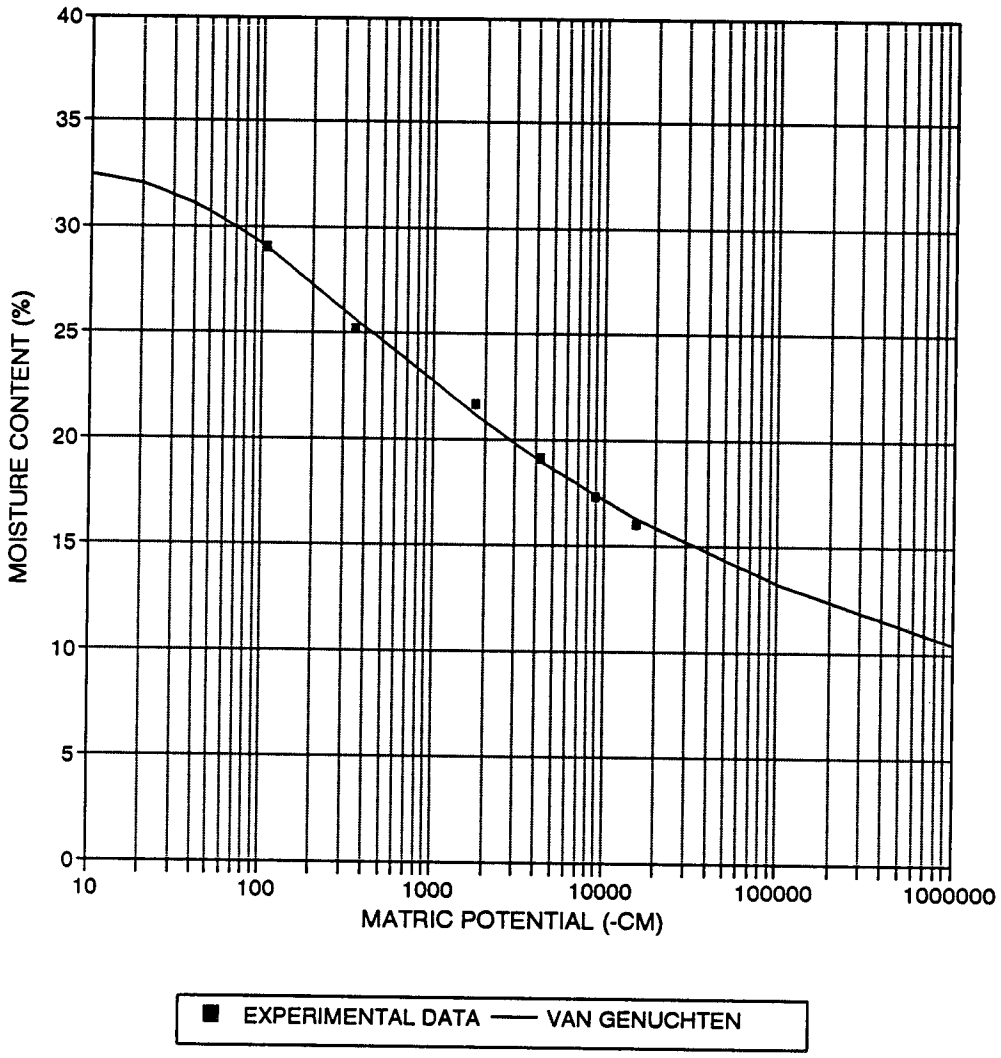
40
35
30
25
20
15
10
5
0
MOISTURE CONTENT (%)
10
100
1000
10000
100000
1000000
MATRIC POTENTIAL (-CM)
EXPERIMENTAL DATA
VAN GENUCHTEN

5.0 FEET

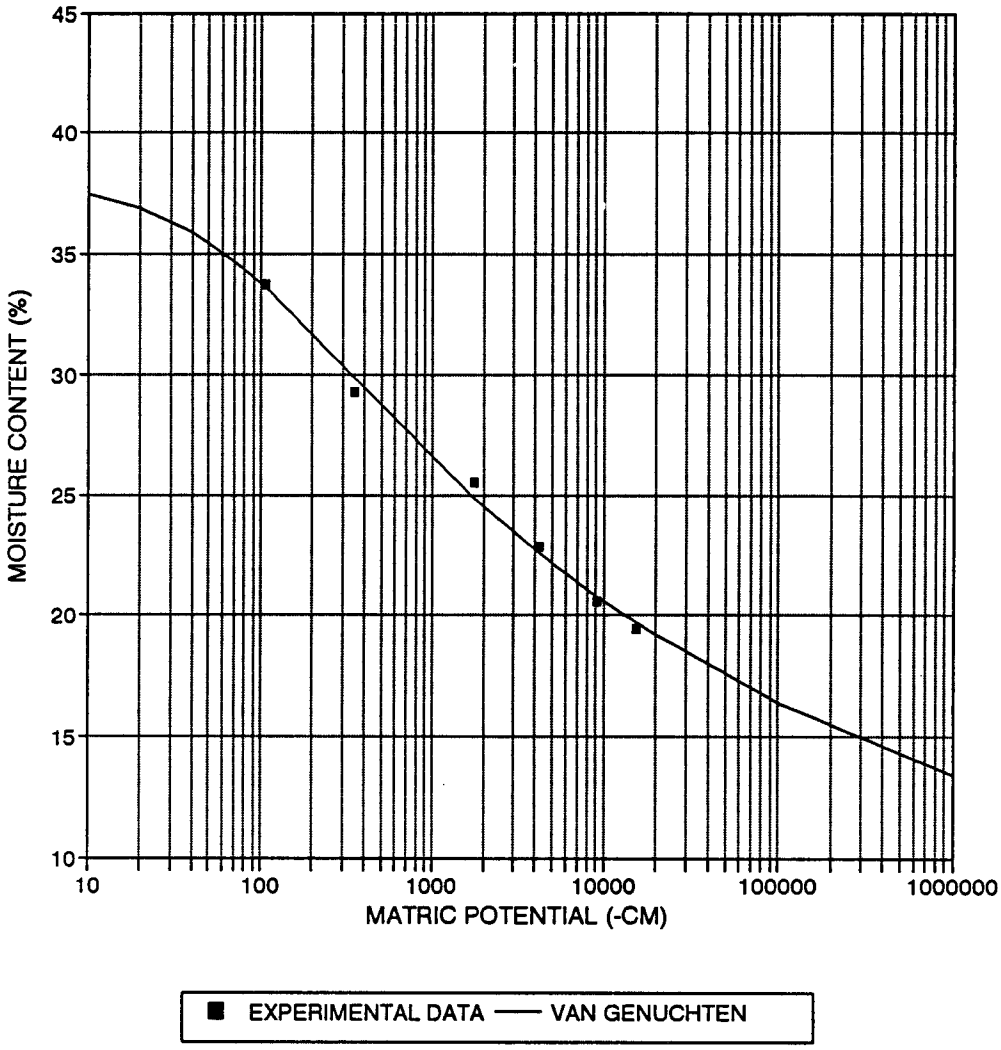
45
40
35
30
25
20
15
10
MOISTURE CONTENT (%)
10
100
1000
10000
100000
1000000
MATRIC POTENTIAL (-CM)
EXPERIMENTAL DATA
VAN GENUCHTEN

5.5 FEET

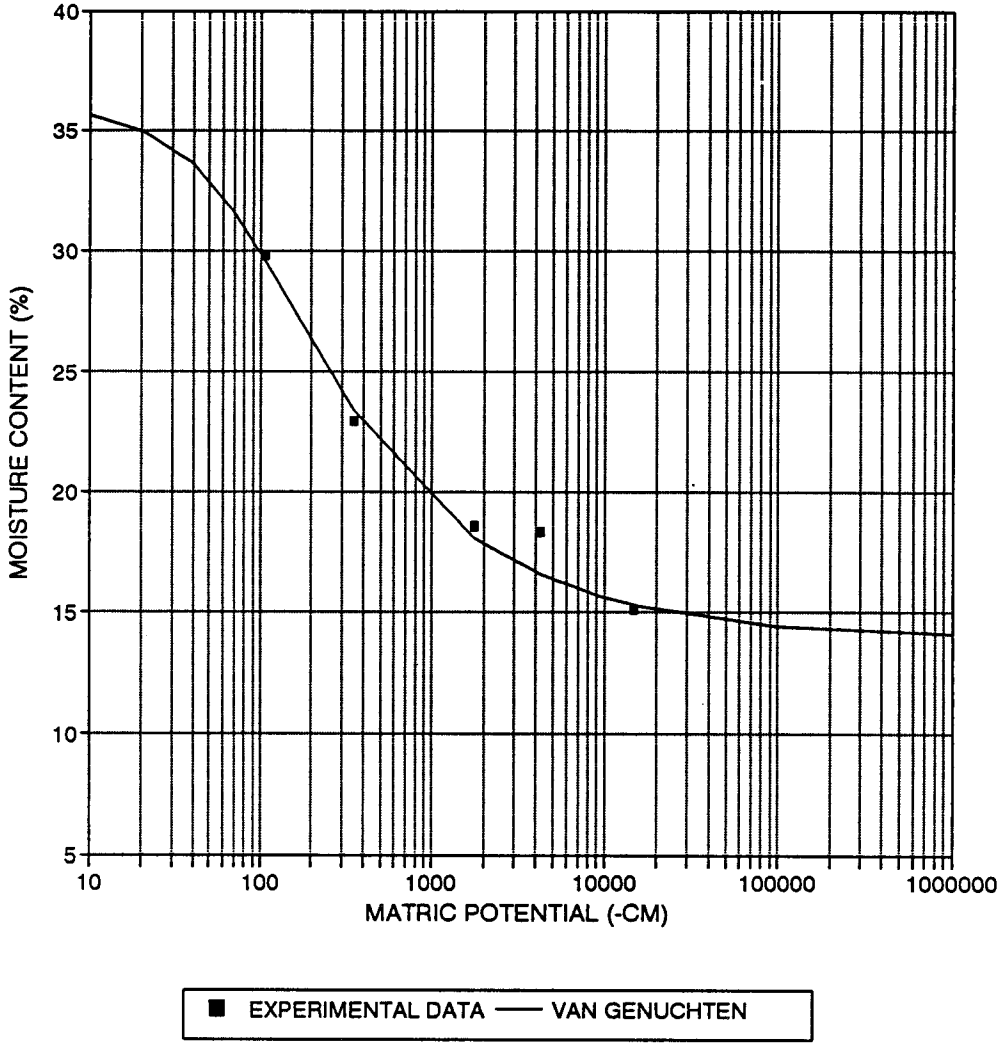
40
35
30
25
20
15
10
5
MOISTURE CONTENT (%)
10
100
1000
10000
100000
1000000
MATRIC POTENTIAL (-CM)
EXPERIMENTAL DATA
VAN GENUCHTEN

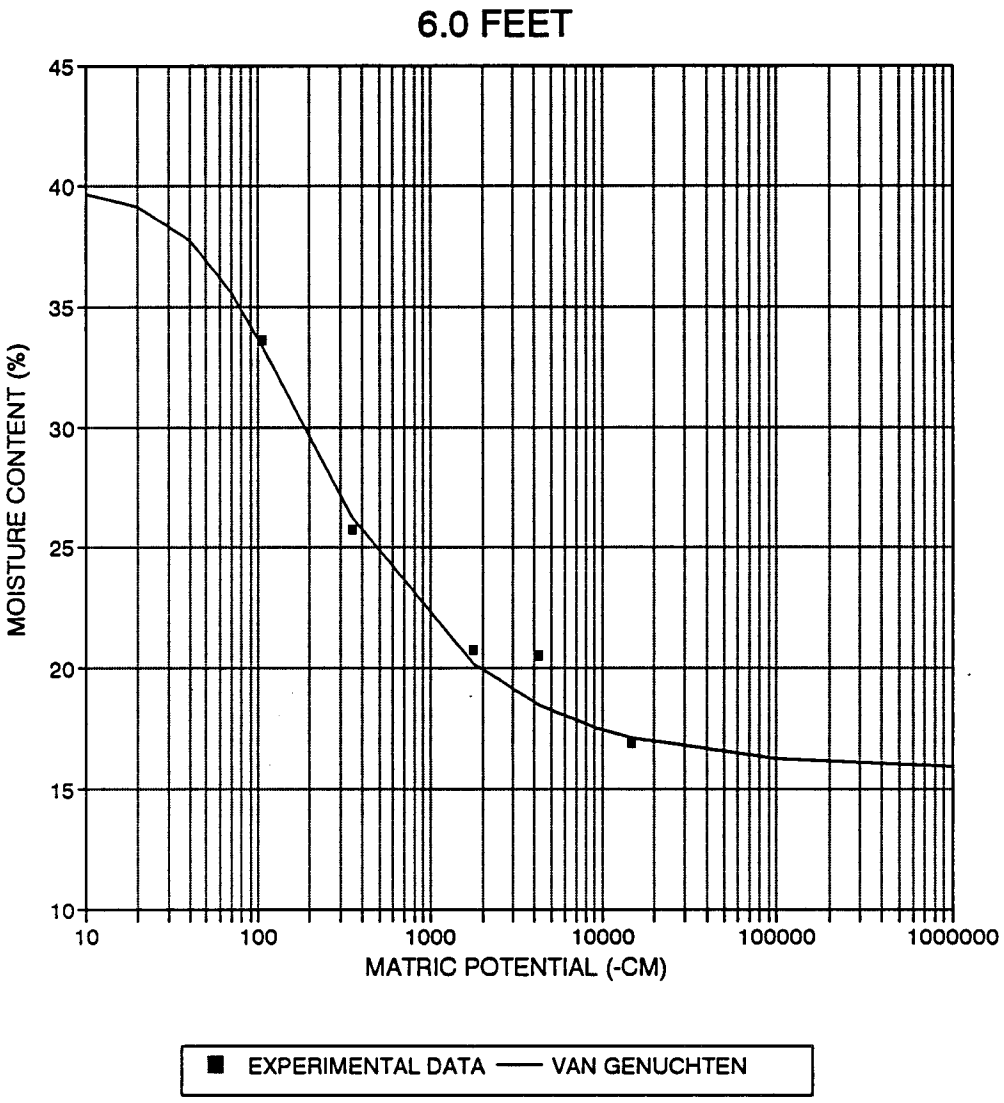
6.0 FEET
45
40
35
30
25
20
15
10
MOISTURE CONTENT (%)
10
100
1000
10000
100000
1000000
MATRIC POTENTIAL (-CM)
EXPERIMENTAL DATA
VAN GENUCHTEN

6.5 FEET

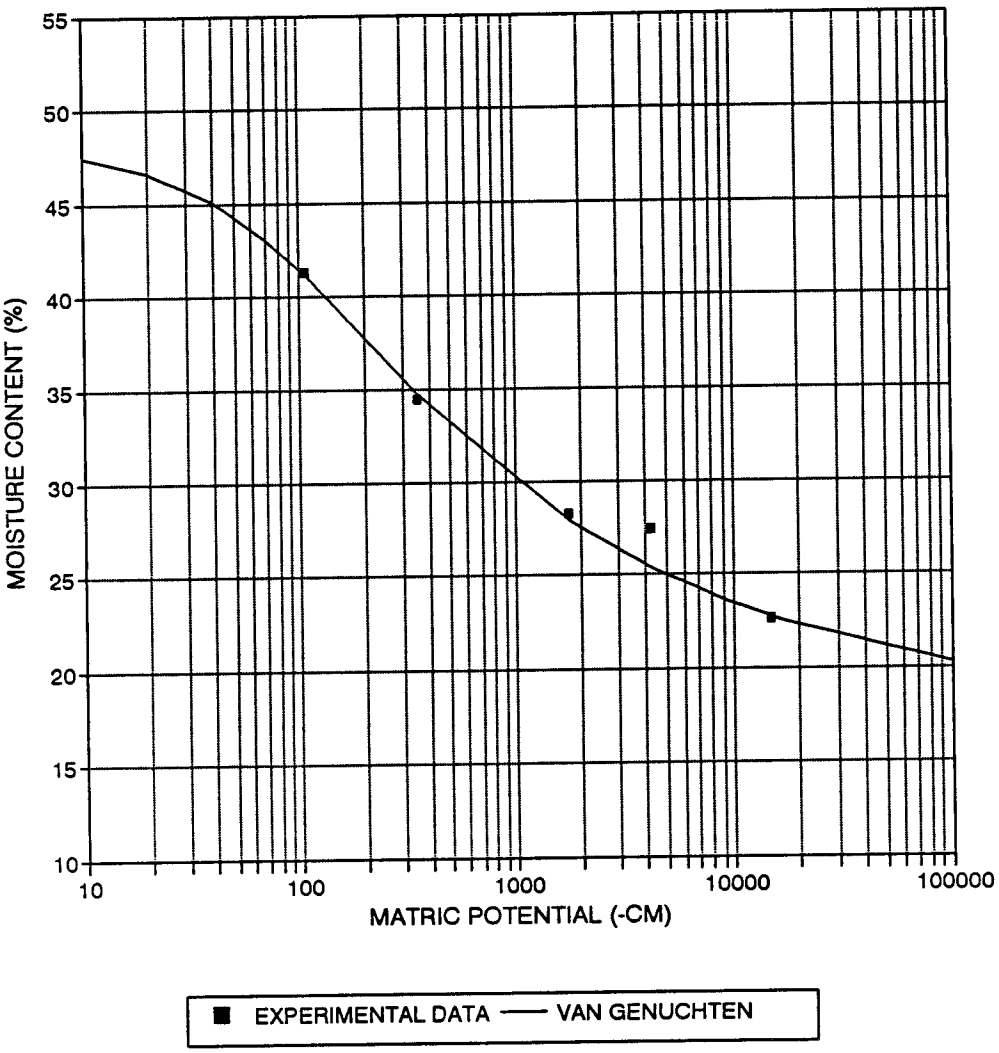
55
50
45
40
35
30
25
20
15
10
MOISTURE CONTENT (%)
10
100
1000
10000
100000
MATRIC POTENTIAL (-CM)
EXPERIMENTAL DATA
VAN GENUCHTEN

7.0 FEET

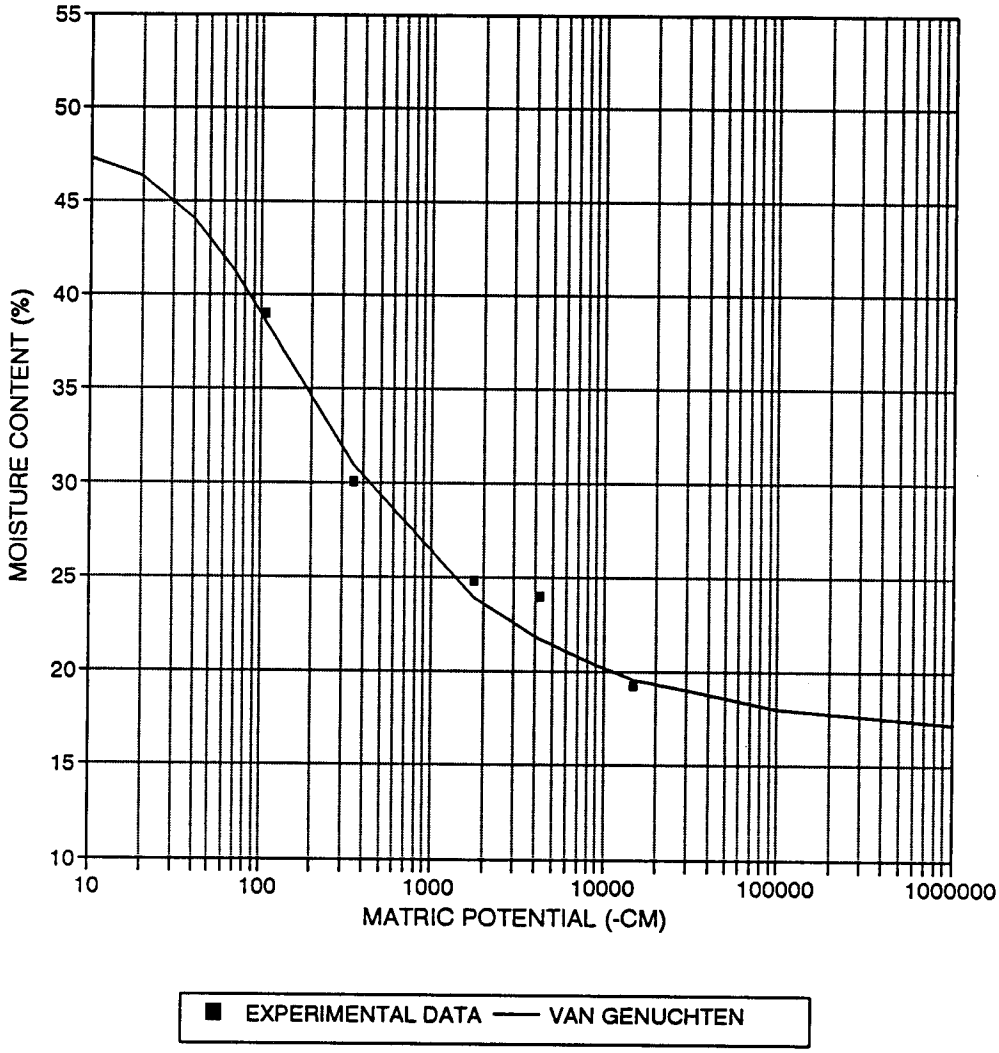
55
50
45
40
35
30
25
20
15
10
MOISTURE CONTENT (%)
10
100
1000
10000
100000
1000000
MATRIC POTENTIAL (-CM)
EXPERIMENTAL DATA
VAN GENUCHTEN

8.5 FEET

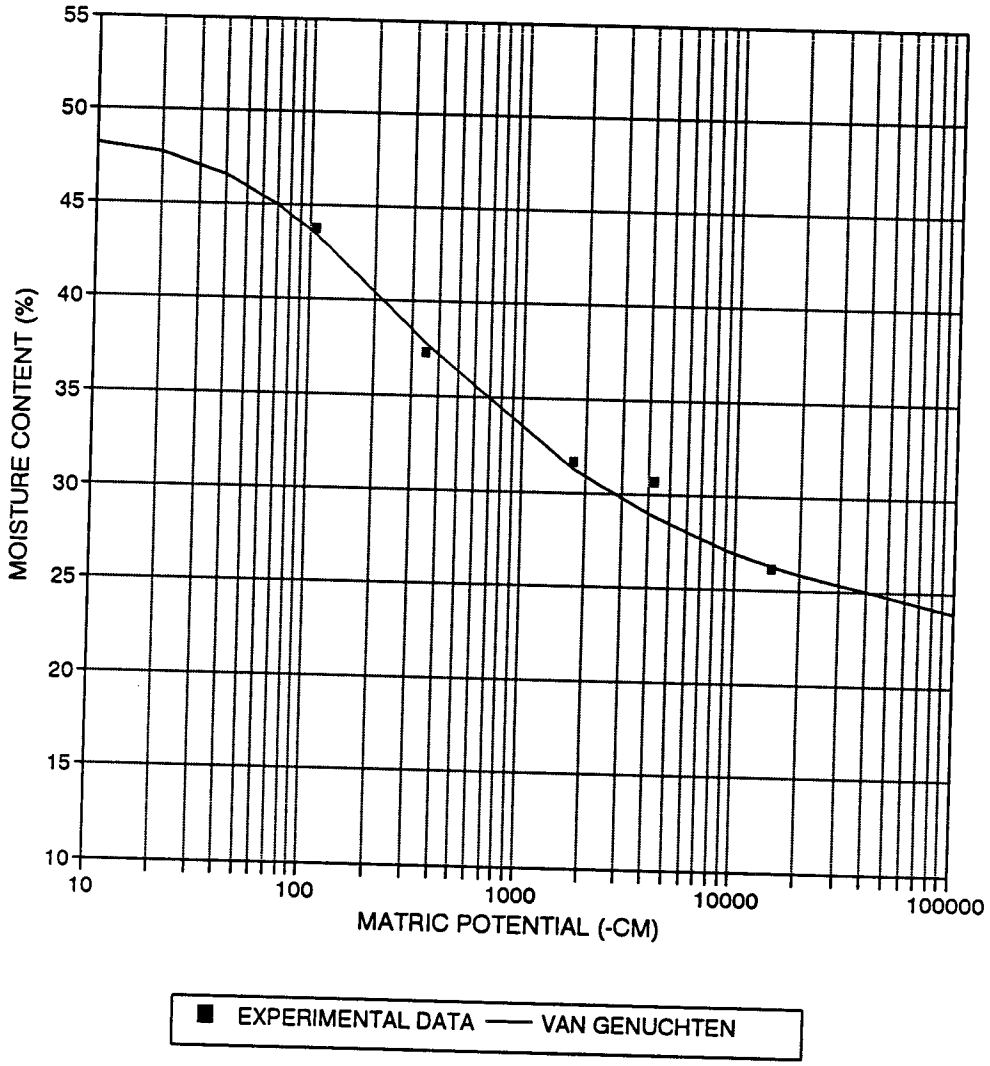
55
50
45
40
35
30
25
20
15
10
MOISTURE CONTENT (%)
10
100
1000
10000
100000
MATRIC POTENTIAL (-CM)
EXPERIMENTAL DATA
VAN GENUCHTEN

9 FEET

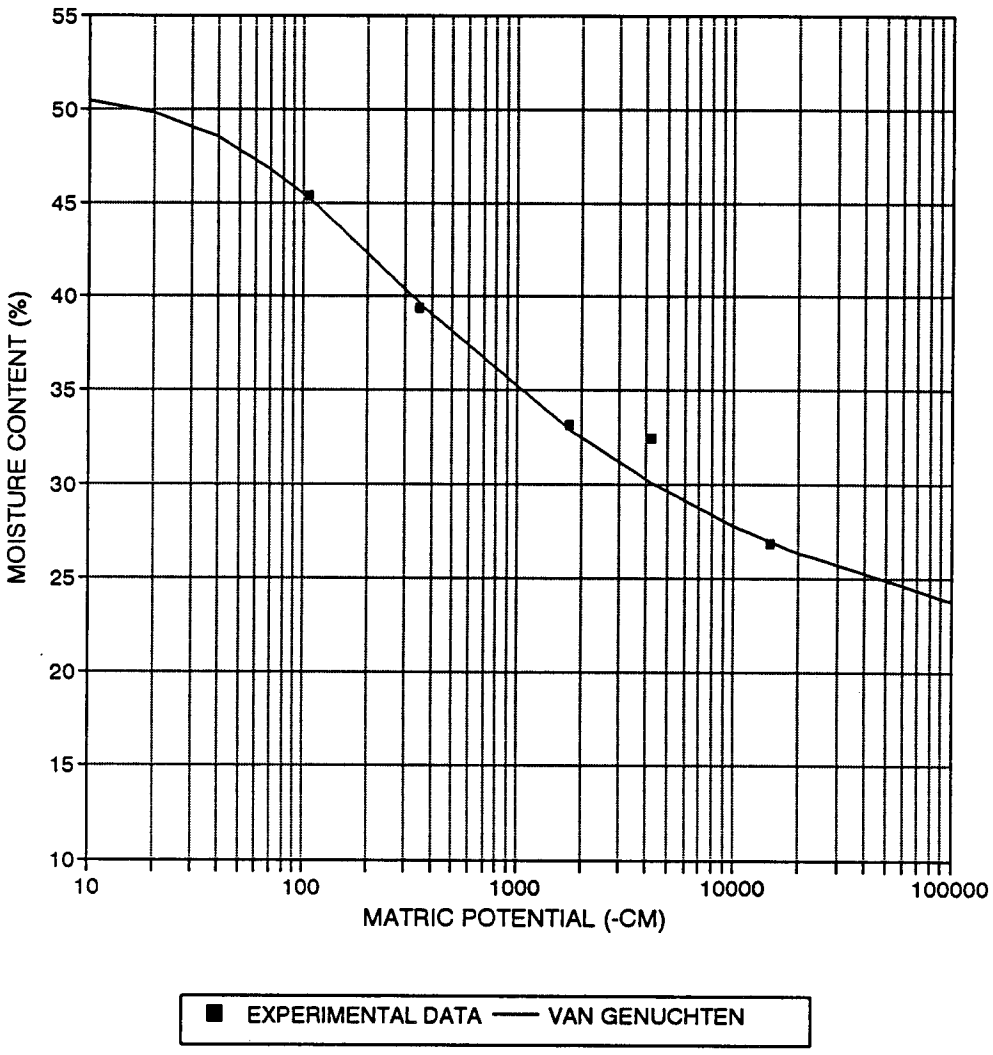
55
50
45
40
35
30
25
20
15
10
MOISTURE CONTENT (%)
10
100
1000
10000
100000
MATRIC POTENTIAL (-CM)
EXPERIMENTAL DATA
VAN GENUCHTEN

Appendix E

PRECIPITATION DATA

Precipitaion Data
Golden, Colorado

Date	Precipitatio (inches)	Date	Precipitatio (inches)	Date	Precipitatio (inches)
09/07/91	0.04	03/28/92	0.62	07/17/92	0.16
09/10/92	0.07	03/30/92	0.18	07/19/92	0.05
09/11/92	0.06	03/31/92	0.05	07/20/92	0.06
09/12/92	0.07	04/11/92	0.10	07/21/92	0.02
09/13/92	0.14	04/14/92	0.16	07/24/92	0.05
09/18/91	0.30	04/15/92	0.12	07/25/92	0.09
09/30/91	0.26	04/16/92	0.07	07/26/92	0.02
10/04/91	0.16	04/22/92	0.13	08/01/92	0.02
10/24/91	0.13	05/09/92	0.13	08/03/92	0.10
10/25/92	0.05	05/19/92	0.18	08/14/92	0.31
10/28/92	0.43	05/21/92	0.39	08/22/92	0.28
10/30/91	0.30	05/22/92	0.18	08/23/92	0.13
11/01/91	0.33	05/24/92	0.06	08/24/92	2.85
11/06/91	0.04	05/25/92	0.58	08/25/92	0.05
11/07/91	0.06	05/26/92	0.15		
11/10/91	0.12	05/27/92	0.18		
11/14/91	0.41	05/28/92	0.08		
11/15/91	0.09	05/30/92	0.02		
11/16/91	0.37	05/31/92	0.36		
11/17/91	0.70	06/01/92	0.39		
11/18/91	0.35	06/05/92	0.14		
11/19/91	0.32	06/07/92	0.10		
11/21/92	0.08	06/08/92	0.05		
11/22/92	0.03	06/13/92	0.02		
11/28/92	0.12	06/14/92	0.01		
11/29/91	0.22	06/19/92	0.05		
11/30/91	0.31	06/23/92	0.02		
12/13/91	0.05	06/25/92	0.10		
12/31/91	0.05	06/26/92	0.10		
01/07/92	0.26	06/28/92	0.03		
01/12/92	0.45	07/01/92	0.06		
01/14/92	0.16	07/02/92	0.23		
03/04/92	1.37	07/07/92	0.04		
03/08/92	1.23	07/08/92	0.02		
03/09/92	1.56	07/10/92	0.04		
03/18/92	0.17	07/11/92	0.07		
03/22/92	0.35	07/12/92	0.19		
03/24/92	0.23	07/16/92	0.20		

Precipitation Data
Van Bibber Creek

Date	Precipitatio (inches)	Date	Precipitatio (inches)
09/09/91	0.04	06/15/91	0.08
09/10/92	0.04	06/25/92	0.04
09/11/92	0.20	06/26/92	0.08
09/13/91	0.12	06/27/92	0.12
09/18/91	0.12	07/02/92	0.04
09/29/91	0.16	07/07/92	0.04
09/30/91	0.04	07/19/92	0.08
10/04/91	0.12	08/06/92	0.04
10/24/91	0.12	08/08/92	0.04
10/25/92	0.08	08/14/92	0.16
10/29/92	0.04	08/15/92	0.04
10/31/91	0.12	08/16/92	0.04
11/02/91	0.04	08/17/92	0.08
11/03/91	0.08	08/23/92	0.16
11/04/91	0.08	08/24/92	2.01
11/06/91	0.04	08/25/92	0.04
03/28/92	0.47		
03/30/92	0.16		
04/01/92	0.04		
04/14/92	0.08		
04/15/92	0.04		
04/16/92	0.04		
05/10/92	0.08		
05/20/92	0.08		
05/21/92	0.08		
05/22/92	0.04		
05/25/91	0.20		
05/26/91	0.12		
05/27/91	0.08		
05/28/92	0.04		
05/30/92	0.08		
05/31/92	0.31		
06/01/92	0.20		
06/02/91	0.04		
06/05/91	0.04		
06/07/92	0.12		
06/09/92	0.04		
06/11/92	0.04		

Appendix F

ET.FOR FORTRAN SOURCE CODE

```
C ***********************************************************************
C  *                                                                     *
C  *                              ET.FOR                                 *
C  *                                                                     *
C  *                          NICHOLAS KIUSALAAS                         *
C  *                       COLORADO SCHOOL OF MINES                      *
C  *                            GOLDEN, COLORADO                         *
C  *                                                                     *
C  *                                                                     *
C  *                                                                     *
C ***********************************************************************
C
C
C       THIS PROGRAM CALCULATES POTENTIAL EVAPOTRANSPIRATION USING
C       THE PENMAN FAO-24 EQUATION (DOORENBOS & PRUITT, 1977).
C       IT REQUIRES HOURLY WIND SPEED, RELATIVE HUMIDITY,
C       MAXIMUM TEMPERATURE, MINIMUM TEMPERATURE, BAROMETRIC
C       PRESSURE, AND SOLAR RADIATION TO PERFORM ET CALCULATIONS.
C
C
      REAL*8 TMAX(24),TMIN(24),WIND(24),WIND2(24),RS(24),PRESS(24),
     &X(24),Y(24),EMAX(24),EMIN(24),EMEAN(24),EDEW(24),EDEFF(24),
     &RB(24),ELEV,LAT,A,B,A1,ET(24),ETMM,ETINCH,PCONV,
     &B1,C,RSCONV,RCONV,ALPHA,HEIGHT,CP,GAMMA(24),DELTA(24),
     &CORR,WCORR,TKMAX(24),TKMIN(24),RH(24),RSO(1000),LAMBDA(24),
     &PI,TMEAN(24),RN(24),RBO(24)
      INTEGER DAY,MONTH,YEAR,JULIAN,DAYCNT,NCNT,TIME(24),
     &CALDAY
      CHARACTER*14 INPUT,DAILY,HOURLY,INTER
      CHARACTER*2 DRIVE
      CHARACTER*16 FILIN,FILOUT,FILEOUT
C.....
C     OPEN INPUT FILE
C.....
      WRITE(*,6000)
      READ(*,6001) DRIVE
      WRITE(*,50)
      READ (*,6001)INPUT
      WRITE(FILIN,1)DRIVE,INPUT
      OPEN(5,FILE=INPUT,STATUS='OLD')
C.....
C     OPEN HOURLY AND DAILY SUMMARY FILES, PRINT OUTPUT HEADER
C     AND READ CARDS 1 - 3
C.....
      WRITE (*,100)
      READ (*,6001)HOURLY
      WRITE(FILOUT,1)DRIVE,HOURLY
      OPEN(10,FILE=HOURLY,STATUS='NEW')
      WRITE (*,200)
      READ (*,6001)DAILY
      WRITE(FILEOUT,1)DRIVE,DAILY
      OPEN(15,FILE=DAILY,STATUS='NEW')
      WRITE (*,250)
      READ (*,6001)INTER
      WRITE(FILEOUT,1)DRIVE,DAILY
      OPEN(20,FILE=INTER,STATUS='NEW')
```

```
      WRITE(*,7000)
      READ(5,*) JULIAN,CALDAY
      READ(5,*) ELEV,LAT,HEIGHT
      READ(5,*) RSCONV,RCONV,PCONV,WCORR
C.....
C     INITIALIZE VARIABLES
C.....
      B1 = -.139
      CP =  0.001013
      PI = 3.1415927
      C = 2.93
C....
C     WRITE DAILY AND HOURLY SUMMARY HEADER
C....
      WRITE(15,500)
      WRITE(15,600)
      WRITE(10,4000)
      WRITE(20,4050)
C
      DO 10, I = 1,1000
C.....
C     READ AND WRITE THE DAY, MONTH AND YEAR
C.....
      READ(5,300,ERR=10)MONTH,DAY,YEAR
      WRITE(10,400)MONTH,DAY,YEAR
      WRITE(20,400)MONTH,DAY,YEAR
C.....
C     CALCULATE RSO, ALPHA, AND A1
C.....
                A = 31.54 - .273*LAT + .00078*ELEV
                B = -.30 + .268*LAT + .00041*ELEV
                RSO(I) = A + B*COS(((2*PI*CALDAY)/365)-C)
                A1 = 0.26 + 0.1*EXP(-(.0154*(30*MONTH+DAY-207))**2)
                ALPHA = 0.29 + 0.06*SIN(30*(MONTH + 0.033*DAY + 2.25))
C.....
C     READ HOURLY DATA
C.....
      DO 20, J = 1,24
                READ (5,*)TIME(J),WIND(J),TMAX(J),TMIN(J)
     &                  ,RH(J),RS(J),PRESS(J)
                        TMAX(J) = 5.0/9.0*(TMAX(J)-32.0)
                        TKMAX(J) = TMAX(J) + 273.0
                        TMIN(J) = 5.0/9.0*(TMIN(J)-32.0)
                        TKMIN(J) = TMIN(J) + 273.0
                        TMEAN(J) = (TMAX(J) + TMIN(J))/2
                        EMAX(J) = EXP((16.78*TMAX(J)-116.9)/(TMAX(J)
     &                             + 237.3))
                        EMIN(J) = EXP((16.78*TMIN (J)-116.9)/(TMIN(J)
     &                              + 237.3))
                        EMEAN(J) = EXP((16.78*TMEAN(J)-116.9)/(TMEAN(J)
     &                              + 237.3))
                        EDEW(J) = EMEAN(J)*RH(J)/100.0
                        EDEFF(J) = EMEAN(J) - EDEW(J)
                        PRESS(J) = PRESS(J)*PCONV
                        RS(J) = RS(J) * RSCONV
                        WIND(J) = WIND(J)*WCORR
```

```
C.....
C     CALCULATE RBO
C.....
                RBO(J) = (A1 + B1*(EDEW(J)**0.5))*4.9E-9*
     +          ((TKMAX(J)**4 + TKMIN(J)**4)/2.0)
C.....
C     CALCULATE RB
C.....
                IF (RS(J)/RSO(I).GT.0.7)THEN
                        A = 1.126
                        B = -.07
                ELSE
                        A = 1.017
                        B = -0.006
                END IF
                RB(J) = (A*RS(J)/RSO(I) + B)*RBO(J)
C.....
C     CACULATE RN, WIND2, DELTA, LAMBDA, AND GAMMA
C.....
                RN(J) = (1 - ALPHA)*RS(J) - RB(J)
                RN(J) = RN(J)*RCONV
                WIND2(J) = WIND(J)*(2.0/HEIGHT)**0.2
                DELTA(J) = (4098*EMEAN(J))/(TMEAN(J) + 237.3)**2
                LAMBDA(J) = 2.501 - ((2.361E-3)*TMEAN(J))
                GAMMA(J) = (CP*PRESS(J))/(.622*LAMBDA(J))
   20 CONTINUE
C.....
C     CACULATE  ET
C.....
      ETMM = 0
      ETINCH = 0
      DO 40, IJ = 1, 24
                X(IJ) = DELTA(IJ)/(DELTA(IJ) + GAMMA(IJ))
                Y(IJ) = GAMMA(IJ)/(DELTA(IJ) + GAMMA(IJ))
                ET(IJ) = X(IJ)*RN(IJ)+Y(IJ)*2.7*(WIND2(IJ)
     &                    * 0.01 + 1.0)*EDEFF(IJ)
                IF(ET(IJ).LT.0)THEN
                ETMM = ETMM
                ETINCH = ETINCH
                ELSE IF(ET(IJ).GE.0)THEN
                ETMM = ETMM + ET(IJ)/24
                ETINCH =  ETINCH + (ET(IJ)/24)/25.4
                END IF
  40  CONTINUE
C.....
C     PRINT RESULTS
C.....
      DO 60, IK = 24,1,-1
                WRITE (10,4500)TIME(IK),DELTA(IK),GAMMA(IK),
     &          WIND2(IK),EDEFF(IK),RN(IK),ET(IK)
                WRITE (20,4600)CALDAY,ALPHA,A1,B1,
     &          RSO(I),RS(IK),RBO(IK),RB(IK),EMEAN(IK)
     &          ,EDEW(IK),LAMBDA(IK),DELTA(IK),GAMMA(IK)
  60  CONTINUE
C.....
      WRITE (15,5000)JULIAN,MONTH,DAY,YEAR,ETMM,ETINCH
```

```
      JULIAN = JULIAN + 1
      IF (CALDAY.LT.365) THEN
                CALDAY = CALDAY + 1
      ELSE IF(CALDAY.EQ.365)THEN
                CALDAY = 1
      END IF
  10  CONTINUE
C
C
 1    FORMAT(A2,A14)
 50   FORMAT(' INPUT DATA FILE NAME -----> ',$)
 100  FORMAT(' INPUT NAME OF THE HOURLY SUMMARY FILE -----> ',$)
 200  FORMAT(' INPUT NAME OF THE DAILY SUMMARY FILE -----> ',$)
 250  FORMAT(' INPUT NAME OF THE INTERMEDIATE VALUE FILE----> ',$)
 300  FORMAT(I2,1X,I2,1X,I2)
 400  FORMAT(I2,'/',I2,'/',I2)
 500  FORMAT(2X,'JULIAN',9X,'DATE',12X,'ET',9X,'ET')
 600  FORMAT(3X,'DATE',26X,'(mm)',5X,'(inches)')
 4000 FORMAT(1X,'DATE',4X,'TIME',2X,'DELTA',3X,'GAMMA',
     &4X,'WIND',2X,'VAPOR DEFF',4X,'RN',3X,'ET (mm/day)')
 4050 FORMAT('CALDAY',3X,'ALPHA',2X,'A1',2X,'B1',3X,'RSO',3X,'RS',
     &      4X,'RBO',3X,'RB',3X,'EMEAN',1X,'EDEW',1X,'LAMBDA',
     &      1X,'DELTA',1X,'GAMMA')
 4500 FORMAT(9X,I4,1X,F6.3,2X,F6.4,2X,F6.2,2X,F6.3,5X,
     &F6.3,3X,F6.2)
 4600 FORMAT(1X,I5,1X,F5.2,1X,F5.3,1X,F5.3,1X,F5.2,1X,F5.2,1X,F5.2,
     $      1X,F5.2,1X,F5.2,1X,F5.2,1X,F5.3,1X,F5.3,1X,F5.3)
 5000 FORMAT(2X,I5,9X,I2,'/',I2,'/',I2,7X,F9.5,4X,F9.5)
 6000 FORMAT(/' SELECT DEFAULT DRIVE, E.G., A:, B:, ETC. ---> ',$)
 6001 FORMAT(A)
 7000 FORMAT(////'  WORKING ...'//)
      CLOSE(5)
      CLOSE(10)
      CLOSE(15)
 6002 STOP
      END
```

Appendix G

RESULTS OF POTENTIAL EVAPOTRANSPIRATION CALCULATIONS

Date	Potentail ET (inches)	Date	Potentail ET (inches)	Date	Potentail ET (inches)	Date	Potentail ET (inches)	Date	Potentail ET (inches)
08/01/91	0.185	09/09/91	0.218	10/18/91	0.111	11/26/91	0.068	01/04/92	0.059
08/02/91	0.125	09/10/91	0.135	10/19/91	0.173	11/27/91	0.107	01/05/92	0.079
08/03/91	0.023	09/11/91	0.153	10/20/91	0.127	11/28/91	0.011	01/06/92	0.050
08/04/91	0.101	09/12/91	0.146	10/21/91	0.129	11/29/91	0.032	01/07/92	0.018
08/05/91	0.174	09/13/91	0.139	10/22/91	0.145	11/30/91	0.023	01/08/92	0.035
08/06/91	0.159	09/14/91	0.165	10/23/91	0.109	12/01/91	0.029	01/09/92	0.052
08/07/91	0.153	09/15/91	0.138	10/24/91	0.059	12/02/91	0.039	01/10/92	0.079
08/08/91	0.164	09/16/91	0.120	10/25/91	0.073	12/03/91	0.061	01/11/92	0.073
08/09/91	0.137	09/17/91	0.147	10/26/91	0.151	12/04/91	0.073	01/12/92	0.030
08/10/91	0.173	09/18/91	0.044	10/27/91	0.245	12/05/91	0.093	01/13/92	0.041
08/11/91	0.186	09/19/91	0.121	10/28/91	0.033	12/06/91	0.098	01/14/92	0.060
08/12/91	0.093	09/20/91	0.145	10/29/91	0.032	12/07/91	0.087	01/15/92	0.055
08/13/91	0.087	09/21/91	0.207	10/30/91	0.021	12/08/91	0.051	01/16/92	0.065
08/14/91	0.151	09/22/91	0.112	10/31/91	0.048	12/09/91	0.081	01/17/92	0.042
08/15/91	0.154	09/23/91	0.184	11/01/91	0.028	12/10/91	0.072	01/18/92	0.039
08/16/91	0.163	09/24/91	0.120	11/02/91	0.036	12/11/91	0.042	01/19/92	0.076
08/17/91	0.164	09/25/91	0.171	11/03/91	0.075	12/12/91	0.082	01/20/92	0.085
08/18/91	0.138	09/26/91	0.199	11/04/91	0.103	12/13/91	0.121	01/21/92	0.081
08/19/91	0.139	09/27/91	0.212	11/05/91	0.106	12/14/91	0.090	01/22/92	0.077
08/20/91	0.151	09/28/91	0.199	11/06/91	0.053	12/15/91	0.084	01/23/92	0.112
08/21/91	0.178	09/29/91	0.145	11/07/91	0.035	12/16/91	0.138	01/24/92	0.090
08/22/91	0.200	09/30/91	0.037	11/08/91	0.118	12/17/91	0.052	01/25/92	0.092
08/23/91	0.187	10/01/91	0.055	11/09/91	0.113	12/18/91	0.041	01/26/92	0.083
08/24/91	0.217	10/02/91	0.055	11/10/91	0.039	12/19/91	0.030	01/27/92	0.069
08/25/91	0.207	10/03/91	0.055	11/11/91	0.061	12/20/91	0.020	01/28/92	0.099
08/26/91	0.215	10/04/91	0.073	11/12/91	0.117	12/21/91	0.070	01/29/92	0.077
08/27/91	0.162	10/05/91	0.102	11/13/91	0.123	12/22/91	0.064	01/30/92	0.088
08/28/91	0.131	10/06/91	0.168	11/14/91	0.074	12/23/91	0.051	01/31/92	0.110
08/29/91	0.151	10/07/91	0.168	11/15/91	0.014	12/24/91	0.047	02/01/92	0.097
08/30/91	0.175	10/08/91	0.234	11/16/91	0.011	12/25/91	0.056	02/02/92	0.092
08/31/91	0.190	10/09/91	0.156	11/17/91	0.045	12/25/91	0.045	02/03/92	0.092
09/01/91	0.249	10/10/91	0.145	11/18/91	0.045	12/27/91	0.043	02/04/92	0.043
09/02/91	0.161	10/11/91	0.150	11/19/91	0.044	12/28/91	0.079	02/05/92	0.065
09/03/91	0.160	10/12/91	0.205	11/20/91	0.087	12/29/91	0.074	02/06/92	0.071
09/04/91	0.194	10/13/91	0.146	11/21/91	0.066	12/30/91	0.049	02/07/92	0.061
09/05/91	0.172	10/14/91	0.123	11/22/91	0.040	12/31/91	0.032	02/08/92	0.045
09/06/91	0.189	10/15/91	0.155	11/23/91	0.064	01/01/92	0.039	02/09/92	0.076
09/07/91	0.172	10/16/91	0.187	11/24/91	0.061	01/02/92	0.081	02/10/92	0.100
09/08/91	0.207	10/17/91	0.199	11/25/91	0.066	01/03/92	0.084	02/11/92	0.057

Date	Potentail ET (inches)	Date	Potentail ET (inches)	Date	Potentail ET (inches)	Date	Potentail ET (inches)	Date	Potentail ET (inches)
02/12/92	0.058	03/22/92	0.064	04/30/92	0.247	06/08/92	0.093	07/17/92	0.115
02/13/92	0.079	03/23/92	0.105	05/01/92	0.270	06/09/92	0.112	07/18/92	0.182
02/14/92	0.093	03/24/92	0.072	05/02/92	0.126	06/10/92	0.155	07/19/92	0.192
02/15/92	0.099	03/25/92	0.127	05/03/92	0.157	06/11/92	0.121	07/20/92	0.103
02/16/92	0.067	03/26/92	0.136	05/04/92	0.179	06/12/92	0.150	07/21/92	0.140
02/17/92	0.126	03/27/92	0.179	05/05/92	0.200	06/13/92	0.185	07/22/92	0.153
02/18/92	0.093	03/28/92	0.062	05/06/92	0.219	06/14/92	0.230	07/23/92	0.175
02/19/92	0.103	03/29/92	0.097	05/07/92	0.209	06/15/92	0.176	07/24/92	0.141
02/20/92	0.102	03/30/92	0.114	05/08/92	0.177	06/16/92	0.216	07/25/92	0.081
02/21/92	0.089	03/31/92	0.050	05/09/92	0.199	06/17/92	0.188	07/26/92	0.104
02/22/92	0.091	04/01/92	0.091	05/10/92	0.089	06/18/92	0.217	07/27/92	0.167
02/23/92	0.099	04/02/92	0.102	05/11/92	0.187	06/19/92	0.131	07/28/92	0.228
02/24/92	0.081	04/03/92	0.148	05/12/92	0.097	06/20/92	0.110	07/29/92	0.181
02/25/92	0.076	04/04/92	0.154	05/13/92	0.197	06/21/92	0.169	07/30/92	0.156
02/26/92	0.115	04/05/92	0.175	05/14/92	0.152	06/22/92	0.158	07/31/92	0.173
02/27/92	0.138	04/06/92	0.155	05/15/92	0.223	06/23/92	0.196	08/01/92	0.156
02/28/92	0.141	04/07/92	0.123	05/16/92	0.195	06/24/92	0.210	08/02/92	0.151
02/29/92	0.134	04/08/92	0.158	05/17/92	0.178	06/25/92	0.072	08/03/92	0.124
03/01/92	0.118	04/09/92	0.126	05/18/92	0.219	06/26/92	0.097	08/04/92	0.124
03/02/92	0.128	04/10/92	0.155	05/19/92	0.254	06/27/92	0.156	08/05/92	0.155
03/03/92	0.096	04/11/92	0.107	05/20/92	0.313	06/28/92	0.158	08/06/92	0.201
03/04/92	0.013	04/12/92	0.176	05/21/92	0.153	06/29/92	0.185	08/07/92	0.132
03/05/92	0.043	04/13/92	0.186	05/22/92	0.043	06/30/92	0.239	08/08/92	0.189
03/06/92	0.096	04/14/92	0.135	05/23/92	0.090	07/01/92	0.100	08/09/92	0.196
03/07/92	0.094	04/15/92	0.090	05/24/92	0.125	07/02/92	0.111	08/10/92	0.131
03/08/92	0.039	04/16/92	0.037	05/25/92	0.037	07/03/92	0.192	08/11/92	0.126
03/09/92	0.044	04/17/92	0.144	05/26/92	0.092	07/04/92	0.196	08/12/92	0.049
03/10/92	0.072	04/18/92	0.188	05/27/92	0.026	07/05/92	0.218	08/13/92	0.113
03/11/92	0.076	04/19/92	0.190	05/28/92	0.083	07/06/92	0.208	08/14/92	0.099
03/12/92	0.084	04/20/92	0.150	05/29/92	0.123	07/07/92	0.149	08/15/92	0.166
03/13/92	0.108	04/21/92	0.139	05/30/92	0.084	07/08/92	0.105	08/16/92	0.146
03/14/92	0.115	04/22/92	0.118	05/31/92	0.062	07/09/92	0.196	08/17/92	0.071
03/15/92	0.141	04/23/92	0.169	06/01/92	0.059	07/10/92	0.178	08/18/92	0.103
03/16/92	0.152	04/24/92	0.161	06/02/92	0.161	07/11/92	0.153	08/19/92	0.163
03/17/92	0.054	04/25/92	0.138	06/03/92	0.166	07/12/92	0.084	08/20/92	0.146
03/18/92	0.041	04/26/92	0.151	06/04/92	0.162	07/13/92	0.129	08/21/92	0.195
03/19/92	0.063	04/27/92	0.198	06/05/92	0.150	07/14/92	0.146	08/22/92	0.200
03/20/92	0.128	04/28/92	0.202	06/06/92	0.109	07/15/92	0.145	08/23/92	0.100
03/21/92	0.032	04/29/92	0.200	06/07/92	0.145	07/16/92	0.061	08/24/92	0.015